Meteor Berichte

Mid-Atlantic Expedition 2005

Cruise No. 64

MARSÜD 2

2 April – 6 June 2005, Mindelo (Cape Verde) – Dakar (Senegal)

K. Haase, K. Lackschewitz

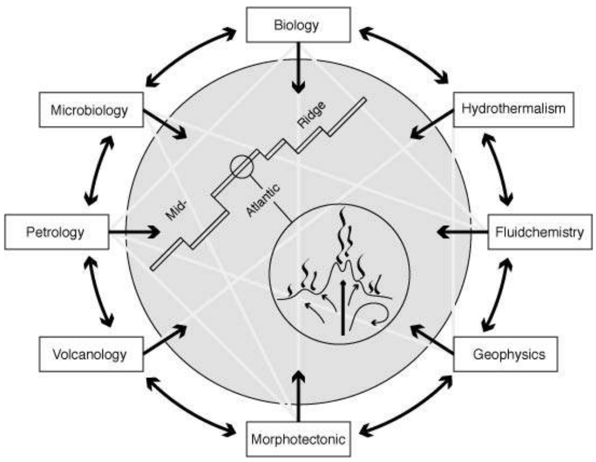

Editorial Assistance:

Senatskommission für Ozeanographie der Deutschen Forschungsgemeinschaft
MARUM - Zentrum für Marine Umweltwissenschaften der Universität Bremen

Leitstelle Deutsche Forschungsschiffe
Institut für Meereskunde der Universität Hamburg

2012

The METEOR-Berichte are published at irregular intervals. They are working papers for people who are occupied with the respective expedition and are intended as reports for the funding institutions. The opinions expressed in the METEOR-Berichte are only those of the authors.

The METEOR expeditions are funded by the *Deutsche Forschungsgemeinschaft (DFG)* and the *Bundesministerium für Bildung und Forschung (BMBF)*.

The reports are available in PDF format from http://www.dfg-ozean.de/.

Editor:
DFG Senatskommission für Ozeanographie
c/o MARUM – Zentrum für Marine Umweltwissenschaften
Universität Bremen
Leobener Strasse
28359 Bremen

Authors:
PD Dr. Karsten Haase
Institut für Geowissenschaften der Christian-Albrechts-Universität zu Kiel, Abteilung Geologie
Olshausenstr. 40
D-24118 Kiel / Germany
Telefon: +49-431-880-2865
Telefax: +49-431-880-4376
e-mail: kh@gpi.uni-kiel.de
http://www.ifg.uni-kiel.de

Dr. Klas Lackschewitz
Leibniz-Institut für Meereswissenschaften
Dienstgebäude Ostufer
Wischhofstr. 1-3
D-24148 Kiel / Germany
Telefon: +49-431-600-2132
Telefon: +49-431-600-2132
http://www.ifm-geomar.de
e-mail: klackschewitz@ifm-geomar.de

Citation: Karsten Haase, Klas Lackschewitz, RV METEOR, Cruise Report M64/L1, M64/L2, Mid-Atlantic Expedition 2005, MARSÜD 2, 118 pp., DFG Senatskommission für Ozeanographie

ISSN 2195-8475

Table of Contents **Page**

Table of Contents Part 1 (M64/1)

Table of Contents Part 2 (M64/2)

Abstract

The three main goals of the **M64/1 cruise** were to study the (1) volcanic, hydrothermal, and biological processes at the newly discovered vents at 4°48'S on the Mid-Atlantic Ridge (MAR), (2) sample an extensive young volcanic eruption site at 8°48'S, and (3) explore and find more hydrothermally active regions on the MAR further south. Thus, the first part of the cruise was dedicated to the observation and sampling of the three hydrothermal sites near 4°48'S, which had been discovered in the previous month during a British-American cruise. Seven dives with the MARUM (Univ. of Bremen) remotely operated vehicle (ROV) were performed at the sites near 4°48'S which yielded numerous fluid, biological and rock samples as well as photographic and film material and measurements. The most important results were the observation of a boiling fluid at 3000 m water depth with a temperature of 400°C, a change of the mineralogy of the precipitated minerals at these vents, and evidence for very young volcanism. It appears that a recent volcanic eruption led to a significant change in the composition and temperature of the fluids. The second main study area of M64/1 was a large volcanic field on segment A2 at 8°48'S which was identified on the side-scan maps of the M62/5. This feature was sampled during two ROV dives and with the wax corer. First results indicate that the volcanism in this field may be older than originally suggested by the reflectivity and preliminary geochemical data imply that the large lava formations consist of two chemically distinct lava types. Thus, although the lava field probably formed within a brief period of time, the composition of the lavas in the northern part is different from the southern part implying different magma reservoirs. The third studied area was the northern part of segment A3 which is relatively shallow (about 1500 m depth) and lies on thickened oceanic crust (about 11 km thick). Here, we found a new hydrothermal field, the so-called Lilliput diffuse field, which is the southernmost known hydrothermal field along the MAR. The occurrence of predominantly juvenile mussels suggests recent reactivation of the hydrothermal activity, possibly following an eruptive event.

The investigations of **cruise M64/2** are a continuation of the program started in 2004 (cruise M60/3) between 14°45'N and 15°05'N on the Mid-Atlantic Ridge. While basic geochemical and biological studies were carried out during the 2004 cruise in the Logatchev hydrothermal field, the emphasis of the 2005 cruise was on the temporal variability of fluid emanations, fluid temperature and chemistry, microbial activities and associated fauna at selected hydrothermal vent sites. Biological, microbiological, petrological and hydrological samples were taken using the ROV, TV-grab, and CTD where several fluid chemical parameters as well as, for example, methane oxidation rates were determined immediately on board. Hydrothermal fluids and sulfides were sampled at several of the hydrothermal chimneys in order to determine the differences in composition between the different structures of this ultramafic-hosted site. Plume exploration and mapping of the seafloor with the ROV revealed more hydrothermal activity in the area of the Logatchev field. Several long-term observation systems were successfully installed on the seafloor in order to measure the variation of temperature at a hydrothermal vent mussel bed, the temperature variation in the bottom water, as well as the seafloor tilt and pressure variations. Furthermore, several experiments were conducted to determine variations of

temperature and fluid compositions in the range of several hours to days which were combined with the sampling of fauna at the respective vents. The results of these measurements will allow the study of the links between the geochemical energy supply from hydrothermal fluids and the vent organisms. Geochemical gradients in vent fluids along mussel beds were determined and mussels were collected along these gradients for analysis of the biomass and activity. Furthermore, a relocation experiment of hydrothermal mussels was carried out where the mussels were removed from hydrothermal activity in order to determine the temporal evolution of the methane oxidation rates and the relationship between symbionts and host mussels.

Zusammenfassung

Die drei Hauptziele der **M64/1 Ausfahrt** waren (1) die Untersuchung der vulkanischen, hydrothermalen und biologischen Prozesse an den neu entdeckten Quellen bei 4°48'S am Mittelatlantischen Rücken (MAR), (2) die Beprobung eines ausgedehnten jungen Vulkanfeldes bei 8°48'S, sowie (3) die Exploration nach weiteren hydrothermalen Quellen am südlichen MAR. Während des ersten Teils der Fahrt wurden die drei hydrothermal aktiven Felder untersucht und beprobt, die während einer Britisch-Amerikanischen Fahrt einen Monat zuvor entdeckt wurden. Sieben Tauchgänge mit dem Remotely Operated Vehicle (ROV) des MARUM (Univ. Bremen) wurden bei 4°48'S durchgeführt und ergaben eine Vielzahl von Fluid-, Biologie- und Gesteinsproben sowie umfangreiches Foto- und Filmmaterial und viele direkte Messergebnisse. Die wichtigsten Ergebnisse bestanden in der Entdeckung von kochenden Fluiden mit einer Temperatur von 400°C bei einer Wassertiefe von 3000 m, eines Wechsels der mineralogischen Zusammensetzung der Präzipitate an den Austritten sowie der Anzeichen für sehr jungen Vulkanismus in dem Gebiet. Offenbar führte eine rezente vulkanische Eruption zu einem signifikanten Wechsel in der Zusammensetzung und Temperatur der Fluide. Das zweite Untersuchungsgebiet der M64/1 war ein großes Vulkanfeld auf dem Segment A2 bei 8°48'S, das auf den Side-scan-Karten der M62/5 identifiziert wurde. Diese Struktur wurde mit zwei ROV-Tauchgängen und mit dem Vulkanitstoßrohr beprobt. Erste Ergebnisse zeigen, daß der Vulkanismus dieses Feldes offenbar älter ist als nach der Reflektivität angenommen und vorläufige geochemische Daten deuten an, daß das Lavafeld aus zwei chemisch unterschiedlichen Laven besteht. Obwohl die Laven vermutlich gleichzeitig eruptierten, stammen die aus dem Norden und die aus dem Süden des Lavafeldes von unterschiedlichen Magmenreservoiren. Das dritte untersuchte Gebiet umfasste den nördlichen Bereich des Segments A3, das relativ flach liegt (ca. 1500 m Wassertiefe) und eine verdickte Kruste (ca. 11 km dick) aufweist. Hier wurde ein neues hydrothermal aktives Feld gefunden, das sogenannte Lilliput Feld, das das südlichste bekannte Hydrothermalfeld auf dem MAR darstellt. Die Dominanz von juvenilen Muscheln an den Austrittsstellen deutet darauf hin, daß dieses hydrothermale Feld reaktiviert wurde, wahrscheinlich in Folge einer vulkanischen Eruption und der Intrusion eines Dikes.

Die Untersuchungen der **Fahrt M64/2** stellt eine Fortsetzung des Programmes von 2004 (Ausfahrt M60/3) im Gebiet zwischen 14°45'N und 15°05'N am MAR dar. Während die grundlegenden geochemischen und biologischen Studien im Logatchev Hydrothermalfeld

während der Fahrt in 2004 durchgeführt wurden, lag der Schwerpunkt der Fahrt in 2005 auf der Untersuchung der zeitlichen Variabilität der Fluidaustritte, der Fluidtemperatur und –zusammensetzung, sowie der mikro- und makrobiologischen Aktivität an ausgewählten hydrothermalen Austritten. Biologische, mikrobiologische, petrologische und hydrologische Proben wurden mit dem ROV, TV-Greifer und der CTD genommen und eine Vielzahl von Parametern der Fluidzusammensetzung und z.B. die Methan-Oxidationsrate wurden an Bord bestimmt. Hydrothermale Fluide und Präzipitate wurden an einigen Austritten beprobt, um die Bildungsbedingungen verschiedener Minerale in Relation zu den verschiedenen Vents zu bestimmen. Die Plume Exploration und Kartierung des Meeresbodens ergab mehrere neue Gebiete mit hydrothermaler Aktivität in der Umgebung des Logatchev Feldes. Verschiedene Langzeit-Beobachtungssysteme wurden erfolgreich am Meeresboden installiert, um die zeitliche Variation der Temperatur an einem hydrothermalen Muschelfeld und im Bodenwasser sowie die zeitliche Variation der Neigung und des Druckes des Meeresbodens zu bestimmen. Weiterhin wurden mehrere Experiment durchgeführt, um die Änderungen der Temperatur und der Zusammensetzung der Fluide über den Zeitraum von mehreren Stunden bis Tagen festzustellen. Diese Untersuchungen wurden mit einer Beprobung der Fauna kombiniert, um entsprechend Aussagen über die Organismen an den Vents zu treffen. Die Ergebnisse werden die Zusammenhänge zwischen der geochemischen Energiezufuhr durch hydrothermale Fluide und den Ventorganismen aufzeigen. Geochemische Gradienten in den Fluiden entlang von Muschelfeldern wurden bestimmt und Muscheln entlang der Gradienten beprobt, damit die Biomasse und biologische Aktivität untersucht werden kann. Weiterhin wurden in einem Umsetzungsexperiment mit hydrothermalen Muscheln die zeitliche Entwicklung der Methanoxidationsrate und die Beziehung zwischen Wirtsmuschel und Symbionten untersucht.

Research Objectives

Mid-ocean ridges are unique features of the Earth where energy and material is exchanged between the Earth's interior and the surface. The two M64 cruises were part of the DFG Priority Programme 1144 "From Mantle to Ocean: Energy, material and life cycles on spreading axes" designed to obtain a four-dimensional picture of the processes operating at mid-ocean ridges. In this context the overall goals of the planned investigations are as follows: (1) to determine the volcanic and tectonic dynamics operating at mid-ocean ridges as well as the geochemical and biological processes occurring at active hydrothermal vent areas shall be characterised in detail as a function of space and time and (2) to link the hydrothermal processes to the volcanic activity on the axis.

The target area of Leg 64/1 (Fig. 1) is one of the two key areas of the Priority Programme 1144 on the Mid-Atlantic-Ridge (MAR) planned to be investigated by petrologists, biologists, chemists, geochemists, geophysists and oceanographers. It is situated between 4 and 12°S along the MAR south of the Ascension fracture zone (Figure M64/1-1). This section of the MAR is highly variable in morphology, crustal thickness, and magma composition and is thus an ideal region to study the diversity of magma transport and volcanic eruption processes and their influence on the formation and evolution of hydrothermal vents and associated biological processes. Leg M64/1 was a follow-up cruise of Leg M62/5 during which the foundation for this cruise – a detailed geologic and tectonic map of the seafloor and the position of hydrothermal plumes – has been obtained by using a TOBI combination of deep towed sidescan and nephelometry and a Remotely Operated Vehicle (ROV) and a CTD/Rosette. Based on this data our research group selected hydrothermally active sites and characterised them volcanologically, geochemically and biologically by taking and analysing rock samples, samples of hydrothermal fluids, samples of the micro- and macro fauna and samples of the water column in the vicinity of those vent areas.

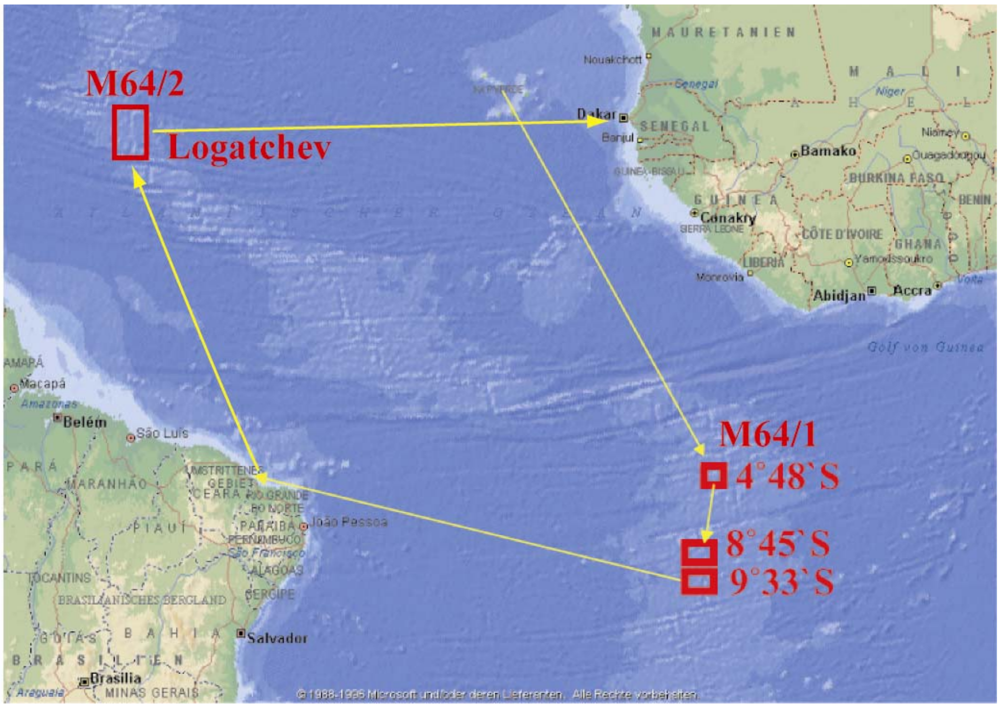

Fig. 1 Map of the central Atlantic Ocean showing the ports and working areas of the two M64 cruises.

The investigations of Leg M64/2 were a continuation of a programme started in 2004 at 15°N on the MAR (cruise M60/3 and respective proposals). Whereas during the 2004 cruise basic geochemical and biological studies have been carried out in the Logatchev field at 15°N, the emphasis of the M64/2 cruise lay on the temporal variability of fluid emanations, fluid temperature and chemistry, microbial activities and associated fauna at selected hydrothermal vent sites. In order to assess long-term variations in hydrothermal activity of the Logatchev Hydrothermal Field, a number of environmental monitoring stations were installed which were recovered in 2006. The fluids sampled at the Logatchev field in 2004 are probably of supercritical (>300 bar, >400°C) origin. They showed high iron, methane and hydrogen concentrations, but low sulphide contents, thus providing a very special environment for hydrothermal habitats. The focus of Leg M64/2 was on the determination of the geochemical changes at the different vent sites and their consequences for the hydrothermal ecosystem. As little is known so far about the medium-term variability of complex hydrothermal systems, it is planned to continue these time-dependant studies in the following years. The strength of this interdisciplinary project is the intense interaction of the different working groups of geochemistry, biology and microbiology, which address the different levels of the hydrothermal ecosystem (from the inorganic material of the fluids to the different life forms) and the interfaces between these levels.

Research objectives special to the respective cruises:

M64/1: The aim of the cruise was the detailed determination of the magmatic, volcanic, hydrothermal and biological processes by an interdisciplinary group of scientists consisting of petrologists, volcanologists, fluid geochemists, microbiologists and zoologists. Based on the detailed side-scan maps from Legs M62/5 and CD169 the magmatic geochemistry group obtained samples by ROV from the freshest lava flows and several representative volcanoes on the different segments of the neovolcanic zone of this section of the MAR. Geochemical and isotopic analysis as well as age dating of the lavas will not only reveal the subsurface connections along the different segments, i.e. whether eruptions occur above large dikes or whether each eruption is fed by its own source in the mantle but it will also allow to study the variation of the magma sources with time.

The fluid geochemistry group is going to take samples from hydrothermal vents along this section of the MAR in order to geochemically characterise the different vent fluids. Those fluids will then be compared with the well-known fluids from the northern MAR in relation to the tectonic and geological situation. One important aspect is also the sampling of fluids from different water depths, preferably from sites considerably shallower than 3000 m. This aims at the comparison of subcritically phase-separated fluids with the supercritically phase-separated fluids from the Logatchev field at 15°N. Both types of phase separation produce chemically and physico-chemically very different fluid types. Especially the differences in salinity, gas and metal concentrations are assumed to exert a strong influence on the development of the associated hydrothermal ecosystem and on associated mineral precipitates.

The sulphur isotopic composition of sulphides (and other sulphur species present) will reveal the principal sulphur source as well as the process responsible for their formation. In combination with quantitative data from fluid geochemistry, this will advance our understanding of sulphur cycling and provide important information for a sulphur budget.

The fauna associated with hydrothermal vents is only poorly known so that every new area has mostly new organism taxa. Although neighbouring areas can be grouped biogeographically, the individual communities remain taxonomically very specific. Thus the main work of the zoological group during Leg M64/1 will be to find, sample and than characterise the macro fauna as a function of the hydrothermal habitat. As the fauna of southern MAR hydrothermal vents is entirely unknown the main work of the hydrothermal symbioses group will be to search for symbionts in putative hosts and analyse the symbionts morphology and their spatial distribution in host tissues. The main questions addressed during the cruise are as follows:

• How did the propagating rift segment evolve through time and how is it linked to material transport from the relatively shallow segment A3?
• What is the time span of volcanic eruptions and magmatic phases on this slow-spreading axis?
• What is the spatial and temporal relationship between the abundance, age and volume of eruptive units and the occurrence of hydrothermal vents?
• What are the different formation processes (including phase separation) and how is the respective composition of fluids of the southern MAR obtained?
• What are the basic geochemical differences between subcritically phase-separated fluids compared to supercritically phase-separated fluids at slow-spreading ridges?
• Which distribution patterns of fluid components are observed in the water column?
• What is the impact of the composition of the fluids (due to processes of phase separation) on activities and structure of microbial communities?
• How genetically diverse are the microbial communities along hydrothermal gradients in different types of phase separated fluids?
• Which important microbial groups exist and which ecological niches do they occupy in habitats of the hydrothermal vent environment?
• How is the taxonomic composition of the hydrothermal communities on the southern MAR?
• Which are the zoogeographic relationships of the hydrothermal communities on the southern MAR?
• Which symbioses occur in the southern MAR hydrothermal vents and what is their spatial distribution along physico-chemical gradients of hydrothermal fluids?

<u>M64/2:</u> The overall goal of the proposed cruise is to advance the integrated study of the 15°N hydrothermal sites further through multi-diciplinary characterisation and sampling at several sites. Biological, mineralogical and hydrological samples are to be taken in a well-characterised thermal environment so that the results on the samples can be interpreted in terms of the influence of the important environmental parameter temperature. The cruise is the second in a number of cruises within the 6-year SPP, dedicated to a long-term study in the 15°N area to investigate medium-term variability in the hydrothermally active sites and the related geochemical and biological consequences. Longterm monitoring of all relevant environmental parameters is essential to assess the temporal variability observed in the biogeochemistry of the hydrothermal field. Temperature measurements, the use of sensors and the sampling of fluids to determine the chemical composition of the fluids, material fluxes and spatial and temporal gradients give the basic information to characterize the environment in which the ecosystem develops. Samples for the biologists are chosen in arrangement with the geochemists measuring the different abiotic parameters. The samples are shared between the different groups, analysed in close collaboration and the results will be finally evaluated in the context of all geochemical and microbiological findings with respect to the bio-geo coupling. The aim is to develop an overall model for the temporal and spatial development of the Logatchev hydrothermal ecosystem, which also includes control by general environmental parameters such as water depth and

geological conditions. To fullfil this aim the following single projects comprising different working groups have been designed:

Project I is concerned with the long-term monitoring of hydrothermal activity, conducting the following tasks on this cruise:

- Testing and deployment of long-term monitoring instruments within the Logatchev Hydrothermal Field for recording environmental parameters for one year (the exact locations where monitoring instruments will be installed within the Logatchev Hydrothermal Field will be determined on board in close cooperation with all groups involved in the longterm monitoring effort);
- Profiling of the water column ('tow-yows') to map the extent of the hydrothermal plume in the water column (these investigations are going to be supplemented by current measurements in the water column as well as with an ADCP current meter on the seefloor);

Project II is investigating the geochemistry and biology of hydrothermal vents with different working groups supporting this project. The fluid geochemistry group conducts the following aims and methods:

- Determination of the relevance of hydrothermal cyclicity by measuring the variability of vent fluids in time;
- Determination of the consequences of fluid variability, such as changes in salinity, gas and metal concentrations, for the hydrothermal ecosystems;
- Determination of the importance of variable sulfur and heavy metal speciation and of organic complexation for geochemical and biogeochemical reaction pathways on a temporal and spatial scale;
- Determination of the extension and temporal variability of the plume by mapping with physicochemical sensors and chemical analyses of tracers (gases, metals);
- Determination of the importance of the hydrothermal input for the element budget in the oceanic water column
- Determination of spatial physico- and geochemical gradients for the biologists.

The main aim of the methane group is the investigation of the occurrence and distribution of methane-consuming microbes in hydrothermal systems with a special focus on the process of anaerobic oxidation of methane. The sulfur isotope geochemistry group plans to characterize all major sulfur bearing phases in the fluids, mineral precipitates, altered volcanic rocks, and sediments in order to quantify the principal sulfur source(s) and respective inorganic and possibly biological transfer processes. An important aspect of this study is the correlation of sulfur isotope data from vent fluids with those of mineral precipitates such as chimneys, mounds and crusts in close proximity to the ridge axis. This information provides the foundation for the interpretation of fossil ridge settings in the geological record. The overall aim of the studies of the microbiology goup is the investigation of the influence of temperature on microbial communities. The proposed microbiological work will focus on two major aspects: 1) the diversity of microbial communities as a function of hydrothermal vent habitats, using molecular genetic methods and 2) function related analysis and experiments of these communities. In particular temporal changes in fluid chemistry on microbial communities will be analysed.

The main aim of the metagenomics group is the characterisation of the metabolic capabilities of those microorganisms in hydrothermal systems that are numerically and functionally important, with respect to the coupling between microbiology and geochemistry. The metagenomics approach provides a broader access to the genetic information of uncultivated microorganisms than other commonly used molecular biology methods and is therefore a suitable method to get new insights into the genetic equipment of microbial communities and to find new and interesting genes. The main aim of the hydrothermal symbioses group is the characterisation of the interplay between geochemical energy from hydrothermal fluids and symbiotic communities at the Logatchev vent field. High-resolution temperature measurements of vent fluids conducted during this cruise will allow for the first time a detailed spatial study of the emission of vent water and its influence on the distribution of symbiotic macrofauna. In parallel, the fluid geochemistry groups will investigate whether water temperature is a good indicator for sulfide and methane concentrations in vent fluids. The advantage of using water temperature as an indicator for fluid gradients is the speed and high spatial resolution of digital temperature measurements in contrast to the time consuming and spatially localized sampling of methane and sulfide. The main objectives are:

- Finding of the hotspots of anaerobic oxidation of methane;
- Identification of the methane oxidizing communities;
- Quantification of microbial processes of methane oxidation and sulfate reduction;
- Investigation of the link between methane and sulfur cycles;
- Characterisation of the interaction between microbes and minerals.
- The determination of the genetic diversity of microbial communities and selected activities (sulfur oxidation, hydrogen oxidation) as a function of temperature;
- Setting up of experiments to verify the temperature range and adaptation of microbial groups and species along temperature gradients;
- The identification of important microbial groups and representatives thereof and determine their ecological niches and competitive temperature range in mixed populations;
- The measurement of important physiological functions (sulfur transformations, CO_2 fixation) and identification of microorganisms performing these functions under variation of the temperature.
- The characterisation of the microbial diversity in representative habitats (e.g. hot/cold, sulfide rich/poor, methane rich/poor);
- Analysis of the metagenome data in the context of the results obtained by cultivation and PCR-based sequence retrieval from the same samples by the other groups working on free-living microorganisms;
- Correlation of the results to fluid chemical, geological and biogeochemical data in order to set the focus on the most interesting findings with respect to the bio-geo coupling.
- Determine of the spatial distribution and population structure of symbiotic macrofauna in relation to temperature, sulfide and methane concentrations;
- Assessment of the symbiotic biomass and activity along these gradients;
- Bringing out of short-term (days) and long-term experiments (1 year) in order to assess productivity, growth rates and colonization success of symbiotic macrofauna along vent gradients.

Acknowledgments

We thank Captain Kull and his crew for their help during the cruises. We gratefully acknowledge the cooperation and sharing of information of Chris German and Tim Shank which led to the success of the first part of M64/1. Funding by the Deutsche Forschungsgemeinschaft made possible the two cruises. Furthermore, we gratefully acknowledge the professional patronage and administrative/logistical support of the German Ministry of Foreign Affairs (Berlin), Captain Berkenheger at the Leitstelle Meteor (Hamburg), K. Bohn at VTG-Lehnkering AG (Bremen) and the RF Reederei Forschung GmbH (Bremen).

We wish to thank the German Science Foundation (DFG) for funding the cruise and subsequent analytical work in the framework of the priority programm SPP 1144 "From mantle to ocean: Energy-, material-, and life cycles at spreading axes".

Meteor Berichte

Mid-Atlantic Expedition 2005

Cruise No. 64, Leg 1

MARSÜD 2

2 April – 3 May 2005, Mindelo (Cape Verde) – Fortaleza (Brazil)

K. Haase, C. Flies, S. Fretzdorff, O.Giere, A. Houk, S. Klar, A. Koschinsky, J. Küver, H. Marbler, P. Mason, N. Nowald, C. Ostertag-Henning, H. Paulick, M. Perner, S. Petersen, V. Ratmeyer,W. Schmidt, T. Schott, M. Schröder, R. Seifert, C. Seiter, J. Stecher, H. Strauss, J. Süling, D. Unverricht, M. Warmuth, S. Weber, U. Westernströer

Project Leader: Karsten Haase

METEOR 64
SPP 1144
Vom Mantel zum Ozean
Dakar - Fortaleza - Mindelo

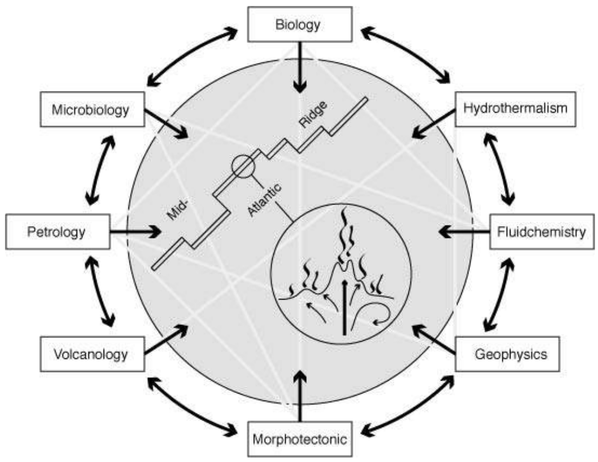

Editorial Assistance:

Senatskommission für Ozeanographie der Deutschen Forschungsgemeinschaft
MARUM - Zentrum für Marine Umweltwissenschaften der Universität Bremen

Leitstelle Deutsche Forschungsschiffe
Institut für Meereskunde der Universität Hamburg

2012

Table of Contents Part 1 (M64/1)

8

1. Leg M64/1

1.1. Participants

	Name	Discipline	Institution
1.	Haase, Karsten, Dr./ Chief scientist	Petrology	IfG Uni Kiel
2.	Flies, Christine, Dr.	Microbiology	GZ Göttingen
3.	Fretzdorff, Susanne, Dr.	Petrology	IfG Uni Kiel
4.	Giere, Olav, Prof. Dr.	Biology	ZIM Hamburg
5.	Houk, Andy	ROV	Schilling Robotics, USA
6.	Klar, Steffen	ROV	MARUM Bremen
7.	Koschinsky, Andrea, Dr.	Fluid chemistry	IU Bremen
8.	Küver, Jan, Dr.	Microbiology	MPA Bremen
9.	Marbler, Herwig, Dr.	Fluid chemistry	IU Bremen
10.	Mason, Pete	ROV	SOC Southampton
11.	Nowald, Nicolas	ROV	MARUM Bremen
12.	Ostertag-Henning, Christian, Dr.	Gas chemistry	BGR Hannover
13.	Paulick, Holger, Dr.	Petrology	MinBonn
14.	Perner, Mirjam	Microbiology	IfM-Geomar Kiel
15.	Petersen, Sven, Dr.	Mineralogy	IfM-Geomar Kiel
16.	Ratmeyer, Volker, Dr.	ROV	MARUM Bremen
17.	Schmidt, Werner	ROV	MARUM Bremen
18.	Schott, Thorsten	Technician	IfM-Geomar Kiel
19.	Schröder, Marcel	ROV	MARUM Bremen
20.	Seifert, Richard, Dr.	Gas chemistry	IFBM Hamburg
21.	Seiter, Christian	ROV	MARUM Bremen
22.	Stecher, Jens, Dr.	Biology	FSI Wilhelmshaven
23.	Strauss, Harald, Prof. Dr.	Fluid chemistry	GPI Münster
24.	Süling, Jörg, Dr.	Microbiology	IfM-Geomar Kiel
25.	Unverricht, Daniel	Petrology	IfG Kiel
26.	Warmuth, Marco	Gas chemistry	IFBM Hamburg
27.	Weber, Stefan	Gas chemistry	IFBM Hamburg
28.	Westernströer, Ulrike	Fluid chemistry	IfG Kiel

Abbreviations:

BGR Hannover: Bundesanstalt für Geowissenschaften und Rohstoffe, Stilleweg 2, D-30655 Hannover

FSI Wilhelmshaven: Forschungsinstitut Senckenberg, Rheinstrasse 190, D-26382 Wilhelmshaven, Germany

GPI Münster: Geologisch-Paläontologisches Institut, Corrensstraße 24, D-48149 Münster, Germany

GZG: Göttinger Zentrum Geowissenschaften GZG, Abt. Geobiologie, Universität Göttingen, Goldschmidtstr. 3, D-37077 Göttingen, Germany

IFBM Hamburg: Institut für Biogeochemie und Meereschemie, Bundesstr. 55, D-20146 Hamburg, Germany

IfG Uni Kiel : Institut für Geowissenschaften, Abteilung Geologie, Christian-Albrechts-Universität zu Kiel, Olshausenstr. 40, D-24118 Kiel, Germany

IfM-Geomar Kiel: Leibniz-Institut für Meereswissenschaften, IFM-GEOMAR, Düsternbrooker Weg 20, D-24105 Kiel, Germany

IfM-Geomar Kiel#: Leibniz-Institut für Meereswissenschaften, IFM-GEOMAR, Dienstgebäude Ostufer, Wischhofstr. 1-3, D-24148 Kiel, Germany

IU Bremen: Geosciences and Astrophysics, Research III, Room 108, School of Engineering and Science, International University Bremen IUB, Campus Ring 8, D-28759 Bremen, Germany

MARUM Bremen: MARUM Zentrum für Marine Umweltwissenschaften, Universität Bremen, Leobener Str, D-28359 Bremen, Germany

MinBonn: Mineralogisches und Petrologisches Institut, Universität Bonn, Poppelsdorfer Schloss, D-53115 Bonn, Germany

MPA Bremen: Department of Microbiology, Bremen Institute for Materials Testing, a Division of the Institute for Materials Science, Paul-Feller-Str. 1, D-28199 Bremen, Germany.

SOC Southampton: Southampton Oceanography Centre, European Way, Empress Dock, Southampton SO14 3ZH, United Kingdom

ZIM Hamburg:

Zoologisches Institut und Zoologisches Museum, Universität Hamburg, Martin-Luther-King-Platz 3, D-20146 Hamburg, Germany

1.2. Research Program

Mid-ocean ridges are unique features of the Earth where energy and material is exchanged between the Earth's interior and the surface. This cruise is part of a DFG Priority Programme "From Mantle to Ocean: Energy, material and life cycles on spreading axes" designed to obtain a four-dimensional picture of the processes operating at mid-ocean ridges. In this context the overall goals of the planned investigations are as follows: (1) to determine the volcanic and tectonic dynamics operating at mid-ocean ridges as well as the geochemical and biological processes occurring at active hydrothermal vent areas shall be characterised in detail as a function of space and time and (2) to link the hydrothermal processes to the volcanic activity on the axis. The target area of Leg 64/1 is one of the two key areas of the Priority Programme 1144 on the Mid-Atlantic-Ridge (MAR) planned to be investigated by petrologists, biologists, chemists, geochemists, geophysists and oceanographers. It is situated between 7 and 12°S along the MAR south of the Ascension fracture zone (Figure M64/1-1). This section of the MAR is highly variable in morphology, crustal thickness, and magma composition and is thus an ideal region to study the diversity of magma transport and volcanic eruption processes and their influence on the formation and evolution of hydrothermal vents and associated biological processes. Leg M64/1 is a follow-up cruise of Leg M62/5 during which the foundation for this cruise – a detailed geologic and tectonic map of the seafloor and the position of hydrothermal plumes – has been obtained by using a TOBI combination of deep towed sidescan and nephelometry and a Remotely Operated Vehicle (ROV) and a CTD/Rosette. Based on this data our research group will select hydrothermally active sites and characterise them volcanologically, geochemically and biologically by taking and analysing rock samples, samples of hydrothermal fluids, samples of the micro- and macro fauna and samples of the water column in the vicinity of those vent areas.

1.3. Narrative of the cruise

The cruise started in Mindelo with some minor problems with the transport of crew members and with the successful loading of the heavy ROV containers with an ancient swimming crane. In the morning of April 2nd FS METEOR left the port of Mindelo and steamed southwards to the first working area on the Mid-Atlantic Ridge near 5°S. Throughout the cruise we had warm and calm weather and only for a couple of days the wind rose to a strength of 6 and the swell increased to about 3 m. In the evening of April 7th we arrived in the first working area at the location of the Turtle Pits hydrothermal field which was discovered only weeks before by a British-American cruise and the location of which was kindly forwarded to us by C. German and T. Shank. During the night the area was mapped with Hydrosweep after we had one CTD/rosette station outside of the ridge area in order to determine the background water composition. Unfortunately, the CTD failed and no water samples were recovered. On the morning of April 8th we performed the first dive (#36, station 108) with the MARUM QUEST ROV and after a few technical problems the ROV reached the seafloor at around noon. Towards the end of the dive we found two inactive black smokers and deployed a sonar buoy. During the night two TV grab and several wax corer stations recovered basaltic lava and CTD/rosette stations were carried out to determine the location of the hydrothermal plume. MAPRs were also deployed with each wax corer and TV grab in order to study the areal extent of the plume. On April 9th the second ROV (#37, station 114) dive found the active chimneys situated in a north-south running depression and we started photographing, sampling and measuring the different structures. Between April 9th and April 15th five dives with the ROV were performed mostly during the day with CTD, wax corer and TV grab stations during the night. In most dives we studied the Turtle Pits field but one dive (#39, station 125) led to the Wideawake mussel field for geological, biological and fluid sampling. On April 16th a very long dive (#42, station 146) was performed starting south of the Turtle Pits field and ending at the Red Lion hydrothermal field where one active smoker was reported by our British-American colleagues. While diving at this location we found four active smokers and numerous inactive structures with a peculiar fauna consisting of impressive numbers of shrimps. After this long dive we had a 24 h transit to the working area at 8°50´S on the MAR.

Work in this area started with a detailed bathymetric survey of the large volcanic field on segment A2. After that the lavas of the volcanic field were sampled using the wax corer and the ROV during two dives in order to study the volcanology and geology of the area. Surprisingly, much of the volcanic field was covered by sediments althought the sidescan maps showed a very high reflectivity. CTD and MAPR stations in the area of the volcanic field did not show any hydrothermal signal and we concluded that the southern part of segment A2 is probably both volcanically and hydrothermally inactive. After three days of work on segment A2 (April 18th to 21st) we continued hydrothermal exploration on segment A3 using wax corers with MAPRs and CTD/rosettes. 186 CTD station showed a strong methane anomaly but the nephelometers did not record any anomalies in the water column. On April 23rd and 24th we performed two dives on the shallowest part of segment A3 near the near-axis seamounts in order to study the volcanology and sample lavas. On the night from April 24th to the 25th five CTD stations defined the location of a potential hydrothermal vent to be within the area between 9°32.5´S and 9°33.0´S. Studying the bathymetric and sidescan maps indicated that the most likely location of a vent would be the neovolcanic zone with a narrow cleft. On the morning of the 25th the ROV dive led us from one of the CTD stations with an anomaly to the east toward the neovolcanic zone. At about 12 o´clock we found the first hydrothermal sediments and mussel shells and at 15:55 we discovered the active low-temperature Lilliput hydrothermal field. The name was given because of the overabundance of small juvenile mussels. Biological, geological and fluid samples were taken. During the night two TV grab stations recovered more hydrothermal sediment, lava and biology from this field. On the next morning the ROV started the dive but technical problems required to retrieve the ROV after 2 hours from the water. The final stations of cruise M64/1 consisted of CTD, wax corer, and TV grab stations and one camera sledge tow across the neovolcanic zone. On the 27th at 15:00 we finished our work and RV METEOR started its voyage to Fortaleza. The ROV team was busy repairing the damage in the high voltage unit of the ROV and was successful so that by the time of arrival in Fortaleza most of the damage was repaired. Early in the morning on May 3rd METEOR arrived in Fortaleza after a very successful cruise.

1.4. Preliminary Results

1.4.1. Geology and petrology

1.4.1.1. Geological setting and lava petrology of the area at 4°48`S on the MAR

(K. Haase, S. Fretzdorff, H. Paulick, D. Unverricht)

The Turtle Pits hydrothermal field occurs in a N-S striking row of collapse pits in a large sheet flow whereas the Wideawake Mussel Field occurs in a jumbled sheet flow. The abundance of fresh glassy sheet flows in the area suggests a very strong volcanic activity and the youngest observed lava covers parts of the Wideawake Mussel Field in the SE and is thus probably less than 10 years old. The segment was seismically active in June 2002 (C. Devey, pers. comm.) and one can speculate whether the seismic activity occurred during the eruption of the lava flow. These observations indicate that this segment of the MAR is currently in a volcanic rather than in a tectonic phase. The tectonic features of the MAR at 4°48´S all strike in N-S direction, for example, the major faults at the rift flanks, minor faults observed during ROV dives as well as volcanic features in the rift. Interestingly, the shallow rift flanks of the MAR at 4°48´S suggest variable volumes of magma production.

The volcanic rocks in the region surrounding the Turtle Pits hydrothermal and Wideawake Mussel fields have been sampled very detailed using the rock corer, TV grab and the ROV. Forty-two samples have been selected from the recovered lavas covering an area of about 3 x 3 km^2. Most of the lavas in this region are very fresh aspheric sheet flows with ropy and jumbled surfaces. Collapse structures with lava pillars are frequent in the sheet flows. Young lava flows also occur in the deep basin between the Turtle Pits hydrothermal field and the axial seamount (e.g. sample 146ROV-2). The freshness and the predominance of sheet flows in the region imply very strong volcanic activity and eruption volumes in this segment of the Mid-Atlantic Ridge. Pillow lavas occur only in few areas, for example, on the small seamount west of the Turtle Pits field and on the very young lavas in the south of the Wideawake Mussel field.

Most lavas are glassy and aphyric without vesicles suggesting that the magmas were undersaturated with volatiles either due to the high water pressure or low volatile concentrations. From the axial seamount and from two locations on the eastern flank of the neovolcanic zone we recovered lavas with large (up to 1 cm) plagioclase crystals. One TV grab station recovered aphyric sheet flows containing abundant gabbroic xenoliths up to 8 cm in diameter with clinopyroxene to 8 mm and slightly smaller plagioclase crystals.

1.4.1.2. Geology and lava petrology of the large volcanic field at 8°50´S

The TOBI sidescan mapping during cruise M62/5A provided structural maps of the MAR between 7 and 12°S. Volcanic features can be very well distinguished and one of the largest and most interesting features in this segment is a volcanic field with a young appearance on the sidescan map. This volcanic field is defined based on a very similar reflectivity that is interpreted as lavas of approximately similar age in an area some 10 km long and 2 km wide. Large parts of the volcanic field consist of flat lava flows but at the western edge two rows of eruption centres are aligned in sigmoidal, about 3 km long lines probably overlying two major feeder dikes for the eruptions. Furthermore, several single volcanic features occur on the volcanic field, most notable being an approximately 50 m high pancake shaped volcano with very steep cliffs. The sidescan map suggested a very young age of the lavas without obvious faults cutting the lavas. However, during the ROV dives we found some cracks and up to 15 m high faults running through the central part of the lava field implying that significant tectonic movements have occurred after ceasing of the volcanic activity, i.e. the segment probably is in a beginning tectonic rather than in a volcanic stage. The lavas are also covered by 1 to 2 cm thick carbonate pteropod/foraminifera ooze, especially in the central part whereas many lavas in the north appear to be less sedimented and younger. This may indicate a variable age of the different parts of the volcanic field.

ROV dives and wax corer from various positions along the volcanic field recovered thirty samples of mostly glassy basalt. We especially sampled different small volcanic cones along the presumed eruption fissure in order to determine the heterogeneity of the erupting magmas. In contrast to the 4°48´S region the predominant lavas in the 8°50´S volcanic field are pillow lavas which appear to cover the central part whereas sheet flows are more abundant in the north. Here we observed frequent changes between pillows and sheet flows during station 159 (dive 44) and we also found collapse structures and lava pillars typical for fast eruptions. Consequently, the eruption volumes and the velocities must have varied with more lava erupting in the north.

1.4.1.3. Geology and lava petrology of the hydrothermal field at 9°33´S

The Lilliput hydrothermal field at about 9°33´S lies in the segment A3 which has a significantly thickened crust of about 11 km thickness based on gravimetric modelling (Minshull et al., 2003). The morphology of the A3 segment is reminiscent of the fast-spreading East Pacific Rise with a neovolcanic zone occurring on a shallow ridge with a narrow cleft rather than in a deep rift typical for the slow-spreading Mid-Atlantic Ridge. The cleft is some 900 m wide and 20 to 30 m deep with an about 10 m high volcanic ridge in the centre. The hydrothermal field lies in a water depth of about 1500 m in a pillow lava flow disrupted by several deep faults striking approximately 345°. South of the hydrothermal field we found very young-looking sheet flow lava flows suggesting that recent volcanic activity occurs in this part of the A3 segment. Possibly, these lava flows represent the heat source for the hydrothermal convection cells. Alternatively, the thick pillow flow itself may have initiated the hydrothermal circulation because hot water was observed to stream out of cracks in large pillows and most of the hydrothermal sediment is Fe-oxide/hydroxide crust.

1.4.2. Description of hydrothermal precipitates

(S. Petersen, H. Paulick)

Hydrothermal precipitates were recovered from the Turtle Pits and Red Lion hydrothermal fields at 4°49'S as well as from the Lilliput hydrothermal field at 9°33'S. The samples consist of massive sulfides, sulfide-oxide-sulfate breccias, and Fe-oxyhydroxides and are described below in detail. Major and trace element geochemical and mineralogical studies will be performed on these samples (S. Petersen, IFM-GEOMAR), as will be sulfur isotopic investigations (H. Strauss, Uni Münster). Selected subsamples were taken for age dating in order to document variations with time (J. Scholten, Univ. Kiel). All samples will be archived at IFM-GEOMAR.

Table 1.1: Hydrothermal precipitates

No.	Date / time	Lat / Long	Depth wire	Comment
Turtle Pits				
114ROV-4	10.04.05/03:55	South Tower 4°48.579'S/ 12°22.420'W	2990 m	Black smoker chimney from SE base of tower (heading 336)
114ROV-5	10.04.05/04:15	South Tower 4°48.579'S/ 12°22.420'W	2990 m	Lower part of structure (heading 294)
114ROV-6	10.04.05/05:00	South Tower 4°48.579'S/ 12°22.420'W	2986 m	Near top of structure at western side (heading 084)
114ROV-7	10.04.05/05:09	South Tower 4°48.579'S/ 12°22.420'W	2986 m	Near top of structure at western side
123ROV-4	11.04.05/13:50	Marker 1 4°48.588'S/ 12°22.414'W	2986 m	Eastern side of Marker 1 chimney, sampled in bionet
123ROV-9	11.04.05/16:50	Pinoccio 4°48.562'S/ 12°22.419'W	2990 m	Small knob on western side of the inactive Pinocchio chimney
124GTV	11.04.05/22:11	4°48.58'S/ 12°22.42'W	2998 m	1000 kg of massive pyrite (inactive chimney) sampled from sheet flow at western edge of the field
130ROV-1	13.04.05/14:39	Mk 2 BS 4°48.573'S/ 12°22.421'W	2985 m	Sampled in bionet during attempt to sample fauna
130ROV-2	13.04.05/14:57	Mk 2 BS 4°48.573'S/ 12°22.421'W	2985 m	Sampled in bionet during attempt to sample fauna
131GTV	13.04.05/21:05	4°48.57'S/ 12°22.37'W	2999 m	Fe-oxyhydroxide stained fresh basalt, plume fallout sampled in graben east of Pinocchio
139GTV	14.04.05/20:17	Mk 2 mound 4°48.573'S/ 12°22.421'W	2985 m	1000 kg of massive sulfide, hematite-magnetite-sulfate material, and chimney debris from western flank of Marker 2 mound
141ROV-6	15.04.05/	4°48.56'S/ 12°22.41'W	2985 m	Six pieces of pyrrhotite-rich chimney material
146ROV-3	16.04.05/20:24	4°47.90'S/ 12°22.62'W	3045 m	Inactive sulfide structure on the way to Red Lion
Red Lion				
146ROV-7	16.04.05/22:57	4°47.82'S/ 12°22.60'W	3048 m	Flange of Shrimp Farm in the Red Lion vent field
Lilliput				
200ROV-5	25.04.05/13:01	9°32.93'S/ 13°12.51'W	1494 m	Fe-oxyhydroxide crusts
200ROV-7	25.04.05/15:48	9°32.88'S/ 13°12.55'W	1495 m	Fe-oxyhydroxide crusts
209GTV	26.04.05/14:53	9°32.86'S/ 13°12.52'W	1511 m	Fe-oxyhydroxide crusts, basalt glass chips and fauna
213GTV	27.04.05/01:58	9°32.83'S/ 13°12.55'W	1513 m	Fe-oxyhydroxide crusts, basalt glass chips and fauna
214GTV	27.04.05/03:55	9°32.84'S/ 13°12.54'W	1511 m	Fe-oxyhydroxide crusts, basalt glass chips and fauna

Turtle Pits area

Station 114ROV:

During this dive chimney samples were recovered from the Southern Tower structure at Turtle Pits. The black smoker samples consist of porous chalcopyrite-rich pieces with minor pyrrhotite and pyrite/marcasite crusts of variable thickness. One sample (114ROV-5) is a larger peace from the trunk of the structure and is characterized by abundant pyrite, chalcopyrite and an anhydrite conduit within the pyrite crust. This seems to indicate that seafloor ingress into the structure is taking place and is channeled within the structure. Sample 114ROV-7 is a small knob of which the core consists entirely of pyrrhotite. A thin crust of pyrite and marcasite is also present. Subsampling: SP=4C1, 4C2, 5B1, 5B2, 5G, 6, 7B; JSch=4B, 5B1, 7B; HS=5, 5C, 5bag, 6, 7

Station 123ROV:

Sample 123ROV-4 was taken on the eastern side of the Marker 1 black smoker complex and is the outer portion of an active chimney (Tmax at this site is close 400°C). The interior of the sample consists of chalcopyrite, pyrite and anhydrite. The outer portion is composed of a 1-5 mm marcasite crust and contains a few cm wide microchimneys on top. Exterior partly oxidized to Fe-oxyhydroxides plus white bacterial-associated globules (sulfur?). Sample 123ROV-9 was sampled at the inactive Pinocchio chimney and is strongly recrystallized. Subsampling: SP=4C1, 4C2, 9/3; JSch=9/3; HS=4A, 4B

Station 124GTV:

This grab was aimed at sampling the sulfide mounds or inactive chimneys at the western flank of Turtle Pits. The target area was approached from the west and the grab was placed on top of a large sulfide boulder. Upon recovery it became evident, that this piece was a block of massive pyrite+/-marcasite with rare black sphalerite. Chalcopyrite is also rare, but slightly enriched in few samples near the interior of the sample. Ribbon texture is abundant in the outer parts of the structure indicating that this chimney was partially characterized by beehive textures. The samples have been grouped according to their texture. More massive samples belong to group 2, while samples characterized by ribbon-like layering were grouped into group 3. Accidently recovered pieces of sheet flow basalt, representing the substrate on which the sulfide block was lying, are group 1. Subsampling: SP=2A2, 2B6, 2C3; JSch=2A3, 2B3; HS=2A6, 2B4, misc.

Station 130ROV:

Few pieces of massive sulfide were co-sampled with the bionet (130ROV-1) and consist of two types of fragments: 1. Chimney interior consisting of anhydrite and chalcopyrite. 2. Chimney crust consisting of pyrite, chalcopyrite and marcasite, partially covered by Fe-oxihydroxides. Sample 130ROV-2 is a hollow chimney structure with 2 cm thick walls of chalcopyrite and marcasite. Interior of the vent (5 x 3 x 2 cm) is lined by 1-3 mm long beautiful bladed pyrrhotite crystals up to 1 mm in diameter. Subsampling: All to SP

Station 139GTV:

The station was targeted at the sulfide mound material of the Turtle Pits hydrothermal field. We approached the area from the west, passed a large boulder that was seen in some of the ROV-dives and placed the grab on the western flank of the Marker 2 mound.

The grab recovered close to 1000 kg of heterogenous sulfide-hematite-magnetite-sulfate material including small relict chimney conduit pipes (group 1), larger chimney pieces consisting of a chalcopyrite-rich interior and variably thick pyrite-marcasite rims (group 2). Sphalerite is a minor component in some of the samples as is late hematite+magnetite occurring as bladed infill in cavities and throughout some of the porous sulfides. Some of the inactive chimneys that were cosampled with the grab are dominated by massive friable chalcopyrite+/-pyrrhotite with only a thin py-mc crusts (group 3). Group 4 consist of gypsum-anhydrite-cemented samples and breccias with varying proportions of hematite, magnetite, chalcopyrite, and pyrite. Group 5 consits of very friable, soft grey material with abundant hematite+/-magnetite with associated greenish to yellow-white clay-like material (group 8). This material may be talc, but only XRD-measurements will prove this. One primary chalcopyrite chimney is characterized by a rim of primary hydrothermal hematite-magnetite separating the interior from the pyrite-marcasite rim (group 6). Some of the anhydrite-cemented samples contain breccias of chalcopyrite conduits (mm to cm-sized) in sulfide sand that resemble conduit breccias in fossil massive sulfide depoits on land (group 7). Subsampling: SP=1A1, 2B2, 2C3, 3C3, 3D2, 3E5, 3H1, 4B2, 4C2, 4D11, 5A2, 5C3, 5D2, 5J2, 6A3, 6B2, 7B4, 7E5; JSch=2B23, 2C3, 3E5, 4D11, 5A2, 5D2; HS=2A3, 2B4, 2C2, 2E2, 2F3, 2G1, 3C1, 4A5, 4C4, 4D2, 4D7, 4G2, 4I, 5E2, 6B3, various gypsum needles.

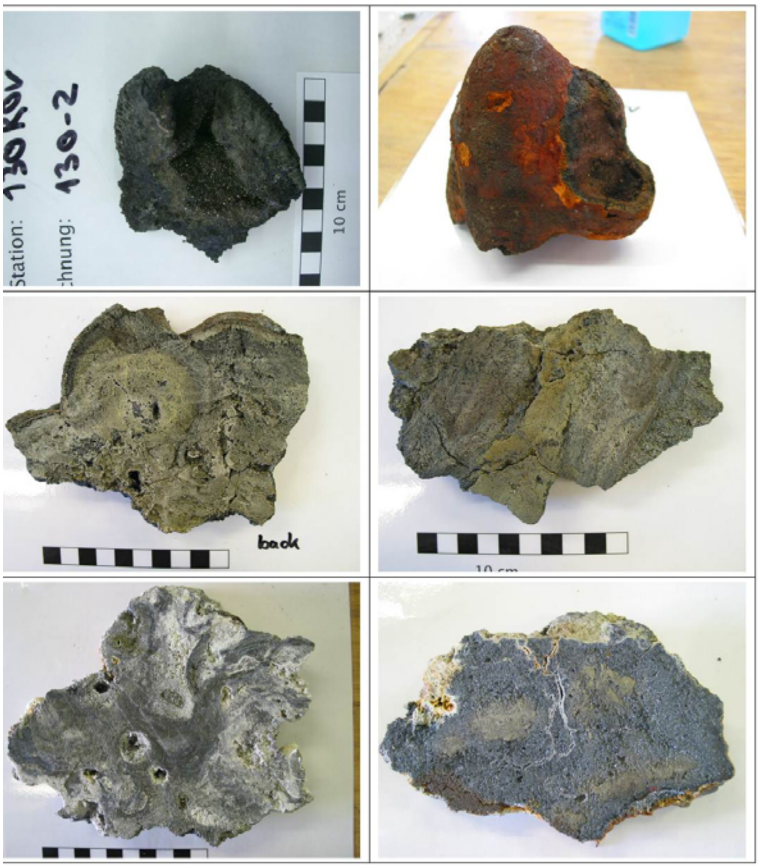

Fig. 1.1 Selected samples from the Turtle Pits hydrothermal field. A) Active chimney conduit with bladed pyrrhotite in the core and a rim of pyrite/marcasite (sample 130ROV-2). B) Inactive chimney knob consisting of a chalcopyrite core, a pyrrhotite-rich zone and an outer rim of pyrite/marcasite stained red by Fe-oxyhydroxides (sample 139GTV-3A). C) Porous inactive chimney composed of pyrite wit a core of chalcopyrite. Multiple growth zones are visible. Late vugs are filled by black sphalerite (sample 139GTV-2F4). D) Massive pyrite cut by dense, recrystallized chalcopyrite. Fractures are lined with grey-metallic hematite-magnetite. E) Massive anhydrite/gypsum breccia with primary clasts of chalcopyrite and abundant grey hematite/magnetite. Individual conduits are lined by gypsum needles (sample 139GTV-4D6). F) Massive hematite/magnetite with relics of chalcopyrite+pyrite. This sample type is characterized by the lack of anhydrite and a clay-like alteration developed as a rim and along fractures (sample 139GTV5A3).

Station 141ROV:

The six pieces from sample 141ROV-6 consists of pyrite-marcasite crust with some chalcopyrite in the interior, which is typically altered (pigeon color). The redbrown outer surface is related to a thin Fe-oxihydroxide coating. One piece with central vug (2 x 3 cm) lined with pyrrhotite + isocubanite(?). Some of the fragments contain 1-3 mm layer of magnetite separating the chacopyrite and pyrite-marcasite zones. Subsampling: All to SP.

Red Lion area

Station 146ROV:

Two sulfide samples were recovered during the transect from Turtle Pits into the rift valley and further north to the Red Lion site. Sample 146ROV-3 is a sulfide knob from an inactive chimney on the way north with a recrystallized interior with irregular cavities lined by sphalerite and chalcopyrite (crystals <1 mm). Bulk of the piece consists of chalcopyrite-marcasite. Crust: 2 mm black Fe-oxihydrixide. One sample was recovered from the Shrimp Farm chimney at the Red Lion hydrothermal field itself. It was sampled at the edge of a large flange and immidiately became a black smoker upon sampling. The sulfide contains abundant sphalerite. Internal cavitiy (2 x 1.5 cm) lined by pyrrhotite (+isocubanite?). A thin crust of pyrite/marcasite is extensively coated by white material (native sulfur?) and orange-brown Fe-oxides. Subsampling: SP=146-3, 146-7; HS=146-3.

Lilliput area

During three TV-grab stations (stations 209GTV, 213GTV, and 214GTV) and one ROV dive (200ROV) hydrothermal Fe-oxyhydroxide-rich crusts were sampled from the Lilliput field. During sampling and upon recovery of the TV-grab it became evident that the Fe-oxyhydroxides are water-saturated muds with only thin crusts. These crusts desintegrated on sampling. In two of the grab stations thin sheets (<<1mm thick) of sulfides (pyrite/marcasite?) appeared. These might be the result of biological. Subsampling: All to SP. One piece of 209GTV to CF.

Fig. 1.2 Fe-oxyhydroxide crusts from the Lilliput hydrothermal field, 9°33'S (sample 209GTV-2).

1.4.3. ROV and OFOS deployments

(H. Paulick, S. Petersen, K. Haase, S. Fretzdorff)

Turtle Pits

The Turtle Pits hydrothermal field is centered at 4°48.58'S / 12°22.42'W in a water depth of 2990 m and occurs within a fracture-controlled small depression. The fracture continues to the north and the south and is marked by aligned collapse pits within sheet flows. The central depression hosting the hydrothermal field is surrounded by sheet flows to the north and to the northwest, whereas jumbled flows are more exposed along the eastern side of the deposit. Turtle Pits itself consists of two mound areas (Marker 1 and Marker 2 sites) composed of sulfide debris with numerous small active black smokers at the top of the mounds (Fig.1.3) A 9.5 m high, active black smoker with vertical walls (Southern Tower) is located to the southeast of Marker 2 mound and is surrounded by a few small diameter black smoker orifice near its base. Two medium-sized inactive black smokers (Pinoccio and Stalagmite) as well as a third, more complex and somewhat older smoker, occur to the north of the active sites, where the central depression narrows to within a few meters. Large toppled chimneys occur to the west of both the Marker 1 and Marker 2 sites, documenting previous periods of hydrothermal activity. Overall the deposit seems to be ~50 in length and up to 30 m wide. Exploration a couple 100 m to either side did not provide evidence for an extension of the deposit. Massive blocks of white (anhydrite-rich?) material are exposed along the northeastern side of the Marker 1 site. Smaller talus blocks of this material are transported into the small graben to the east.

The **Red Lion** hydrothermal field lies ~ 2 km north of the Turtle Pits field and consists of four active chimneys: Shrimp Farm, Zuckerhut, Mephisto, and Tannenbaum. These chimneys are between 4 and 6 m high and sit directly on a pillow lava floor. Three of the chimneys Tannenbaum, Zuckerhut, and Mephisto have a small pedestal of sulfide debris. Small (<0.5 m) inactive chimneys are situated next to Shrimp's Farm and in the vicinity of Zuckerhut. Plume fallout is evident on the pillows in the immediate vicinity of the smoker. Two chimneys, Shrimp Farm and Zuckerhut are characterized by abundant shrimps responsible for the white colour of their tops. The most interesting aspect of these smokers is their flange growth, not commonly reported from seaflooor hydrothermal systems. The conductive cooling of the hydrothermal fluids through the flanges supports a thriving community of shrimp on these two structures. The other two chimneys do not show evidence for flange growth and shrimp are rare.

The distance between these two sites (Turtle Pits and Red Lion) may give evidence for the size of the individual hydrothermal convection cells in the area and provides a tool for the exploration of further sites in similar distance to those two hydrothermal field. This is supported by the discovery of small inactive sulfide deposits in the SW of the deposits suggesting, at least, a potential for additional vent sites in the area.

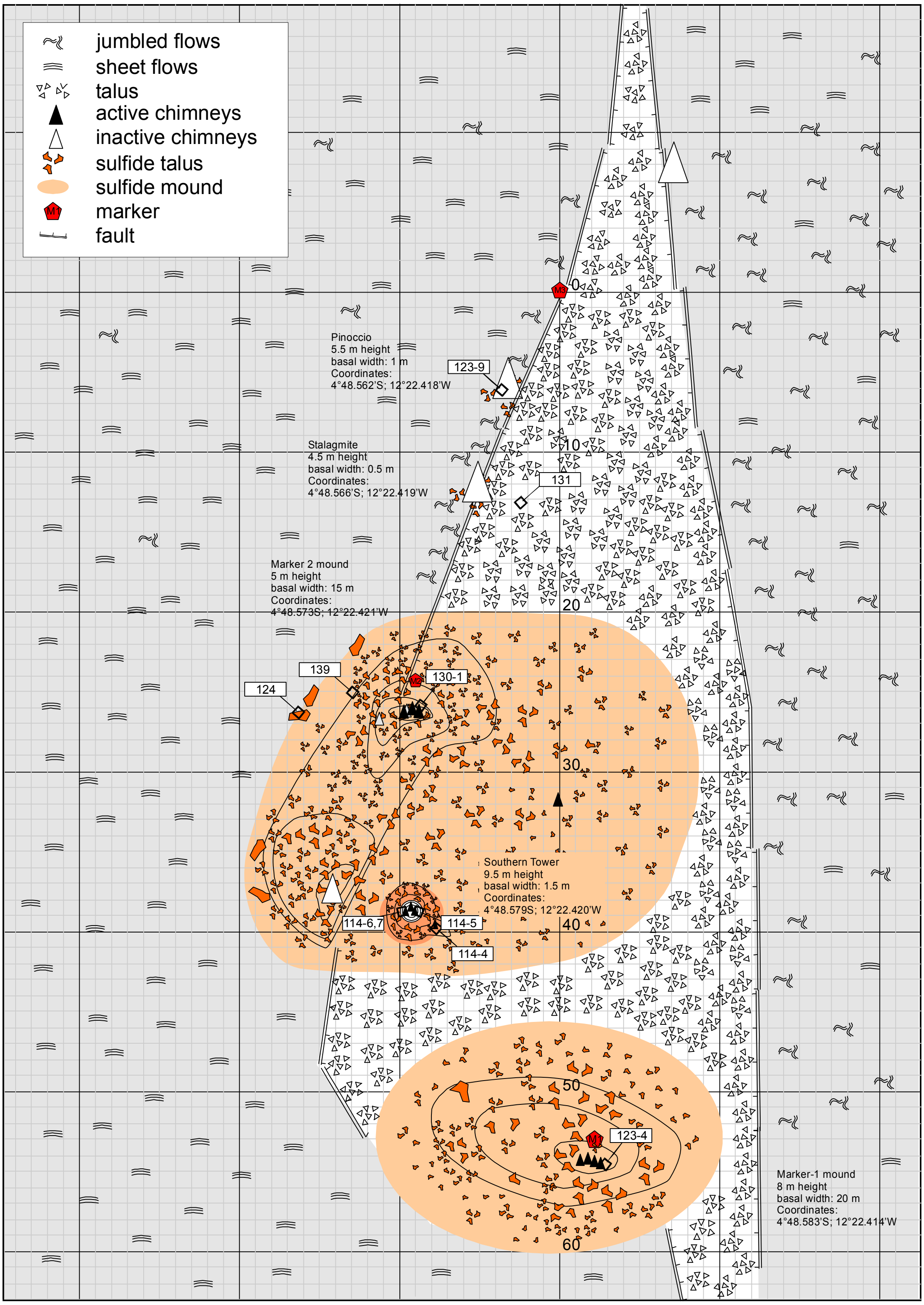

Fig. 1.3 Location of individual chimneys and mounds and geology around the Turtle Pits hydrothermal field, 4°48.58'S. Grid is 10 m.

In addition to detailed investigations of the hydrothermal fields at 4°48'S, several ROV deployments were designed to investigate the volcanic geology of the MAR in detail (eruption-scale). The areas investigated are:

a) the neovolcanic zone between 4°47.76'S (Red Lion) and 4°48.90'S,

b) a „young“ on-axis volcanic center at 8°40’S to 8°50’S (segment A2),
c) the surrounding of the Lilliput hydrothermal field (9°33’S), and
d) on-axis and off-axis volcanic fields in the central A3 segment (9°34.40’S and 9°42.50’S).

Geological maps of these tracks are presented in Fig. 1.4 and in the following the principal observations are summarized.

Neovolcanic zone between 4°47.76’S (Red Lion) and 4°48.90’S

ROV dive 42 (station 146) transgressed ca. 800 m of the neovolcanic MAR at 4°48.90’S which consists mainly of fresh sheet flows including areas with jumbled and lobate flow textures. In contrast, a pillow mound (ca. 30 m high; radius >600 m) in the central portion of this MAR segment is heavily sedimented and locally dissected by tectonic faults indicating a relatively high age. To the north, the neovolcanic zone deepens significantly from 3005 m at 4°48.70’S to 3053 m at 4°47.80’S. Most of this area is dominated by fresh (no sediment cover) jumbled to lobate sheet flows, however, pillow lavas become increasingly abundant to the north. On these pillow flows an inactive black smoker chimney is located at 4°47.90’S and about 200 m further north the active black smokers of the Red Lion hydrothermal field were discovered.

On-axis volcanic center at 8°40’S to 8°50’S (A2 segment)

A relatively young volcanic center was identified in this area of the MAR (segment A2) during Meteor Cruise M62-5 based on side scan images which show highly reflective surfaces undisturbed by tectonic faulting and lineaments defined by coalesced volcanic edifices. The highly reflective surfaces have been interpreted as extensive young lava flows (sheet flows?) fed by voluminous fissure eruptions. Two ROV deployments (dive 43, station 155 and dive 44, station 159) were designed to ground truth these interpretations and obtain eruption scale samples of the basalts.

A 1500 m long transect started in the tectonized western margin of the MAR that consists of pillow basalt and talus breccia. The neovolcanic zone is ca. 900 m wide and characterized by sedimented pillow and lobate flows. The lobate flows are largely restricted to a 350 m wide area that rises by about 20 to 30 m above the surrounding pillow basalts and contact relationships indicate that this structure represents the youngest volcanic eruption. To the east, the terrain is characterized by abundant N-S trending tectonic faults marking the margin of the neovolcanic zone. The basalts sampled during this dive are aphyric to poorly olivine-phyric, providing little petrographic evidence for distinguishing the products of individual eruptions.

To the north, a ca. 1600 m portion of the neovolcanic zone has been investigated during dive 44 (station 159) which crossed a 400 m wide and 50 m high pillow mound. This mound consists of highly plagioclase-phyric basalt (10 vol% plagioclase phenocrysts up to 10 mm) and is covered by a thick blanket of white pelagic sediment that includes local patches of pteropoda shill. Furthermore, colonization by Gorgonaria is also prevalent. In contrast, the aphyric to poorly porphyritic basalt lava flows to the north and south of the pillow mound show only minor biological colonization and variable degrees of sedimentary cover suggesting a younger age. However, contact relationships at the base of the pillow mound are inconclusive in this regard.

Overall, the volcanic plain surrounding the pillow mound is dominated by lobate and ropy sheet flow morphologies including minor intervals with jumbled textures. About 500 m to the north of the mound, a pillow lava flow lacking a sedimentary cover is overlying a jumbled sheet flow. This pillow flow may represent the youngest volcanic eruption in the area.

Lilliput hydrothermal field (9°33'S) and on-axis exploration (9°31.0'S to 9°33.20'S)

The Lilliput hydrothermal field was discovered during ROV dive 47 (Station 200), which was targeted based on CH_4 anomalies in the water column. It consists of abundant, semi-lithified Fe-oxihydroxide accumulations over an area of some 100 x 40 m^2 and mussel colonies at 1495 m water depth that form linear and patchy arrangements following pre-existing cracks and contacts in the underlying basalt pillows. Venting of warm hydrothermal fluids has been observed where cracks within individual pillows and intrapillow space provide primary permeability. Temperatures measured with the sensors mounted on the ROV at a distance of ca. 0.5 m from the vent sites peaked at 5.1 °C.

The Lilliput hydrothermal field (9°32.85'S; 13°13.54'W) is located in the central zone of the neovolcanic MAR. The surrounding area is characterized by fresh, aphyric basalt pillow flows. To the west, there are abundant N-S trending escarpments flanking horst and graben structures. A strongly sedimented pillow mound with abundant Gorgonaria and other biological colonization marks the westernmost location visited during Station 200.

The OFOS track of Station 215 was designed to investigate the neovolcanic zone between 9°31.00'S and 9°33.22'S, an area where substantial CH_4 anomalies have been detected in the water column. In total, 800 images of the seafloor were taken at regular intervals of ca. 30 seconds and a CDT was mounted on the sledge. The entire area to the north of the Lilliput field is dominated by pillow lavas with variable sediment cover and locally abundant cliffs and fissures marking the tectonized western margin of the neovolcanic zone. To the south of the Lilliput field (9°33.00'S to 9°33.22'S) there are fresh pillow basalts and abundant mussels and light gray mats of hydrothermal (?) sediment were discovered at 9°33.20'S / 13°13.51'W (position of Meteor, cable length exceeds water depth by 20 m). This area may be the extension of the Lilliput field along a N-S oriented lineament and represents an important target for further hydrothermal exploration.

On-axis and off-axis volcanic fields at 9°34.40'S and 9°42.50'S (A3 segment)

The central portion of the MAR between the Ascension and Bode Verde Fracture Zones (segment A3) is characterized by shallow water depths (reaching depths <1400 m), the absence of a deep central valley, and numerous off-axis volcanoes concentrated in an area to the east of the MAR (including Grattan Seamount). Two dives were targeted at investigating and sampling the on-axis neovolcanic zone (dive 46, Station 194) and the off-axis volcanic fields (dive 45, Station 188).

The neovolcanic zone at 9°34.38'S consists of about equal proportions of pillow flows and lobate to ropy sheet flows with prominent collapse structures. The basalts are aphyric and biological colonization is rare. The western flank of the active MAR at 13°13.70'W is marked by prominent N-S trending cliffs and the highest point in this area (1427 m) is ca. 50 m above the center of the neovolcanic zone (1470 m). This marginal zone consists exclusively of aphyric pillow basalts with abundant Gorgonaria and other fauna. The glass crusts of these basalts are extensively palagonitized and Mn-oxide/Fe-oxihydroxide coating is common. These observations indicate that the basalts on the western flank are older than the basalts in the neovolcanic zone. The off-axis volcanic fields have been studied at 9°42.50'S in an area located ca. 10 km to the east of the central MAR. Here, 20 to 30 m high pillow mounds are surrounded by extensive plains of white pelagic sediments (foraminiferous ooze) with localized and isolated outcrops of individual pillows and pillow ridges. Furthermore, there are tectonic escarpments with associated talus breccia. The aphyric to poorly porphyritic basalts show extensive palagonitization and coating by Mn-oxides and Fe-oxihydroxides, which, together with the locally abundant biological colonization, indicates that the volcanic activity is relatively old.

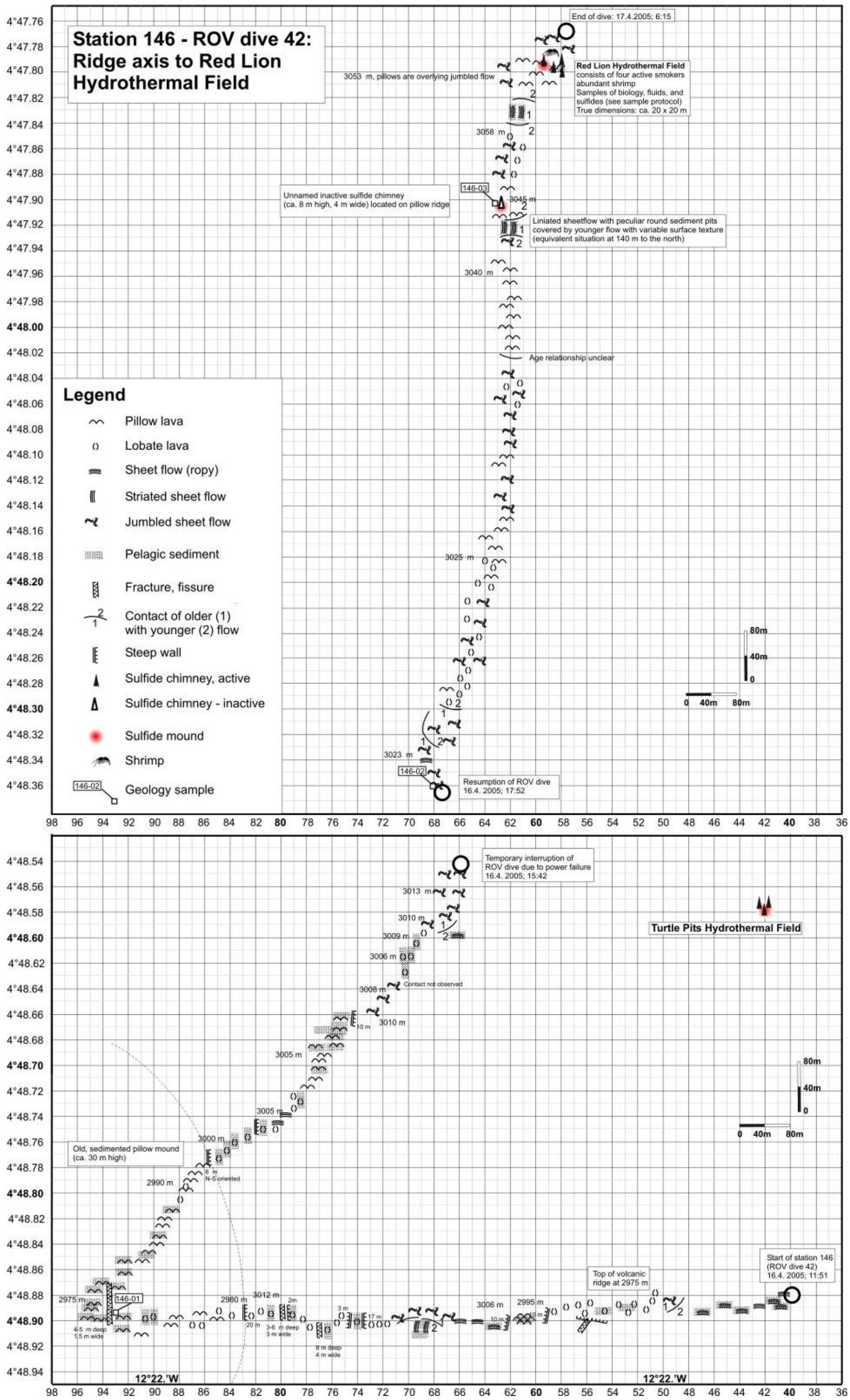

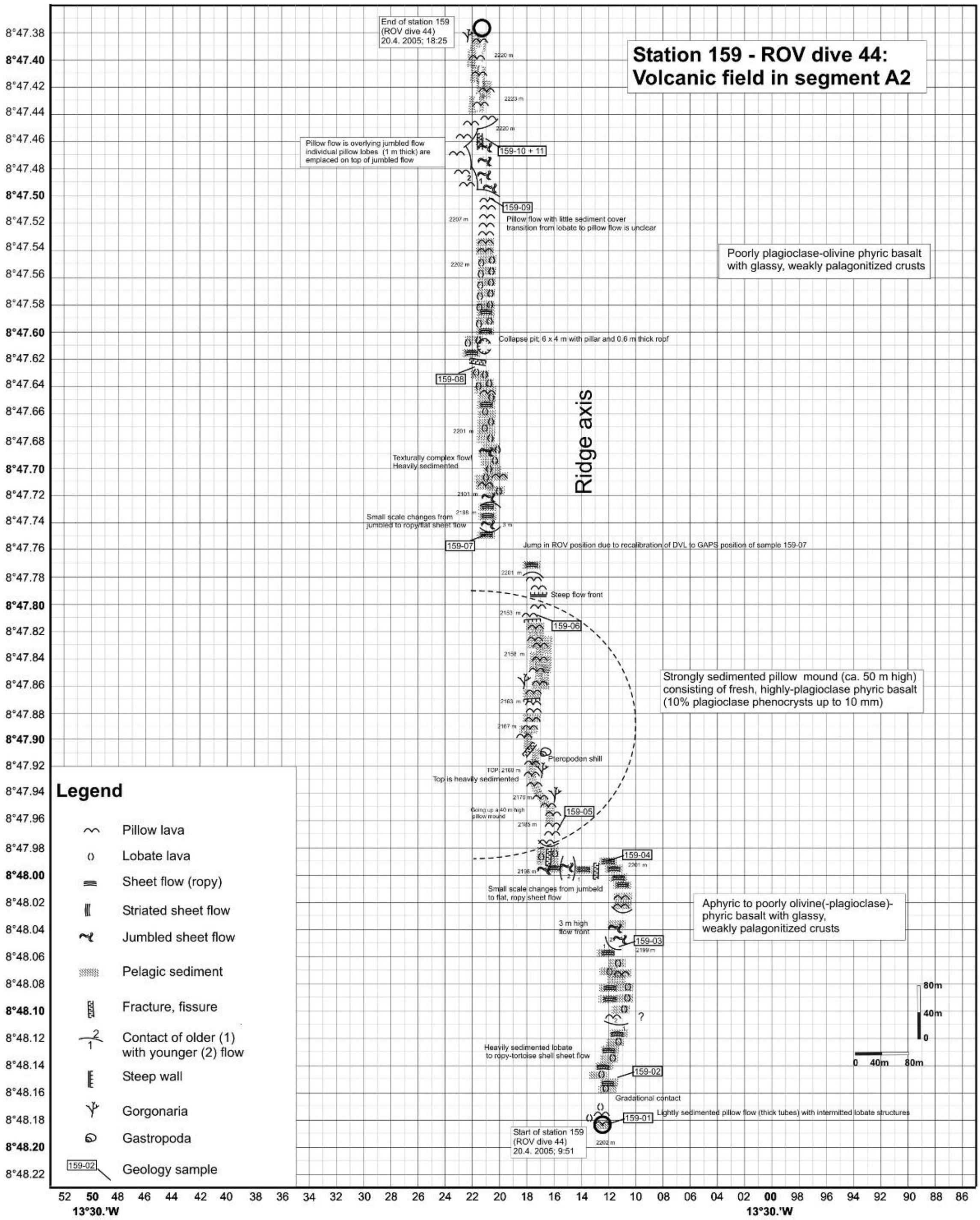
Station 159 - ROV dive 44:
Volcanic field in segment A2
End of station 159
(ROV dive 44)
20.4. 2005; 18:25
Pillow flow is overlying jumbled flow
individual pillow lobes (1 m thick) are
emplaced on top of jumbled flow
159-10 + 11
159-09
Pillow flow with little sediment cover
transition from lobate to pillow flow is unclear
Poorly plagioclase-olivine phyric basalt
with glassy, weakly palagonitized crusts
Collapse pit; 6 x 4 m with pillar and 0.6 m thick roof
159-08
Ridge axis
Texturally complex flow!
Heavily sedimented
Small scale changes from
jumbled to ropy/flat sheet flow
159-07
Jump in ROV position due to recalibration of DVL to GAPS position of sample 159-07
Steep flow front
159-06
Strongly sedimented pillow mound (ca. 50 m high)
consisting of fresh, highly-plagioclase phyric basalt
(10% plagioclase phenocrysts up to 10 mm)
Pteropoden shill
Top is heavily sedimented
159-05
159-04
Small scale changes from jumbeld
to flat, ropy sheet flow
Aphyric to poorly olivine(-plagioclase)-
phyric basalt with glassy,
weakly palagonitized crusts
3 m high
flow front
159-03
Heavily sedimented lobate
to ropy-tortoise shell sheet flow
159-02
Gradational contact
159-01
Lightly sedimented pillow flow (thick tubes) with intermitted lobate structures
Start of station 159
(ROV dive 44)
20.4. 2005; 9:51
Legend
Pillow lava
Lobate lava
Sheet flow (ropy)
Striated sheet flow
Jumbled sheet flow
Pelagic sediment
Fracture, fissure
Contact of older (1)
with younger (2) flow
Steep wall
Gorgonaria
Gastropoda
Geology sample
13°30.'W

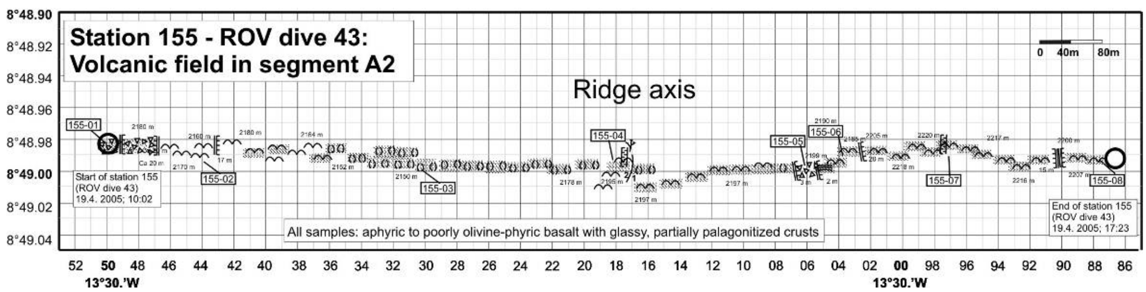
Station 155 - ROV dive 43:
Volcanic field in segment A2
Ridge axis
155-01
Start of station 155
(ROV dive 43)
19.4. 2005; 10:02
155-02
155-03
155-04
155-05
155-06
155-07
155-08
End of station 155
(ROV dive 43)
19.4. 2005; 17:23
All samples: aphyric to poorly olivine-phyric basalt with glassy, partially palagonitized crusts
13°30.'W

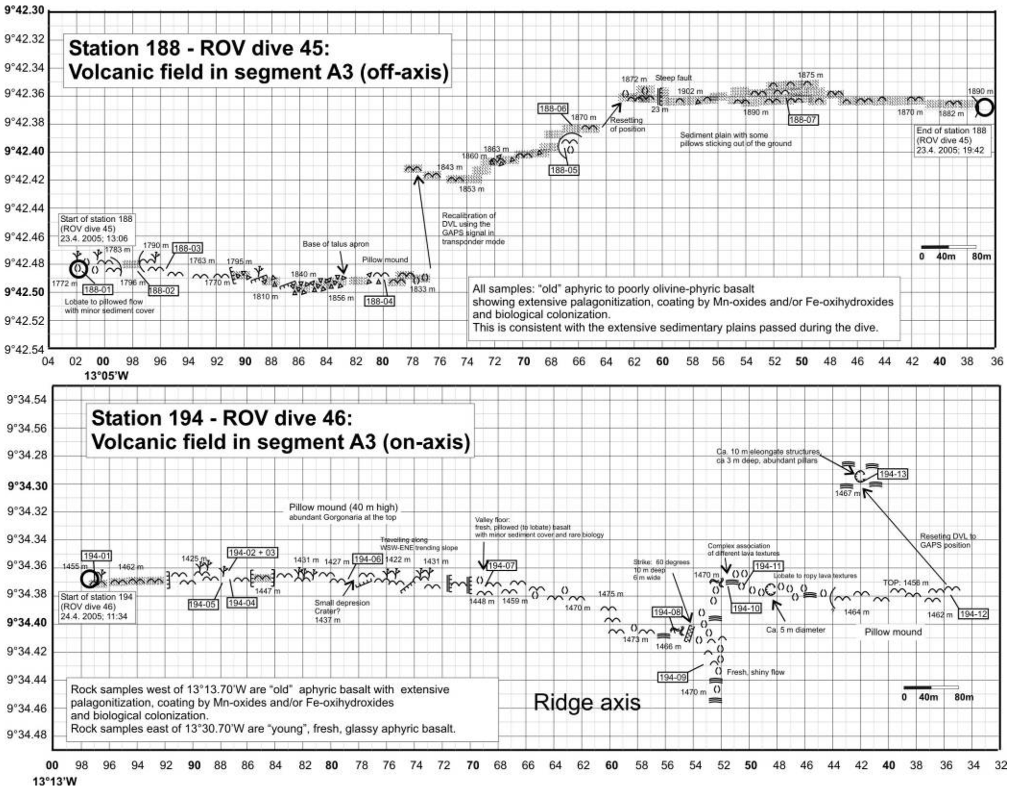

Fig. 1.4 Geology of ROV and OFOS tracks

1.4.4. Fluid Chemistry

(A. Koschinsky, H. Marbler, C. Ostertag-Henning, H. Strauss, U. Westernströer)

Hydrothermal fluids are characterized by their unique chemical and isotopic composition, which is significantly different from ambient seawater (e.g., van Damm, 2004). Scientific objectives for fluid chemical analyses, both on-board and subsequently in the home laboratories, include the detection of hydrothermal plumes in the water column and a quantification of the chemical and isotopic composition of hydrothermal fluids discharging from the ocean crust via distinct vent sites (either through black smokers or diffuse venting).

Three different types of samples were collected for chemical and isotopic analyses: water column samples from the CTD/Rosette, equipped with 24 bottles à 10 l volume; samples from discharging vent sites collected with three Niskin flasks (5 l volume), mounted at the front of the MARUM ROV QUEST; vent fluid samples collected with the new Kiel Pumping System (KIPS: 15 bottles à 675 ml) by inserting a titanium sampling nozzle into the orifice of smoker structures.

1.4.4.1. Fluid Sampling System for MARUM ROV QUEST

For sampling of hydrothermal fluids directly at the vent sites, a pumped flow-through system (Kiel Pumping System, KIPS) mounted on the ROV's starboard back side (Fig. 1.5) was used.

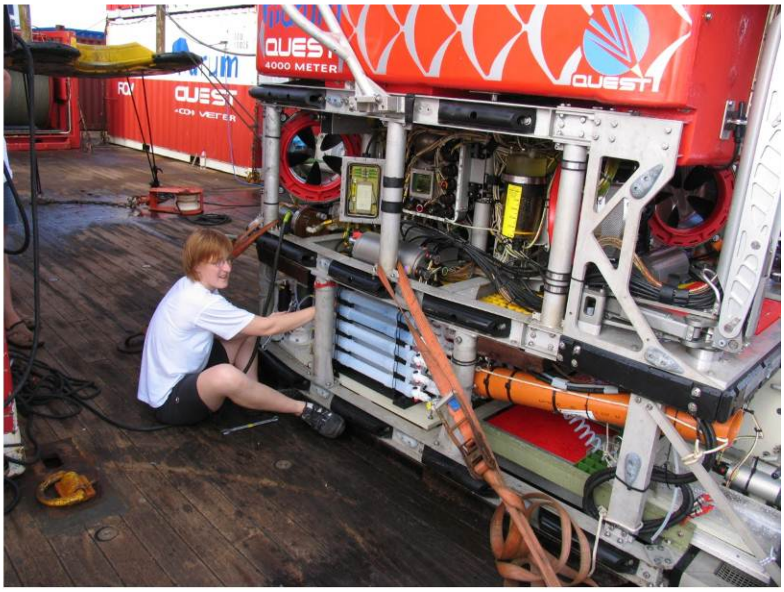

Fig. 1.5 The fluid sampling system "KIPS" mounted on the starboard back side of the Bremen MARUM ROV ("Quest") tool sled

The system was newly constructed and entirely made of inert materials (Teflon, titanium). Samples are collected via a titanium nozzle of 50 cm length which can be directly inserted into the vent orifice by the ROV`s manipulator arm. Parallel to the nozzle is a high-temperature probe measuring the *in situ*-sampling temperature. PFA tubing connects the nozzle to a 18 position-multiport valve motorized by a ROV actuator (SCHILLING, U.S.A) (Fig 1.6). The valve distributes the sample to max 15 individual PFA Teflon flasks with 675 ml volume each. Each bottle is equipped with all-Teflon checkvalves at inlet and outlet. All sample bottles are mounted in three racks A, B, C, with every rack containing five horizontally positioned bottles. For sub-sampling the three racks were transferred to the laboratory. A deep sea pump is mounted downstream to the sample bottles. The system is fully remotely controlled via the ROV control desk.

The system is modular in such a way that a number of bottles can be filled separatedly or interconnected in-line according to the needs of both sample volume and number of samples (c.f., leg M64/2). During leg M64/1 five sample flasks were filled at every sampling location, thus, resulting in sufficient fluid volume (3.4 l) in order to study all aspects of fluid chemistry and dissolved gas composition on sub-samples that are as identical as possible. The bottles were pre-filled with freshwater or seawater. To assure the complete exchange of pre-filled water with sample fluid the total pumping time for 5 in-line bottles was determined experimentally. A total pumping time of 1 hour was applied during the cruise.

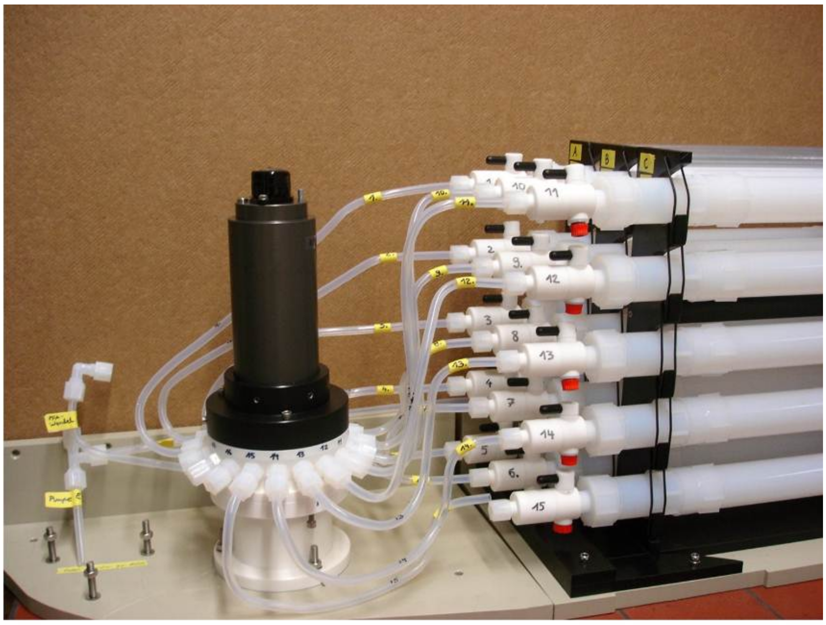

Fig. 1.6 Details of the Kiel fluid sampling system showing actuator-driven PETP multiport valve (left) and PFA tubing to 15 PFA Teflon sampling flasks in 3 racks A, B, C

1.4.4.2. Fluid Sampling and Sample Preparation

Water Column Samples

Based on the depth profiles for temperature, salinity and light transmission, samples were collected at different depths with the CTD/Rosette system, covering the vertical distribution of the hydrothermal plume. Sampling of these waters was performed directly after recovery of the CTD/Rosette system.

Immediately after sampling, pH and Eh were measured. Subsequently, and depending upon future chemical analyses, non-filtered subsamples (with aliquots either non-acidified or acidified to a pH of 2 with suprapure HCl) were stored at 4°C.

Barium sulphate was precipitated from sample aliquots (addition of barium chloride solution at pH 2) for measuring the sulphur and oxygen isotopic compositions of dissolved sulphate. For selected CTD stations, untreated water samples were collected for measuring the oxygen and hydrogen isotopic composition of these waters.

For the CTD stations in the vicinity of the Turtle Pits, Wideawake Mussel Field and Red Lion hydrothermal fields, samples throughout the water column have been collected for the analysis of amino acids in the dissolved and particulate organic material. Water samples were filtered through GF/F glass fibre filters and the filters wrapped in aluminium foil and frozen at -20°C. The organic compounds in the filtrate were concentrated by means of solid phase extraction onto C18 and SCX phases and subsequently stored at -20°C. For selected profiles throughout the water column an aliquot of the samples has been frozen at -20°C for later analysis of the ammonium concentration and its nitrogen isotopic composition.

Vent Fluid Samples

Immediately after recovery of the ROV, all three Niskin flasks (N1, N2, N3) and all bottles from the KIPS were sub-sampled. On small aliquots (20 ml), ph and Eh were measured directly after sampling for all samples.

Aliquots were sub-sampled for the following chemical and isotopic analyses: major and trace elements, selected anions, methane and hydrogen (abundance and isotopic composition), sulphate and sulphide sulphur isotope geochemistry, dissolved inorganic carbon (abundance and isotopic composition), amino acids, ammonium (abundance and nitrogen isotopes).

Unfiltered sample aliquots were collected for gas chemistry, for analyses of dissolved sulphide, for dissolved inorganic carbon, for amino acid analyses, and for ammonium measurements. Similarly, unfiltered water was sub-sampled for microbiological work.

For all other chemical analyses, fluid samples were pressure-filtrated with Nitrogen (99.999%) at 0.5 bar through pre-cleaned 0.2 µm Nuclepore PC membrane filters by means of polycarbonate filtration units (Sartorius, Germany). The filtrates were separated into aliquots for voltammetric and ICP analyses and acidified to pH 1 with 100 µl subboiled concentrated nitric acid per 50 ml (ICP) and with suprapure HCl to pH 2 (voltammetry), respectively. For selected samples, about 150 ml of fluid were filled into specially pre-cleaned bottles and immediately deep-frozen at -20°C. These samples are shipped in frozen state for the determination of organic metal complexation in the home laboratory of the project partner Dr. Sylvia Sander (University of Otago, New Zealand). Some representative samples were deep-frozen or poisoned with $HgCl_2$, respectively, as conservation for organic analyses in the home laboratory.

Procedural blanks were processed in regular intervals. All work was done in a class 100 clean bench (Slee, Germany) using only all-plastic labware (polypropylene, polycarbonate, PFAteflon). Rinse water was ultrapure (>18.2 Mohm), dispensed from a Millipore Milli-Q system.

A total of 227 water column samples, 26 bottle samples from the fluid sampling system, and 17 Niskin samples were collected. After return to the home labs, in Kiel selected samples will be analysed for major (Mg, Ca, Ba, Sr, Na, K, Si, Fe, Mn, B, Cl) and trace element composition (e.g., I, Br, Li, Al, Cs, Ba, Sr, Y-REE, Fe, Mn, Cr, V, Cu, Co, Ni, Pb, U, Mo, As, Sb, W, PGE) by ICP-OES (Spectro Ciros SOP CCD) and ICP-MS using both collision-cell quadrupole (Agilent 7500cs) and high-resolution sector-field based instrumentation (Micromass PlasmaTrace2).

At IUB in Bremen, voltammetry will be used for further trace metal analyses (Zn, Cd, Pb, Cu, Co, Ni, Ti, V, Mo, U, Tl, Pt). ICP-MS and ICP-OES measurements of minor elements and trace metals (see above) will be carried out as well for interlaboratory comparison. Li and Na will be analysed by flame photometry, and photometric methods will be used to determine anionic compounds (silicate, phosphate, sulfate, chloride). The duplicate coverage of some elements with different methods will be used for the evaluation of the methods and the data. The determination of organic complexation of Fe, Cu, and Zn (S. Sander, Univ. Otago) will be done by voltammetric ligand titration.

At the Westfälische Wilhelms-Universität Münster, sulphur (sulphides, sulphates), oxygen (sulphates, fluid samples), and hydrogen (fluid samples) isotope measurements will be performed.

At the Bundesanstalt für Geowissenschaften und Rohstoffe (BGR) in Hannover the amino acid concentrations (HPLC-FD) and their racemization (GC-FID) as well as their isotopic composition (GC-irmMS) will be analysed for selected samples. Additionally, the ammonium concentration and its nitrogen isotopic composition will be investigated. For a set of samples the concentration and carbon isotopic composition of the dissolved inorganic carbon will be analysed by a Finnigan Gasbench-Delta Plus-MS coupling.

1.4.4.3. On-board analyses

pH and Eh Measurements

For all samples collected with the CTD/Rosette, the Niskin flasks and the Kiel Fluid Pumping System, pH and Eh measurements were performed on unfiltered sample aliquots immediately after sampling. Measurements were carried out with WTW electrodes (Ag/AgCl reference electrode).

Chloride Titration

In order to determine whether or not phase separation affected the chemical composition of the hydrothermal fluids, respective fluid samples collected during ROV dives, either with Niskin bottles or with the Kiel Fluid Sampling System, were subjected to chloride concentration analysis. Measurements were performed as titration with 0.1 mM $AgNO_3$-solution, using fluorescene-sodium as the indicator. For reference, samples from a water column profile were also analyzed.

Photometric Determination of Dissolved Inorganic Silica

Silica tends to be enriched in hydrothermal fluids (e.g., van Damm, 2004). Hence, fluid samples and selected CDT/Rosette water column samples were analyzed for their abundance of dissolved silica. The analysis of dissolved silicon compounds in seawater and hydrothermal fluids is based on the formation of α-silicomolybdic acid via complexation of the dissolved silica with ammoniumheptamolybdate (e.g., Grasshoff et al., 1999). Concentration measurements were performed with a biochrom Libra S12 spectral photometer at an extinction of 810 nm. Silica contents in water column samples were measured both in filtered and non-filtered samples. No significant difference was detected.

Photometric Determination of Iron Concentrations

The principle of this method is the determination of an orange-red ferroin complex, which is formed by Fe(II) ions in the fluid sample with 1,10-phenantroline in a pH range of 3-5. In addition to a quantification of Fe(II), it is also possible to measure the Fe_{tot} fraction in the sample by reducing all Fe with ascorbic acid. Fe(III) is determined as difference between Fe_{tot} and Fe(II). Analyses were carried out with a biochrom Libra S12 spectral photometer and the absorption was measured at 511 nm. Fe concentrations were measured only in filtered samples of hydrothermal fluids. The detection limit is about 0.1 ppm. Samples with concentrations above 100 ppm were measured in diluted samples.

Voltammetric Determination of Trace Element Concentrations

For onboard sulfide and trace metal concentration analyses, the electrochemical method of voltammetry was used. Voltammetry is able to differentiate between different redox species and (in combination with UV digestion of the water samples) free and complexed forms of ions in solution and is highly sensitive. All the voltammetric measurements were performed using a Metrohm system comprising a 757 VA Computrace run with a standard PC, an 813 Compact Autosampler and two 765 Dosimats. The three-electrode configuration consisted of the multi-mode electrode (MME) as the working electrode, an Ag/AgCl reference electrode (3 mol l^{-1} KCl), and a platinum wire as the auxiliary electrode.

Immediately after recovery, the unfiltered fluid samples were analysed for total dissolved sulfide in alkaline solution using the method after Metrohm Application Bulletin 199/3e. Filtered aliquots were submitted to a digestion process in a UV Digestor (Model 705, Metrohm), which contains a high pressure mercury lamp (500 W), decomposing organic metal complexes. After 1 hour UV irradiation, the total content of Fe and Mn in all samples and of Zn, Cu, Cd, and Pb in selected samples were determined by the standard addition method. For Fe, the highly sensitive cathodic stripping voltammetric method of Obata and van den Berg (2001) using 2,3-dihydroxinaphthalene as complexing agent was applied in samples with low Fe concentrations, while photometry was used for samples with high Fe concentrations (>0.1 ppm). Mn concentrations were determined using anodic stripping voltammetry in an alkaline ammonia buffer solution (Locatelle and Torsi, 2001). For Cu, Pb, Cd, and Zn analyses samples were buffered at pH 4.6 with 1 M acetate buffer solution and measured by ASV (Application Bulletin Metrohm 231/2).

1.4.4.4. Results from On-Board Analyses

Vent Fluids

The chemical and isotopic characterization of hydrothermal vent fluids is strongly dependent upon the sampling procedure. Dilution with ambient seawater is always likely. In order to qualitatively assess the contribution from seawater, a number of analytical parameters, such as Eh, chloride have been measured on-board. A final quantification of the fluid contribution from a hydrothermal source will be performed by using Mg concentrations (hydrothermal endmember Mg = 0, seawater endmember Mg = 55 mM). These will be measured in the home laboratory.

The pH and Eh measurements for the samples collected directly at the vent sites during ROV deployments clearly reflect the mixture of hot reducing hydrothermal endmember fluid and oxic seawater. Lowest values for the hydrothermally purest samples were 3.83 for pH and –260 mV for Eh. A crossplot of respective data (Fig. 1.7) allows a clear distinction between hydrothermal fluid and seawater. Most extreme values have been measured for samples from the Turtle Pits area (ROV stations 141 and 146). Results obtained from Niskin flask samples are somewhat in between both endmembers, i.e. reducing hydrothermal fluid and oxidized seawater.

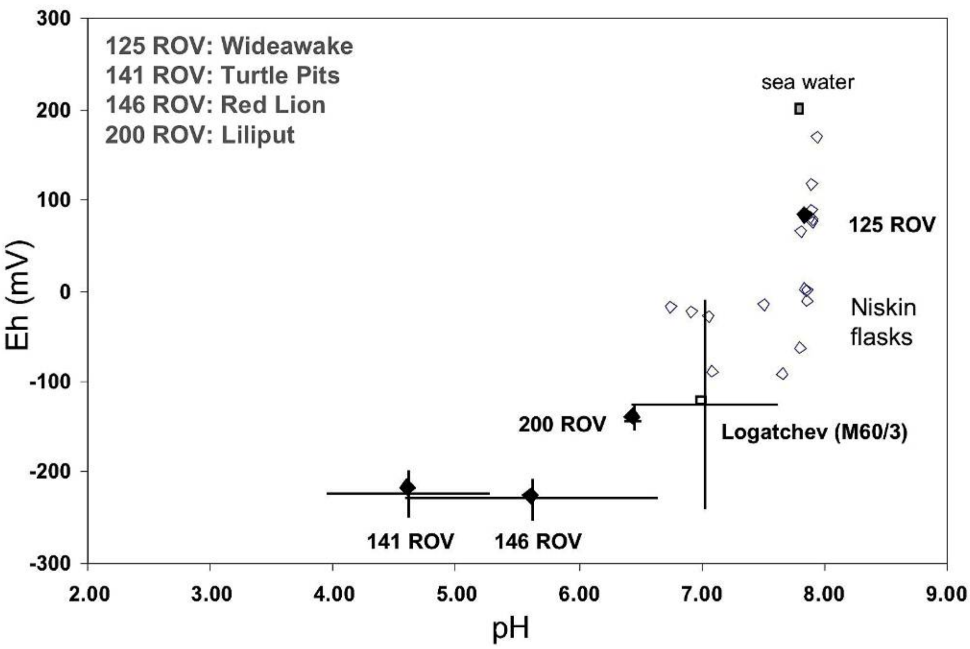

Fig. 1.7. Crossplot of pH and Eh for fluid samples from Niskin flasks and KIPS bottles

Measured sulfide concentrations were less than 1 mg/L in all samples, which may be partly due to the loss of free sulfide through Fe sulfide precipitation during cooling of the hydrothermal fluids. Chloride titrations indicated that the hot vents from the Turtle Pits field have significantly reduced chloride concentrations (minimum value at 13.52 mg/L) compared to a background seawater value of 21.0 mg/L. This clearly indicates that the fluids are phase-separated and that the samples represent the vapor-type phase. Silica is up to 200fold enriched over an average seawater concentration of about 1 mg/L. Si enrichment is typical for hot hydrothermal fluids (as exemplified by samples from ROV stations 141 and 146) due to intensive water-rock interaction. The same applies to Fe and Mn, having highest concentrations of dissolved total Fe of up to 105 mg/L, of which more than 80 % were found to be Fe(II), and up to 0.9 mg/L Mn. It has to be noted that the endmember concentration of Fe, including all Fe bound in the sulfide particles, is significantly higher, but can only be determined later in the home laboratory. Very low concentrations of dissolved Zn (max. 30 µg/L), Cu (max. 7 µg/L), Pb, and Cd were detected, indicating that most of these chalcophilic elements, which are typically enriched in hydrothermal fluids, are strongly bound into the precipitating sulfide particles, parallel to Fe.

Diffuse vent fluids collected from the Lilliput hydrothermal field at 9°33’S are characterized by moderate enrichment of elements that were found to be high in the hot fluids, confirming their mixed fluid – seawater character. They were also significantly reducing (Eh of -137 mV) with slightly lowered pH (6.5).

Water Column Profiles

As Eh measurements are a fast and relatively simple analytical tool, they were used as the first measurement following the recovery of CTD water column samples in order to search for hydrothermal plume indications. For several stations, Eh minima clearly correlate with maxima of other hydrothermal tracers analysed, such as methane, hydrogen, Mn, and Fe concentrations (Fig. 1.8). However, especially when the plume signals were not very pronounced, Eh anomalies were less pronounced or absent. Mn and Fe, were both detected in concentrations significantly above ambient seawater background in samples with very high methane and hydrogen concentrations and from the depth range with high turbidity values. In contrast, respective enrichments could not be detected in samples with lower gas concentrations. This observation can be used as an indicator for the proximity of the source, because the CH_4/Mn or CH_4/Fe ratios typically increase away from the plume due to metal oxidation and particle fallout. As Fe and Mn were determined in unfiltered samples, the data represent total dissolvable concentrations.

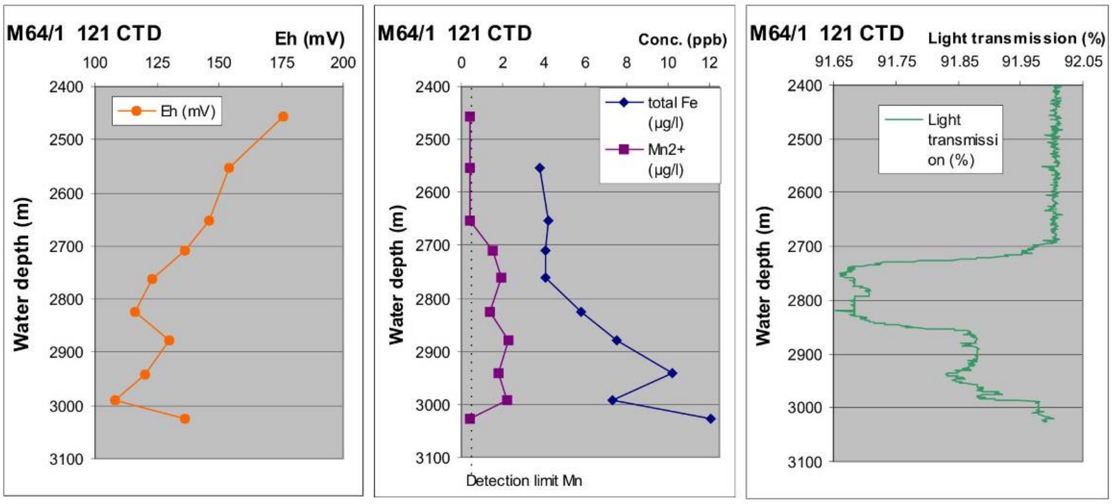

Fig. 1.8 Water column profiles of hydrothermal tracers, indicating the existence of a hydrothermal plume between 2700 and 3000 m water depth at 5°S

1.4.5. Dissolved Gases and Carbon Species

(R. Seifert, S. Weber, M. Warmuth)

1.4.5.1. Introduction

Objective of the work during M64/1 was to localise and characterise hydrothermal fluids and plumes using *in situ* sensors (CTD with sensors for redox and light transmission) and applying on board analytical techniques to determine concentrations of dissolved reactive gases (CH_4, H_2). To elucidate the transformation of carbon species and reduced gases brought along by hydrothermal fluids, a comprehensive set of samples was secured for on shore analysis of stable isotope contributions (H, C, He) of fluid components. Subjects of the study were hydrothermal fluids and plumes of two areas along the MAR - Red Lion / Turtle Pits / Wideawake (04°48'S), and the Lilliput hydrothermal field (9°33'S) with the latter discovered during this cruise.

For this purpose 39 stations were sampled by CTD/Rosette and a total of 252 water samples were obtained from these CTD stations and 6 ROV stations.

1.4.5.2. Samples and Methodology

CTD data were recorded using a SEABIRD CTD Type 911 equipped with a Eh sensor (AMT series 40) and a sensor for light transmission as well as a rosette of 24 10L Niskin bottles. Water samples were taken during lifting keeping the sampler at a certain depth for a short time. A total of 39 stations were performed of which only did failed to yield data. At 107 CTD misfunction of the temperature sensor occurred at about 1100 m water depth caused by seawater entrance at the connection to the data transfer unit. The problem could easily be solved. Data of station 129 CTD were lost by a problem with data recording system on deck. For all other stations data could be recorded and saved for the entire water column.

Light dissolved hydrocarbons were analysed on board applying a purge and trap technique (Seifert et al., 1999). The water sample is stripped by He and analyses in the outflowing gas stream are concentrated in cooled traps at -84°C. After degassing, the trapped gases are released to a gas chromatograph (CARLO ERBA GC 6000) equipped with a packed (activated Al_2O_3) stainless steel column and a flame ionisation detector (FID) to separate, detect and quantify individual components. Recording and calculation of results is performed using a PC operated integration system (BRUKER Chrom Star). Analytical procedures were calibrated daily with commercial gas standards (LINDE). Analyses were generally done within 12 hrs after sampling.

For on board *measurements of dissolved hydrogen* up to 615ml of sample is connected to a high-grade vacuum in an ultrasonic bath and heated until boiling. Aliquots of the released gas are transferred via a septum from the degassing unit into the analytical system. A gas chromatograph (THERMO TRACE) equipped with a packed stainless steel column (Molecular sieve 5A, carrier gas: He) and a pulsed discharge detector (PDD) is used to separate, detect and quantify Hydrogen. Recording and calculation of results is performed using a PC operated integration system (THERMO CHROM CARD A/D). Analytical procedures were calibrated daily with commercial gas standard (LINDE).

For on shore measurements of the *He concentrations and isotopic signature*, water samples were taken immediately after finishing the respective station. The samples were sealed head space free and gastight in copper tubes. Measurements will be performed at the Universität Bremen, Fachbereich 1 (Tracer Oceanography).

Samples for the determination of *$\delta^{13}C$ of the dissolved light hydrocarbons* were obtained by degassing the water samples with a vacuum - ultrasonic technique (see above). Aliquots of the released gas were transferred via a septum from the degassing unit into, gastight glass ampoules filled with NaCl-saturated water for later on shore analysis by GC-Isotope-Ratio-Mass-Spectrometry.

For on shore analysis of *stable carbon isotopes of dissolved inorganic carbon (DIC)*, aliquots of unfiltered sample was spiked with NaOH and BaCl2 directly after recovery to precipitate carbonate species. The analyses of δ^{13}C-DIC will be made by Dual-Inlet-Isotope-Ratio Mass-Spectrometry (THERMO MAT 252).

For on shore analysis of *stable isotopes for dissolved hydrogen*, up to 10mL of gas obtained by vacuum/ultrasonic degassing of sample was frozen on molecular sieve 4A under liquid nitrogen in a pre-vacuated glass vial. The samples will be analysed via a molecular sieve 5A PLOT column and a GC-Isotope-Ratio-Mass-Spectrometer for δ^2H-vlues.

To obtain an overview on the organic components contained in the hydrothermal fluids, selected samples were treated by Solid Phase Extraction (SPE).

1.4.5.3. Results

For the first working area (Turtle Pits, Red Lion, Wideawake) Most CTD profiles obtained in revealed imprints of hydrothermal activity within the water column by anomalies in the transmission profiles and ST diagrams (salinity versus potential temperature). These anomalies were present at a water depth range from 2700 to 3000m (Fig. 1.9). The S/T plots evidence the intrusion of a component relatively depleted in salinity.

Results for concentrations of dissolved methane and hydrogen obtained from CTD/rosette samples on board RV METEOR revealed hydrothermal signatures within the same depth range but do not correlate well with each other and the observed light transmission anomalies (Fig. 1.9).

Samples obtained by ROV directly at the fluid emanations revealed very high concentrations of dissolved hydrogen and Methane. Maximum concentrations found accounted for 0.29 mmol L^{-1} and 0.02 mmol L^{-1} of hydrogen and methane, respectively. The sample was obtained by putting the tip of the fluid sampling system directly into the outlet a black smoker vigorously exhaling boiling fluid (Station 41 ROV; Turtle Pits). The resulting H_2/CH_4 ratio of about 14.7 (Fig. 1.9), that is also found in water samples taken by ROV-based Niskin bottles in the vicinity of the smoker, even exceeds those we found for fluids of the Logachev field (see Table 1.2). A higher ratio is so far only reported for fluids obtained at the EPR at 21°N (Welhan & Craig, 1979). A fluid sample recovered from a black smoker within the Red Lion hydrothermal field (146 ROV) revealed H_2/CH_4 ratio of about 3 with concentrations of CH_4 and H_2 of 26 µmol L^{-1} and 75 µmol L^{-1}, respectively. More precise data on the differences of gas concentrations will only be available after having determined the fluid – seawater mixing ratios. The two sampling locations are about 2 km apart and harbour considerably different vent faunas. More information on the factors holding responsible for the different fluid compositions are expected from on shore analyses of stable isotope signatures and trace metal content. However, the data already available illustrate the presence of compositional distinct black smoker vent fluids and faunas within a relatively narrow area at 04°48’S.

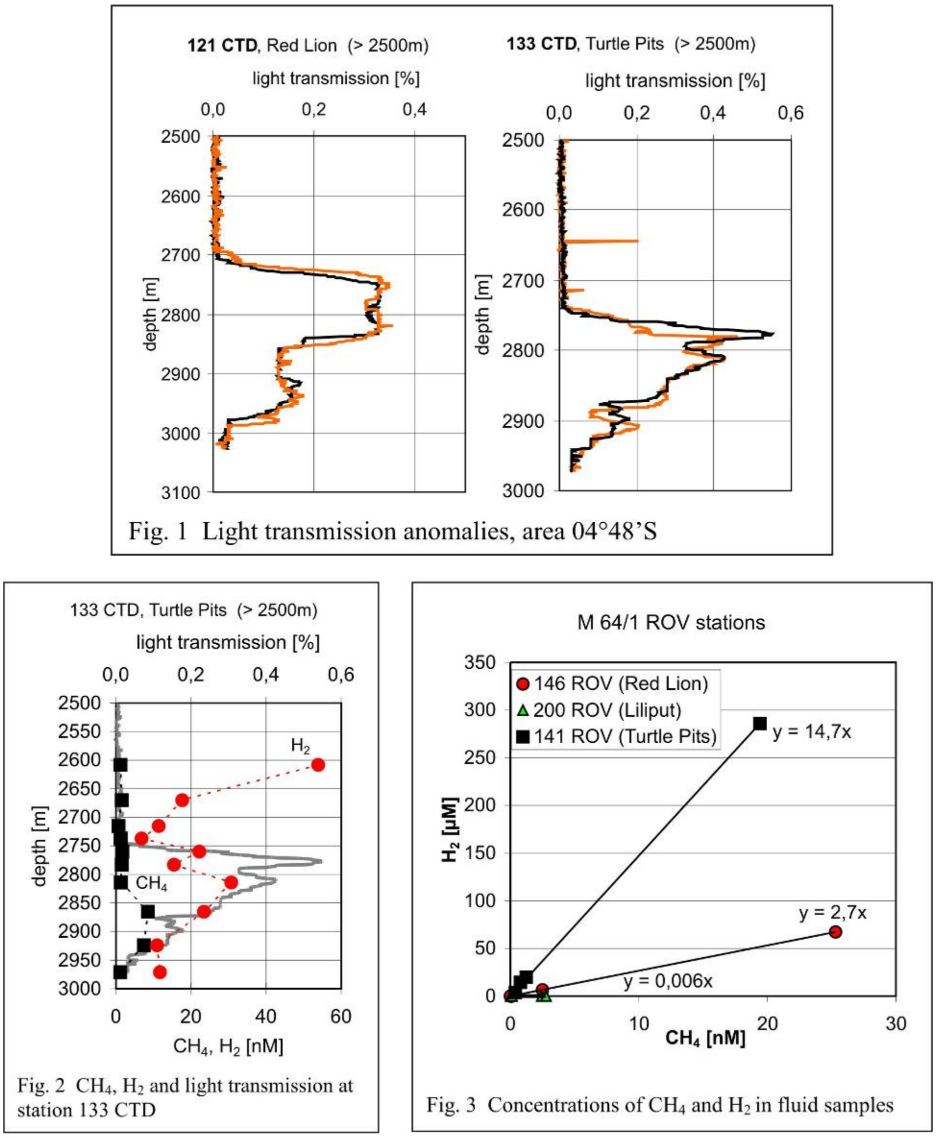

Fig. 1 Light transmission anomalies, area 04°48'S

Fig. 2 CH_4, H_2 and light transmission at station 133 CTD

Fig. 3 Concentrations of CH_4 and H_2 in fluid samples

Fig. 1.9 Light transmission and methane and hydrogen concentrations in selected water profiles and samples.

Table 1.2 CH_4 and H_2 concentrations found in MOR hydrothermal fluids. Note that all data refer to endmembers except those printed in bold (M64/1).

	H_2 [mmol L^{-1}]	CH_4 [mmol L^{-1}]	H_2/CH_4 molar ratio	ref.
Atlantic				
Peridotitic host rocks				
Rainbow 36°14'N, MAR	13, 16	2,5	5.2-6.4	1, 2
Logachev 15°N, MAR	12	2.1	5.7	2, 13
Basaltic host rocks				
Broken Spur 29°N, MAR	0.43 – 1.03	0.07 – 0.13	6.6 – 7.9	3
Menez Gwen 37°17'N, MAR	0.02 – 0.05	1.35 – 2.63	0.01 – 0.02	6
TAG 26°N, MAR	0.15 – 0.37	0.12 – 0.15	1.2 – 2.47	8, 2
MARK 23°N, MAR	0.19 – 0.48	0.02 – 0.06	7.7 – 8.3	10, 11
Lucky Strike 37°17'N, MAR	0.02 – 0.07	0.0 – 0.97	0.03 – 0.07	8

Turtle Pits 04°49‘S, MAR	**0.29**	**0.02**	**14.7**	**14**
Red Lion 04°47‘ S, MAR	**0.08**	**0.03**	**2.87**	**14**
Lilliput 09°33‘ S, MAR	**0.00002**	**0.003**	**0.006**	**14**
Pacific				
Endeavour. JdF, EPR	0.16 – 0.42	1.8 – 3.4	0.1 – 0.12	12
Southern JdF, EPR	0.27 – 0.53	0.08 – 0.12	3.3 – 4.5	9
21°N EPR	0.23 – 1.7	0.06 – 0.09	3.5 – 20	4
Galapagos	0.001 – 0.004	0.1 – 0.4	0.01 – 0.03	5

1: Donval et al., 1997; 2: Charlou et al., 2002; 3: James et al., 1995; 4: Welhan &Craig, 1979; 5: Lilley et al., 1983; 6: Charlou et al., 2000; 7: Kelley et al., 2001; 8: Charlou et al., 1996; 9: Evans et al., 1988; 10: Campbell et al., 1988; 11: Jean-Baptiste et al., 1991; 12: Butterfield et al., 1994; 13: own data M60/3; **14: This work**

Work proceeded by prospecting for hydrothermal activity along the segment A3. Intense survey by CTD and gas measurement failed to recognise any hydrothermal imprint within the water column until station 186 CTD at 09° 27.03'S; 013° 13.99'W revealed considerably enhanced methane concentrations of up to 53 nmol L^{-1} (background < 1 nmol L^{-1}). Further investigation by numerous CTD casts allowed to presuming active hydrothermalism to occur within a relatively narrow area at about 1500 m water depth. An extended area of diffusive fluid outflow accompanied by a dense population of mostly juvenile mussels was spotted and sampled during a ROV dive at this location, the Lilliput hydrothermal field. This is by now the southernmost active hydrothermal area dicovered along the MAR. The emanating fluid was found to be H_2 prone but relatively rich in CH_4 (Fig. 3) with a H_2/CH_4 ratio of 0.006. The distribution of dissolved gases within the area indicates that the Lilliput field does not considerably contribute to the observed anomalies but additional much stronger sources exist. However, no anomalies could be recognised within the CTD records, neither for light transmission nor for temperature. A second ROV attributed to searching for these sources had to be skipped for severe technical problems.

For hydrocarbons of carbon chain lengths from 2 to 4 only saturated homologues were observed (ethane, propane, butanes), but in low concentrations. Molar ratios between methane and higher homologues (C_1/C_{2-4}) were generally above 2000.

1.4.6. Detection of hydrothermal plumes with backscatter MAPR system

(S. Fretzdorff, R. Seifert, C. Ostertag-Henning)

Introduction

The distribution of hydrothermal plumes within the studied areas has been determined with a Pacific Marine Environmental Laboratory (PMEL) Miniature Autonomous Plume Recorder (MAPR; (Baker and Milburn, 1997)) attached to the cabel of a rock-corer, CTD or TV-Grab. The MAPRs include a sensitive light backscatter sensor (LBSS) that provides a relative measure of particle concentration, a 0.001°C resolution thermistor and a strain gauge pressure sensor in a

Ti pressure case. Power supply is warranted by four 9 V alkaline batteries. The sampling rate was usually 10sec during deployment, thus the MAPR recorded data approximately every 5 to 10m in the water column. During the first rock-corer stations the MAPR was attached 200m, and later about 80m above the equipment. During CTD stations 2 to 5 MAPRs were mounted 10, 20, 30m etc. above the CTD. In order to compare the signals of the different MAPRs and literature data, the backscattering intensity has been recalculated to nephelometric turbidity unity (NTUs) according to the expression

$$\Delta \text{NTU} = (V_r - V_b)/a_n$$

where ΔNTU is the plume LBSS anomaly in excess of ambient water, V_r is the raw voltage reading of the LBSS, V_b is the background voltage not affected by hydrothermal plumes, and a_n is a factor unique to each LBSS determined from a laboratory calibration using formazine (Baker et al., 2001). All profiles recorded during individual stations of cruise M64/1 are shown in Figure 1.

Results

MAPRs were attached during 56 deployments of rock-corer, TV-Grab and CTD stations (Fig. 1.10). In the area of Turtle pits, Wideawake mussel field and Red Lion (4°47S to 4°48S) hydrothermal plume signals have been recorded in nearly all stations (Fig. 1.10a). Unfortunately, during the first TV-Grab and rock-corer stations the MAPR was mounted too high above the equipments to trace the complete plume signal (Fig. 1.10a). During the CDT stations and after mounting the MAPR only 80m above the rock-corer distinct plume peaks centred at approximately 200m above the seafloor could be recorded. The plume signals have a vertical extension in the water column between 150 to 200 m (Fig. 1.10a). Only at rock-corer stations 119, 136, and 137 VSR there are no peaks in the recorded nephelometer profiles, probably due to the greater distances (up to 2 km) to the hydrothermal fields. The magnitudes of the anomaly vary from 0.01 up to 0.11 Δ NTU volts which is extremely high compared to other light backscattering peaks recorded in hydrothermally active regions like e.g. along the East Pacific Rise (Baker et al., 2001).

4°47S - 4°48S

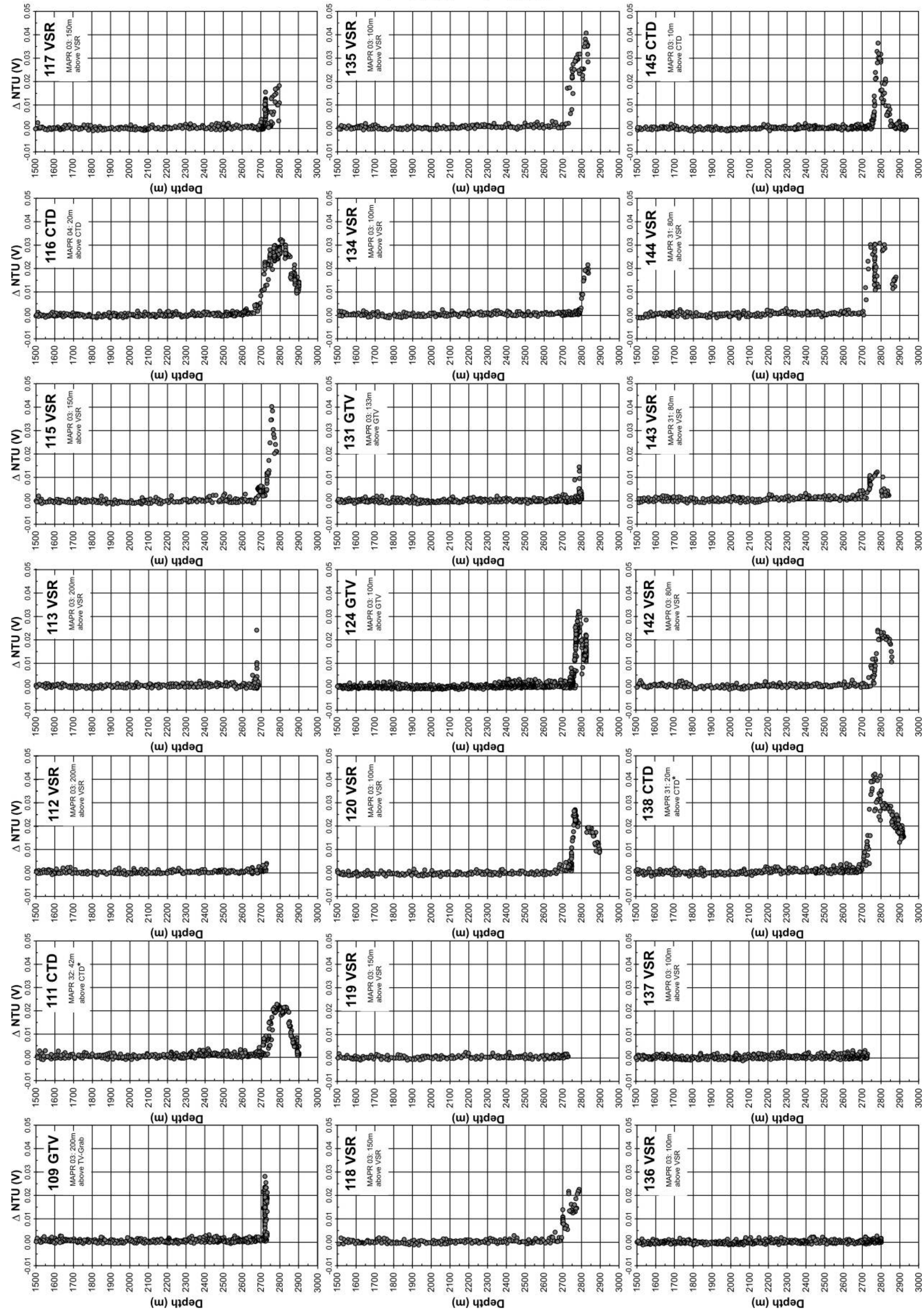

Fig. 1.10a Backscatter profiles (Δ NTU) from CTD and rock-corer stations in the area between 4°47 S - 4°48 S. *one example out of 3 MAPRs.

8°48S - 8°50S

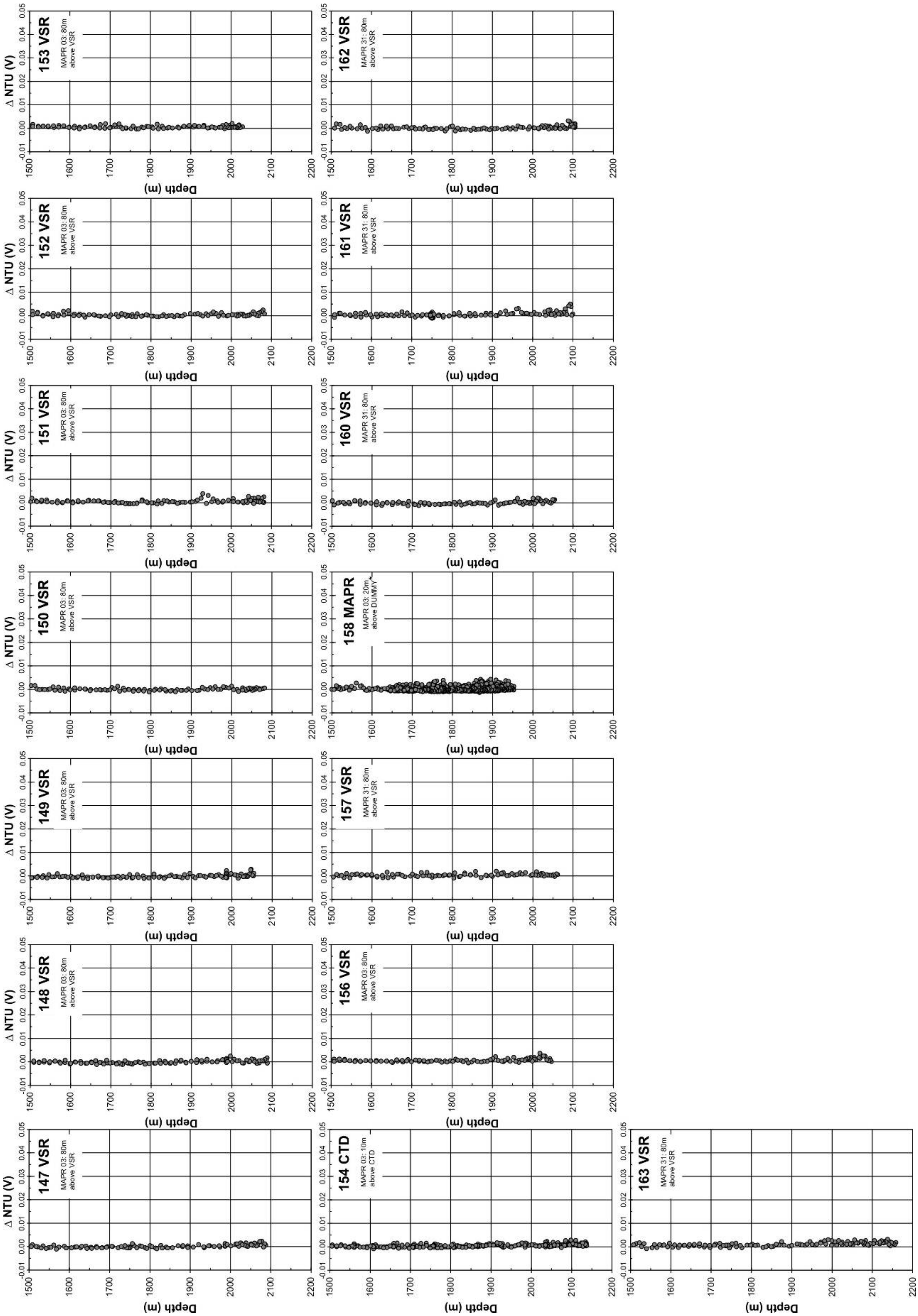

Fig. 1.10b Backscatter profiles (Δ NTU) from CTD and rock-corer stations in the area between 8°48 S - 8°50 S. *one example out of three MAPRs.

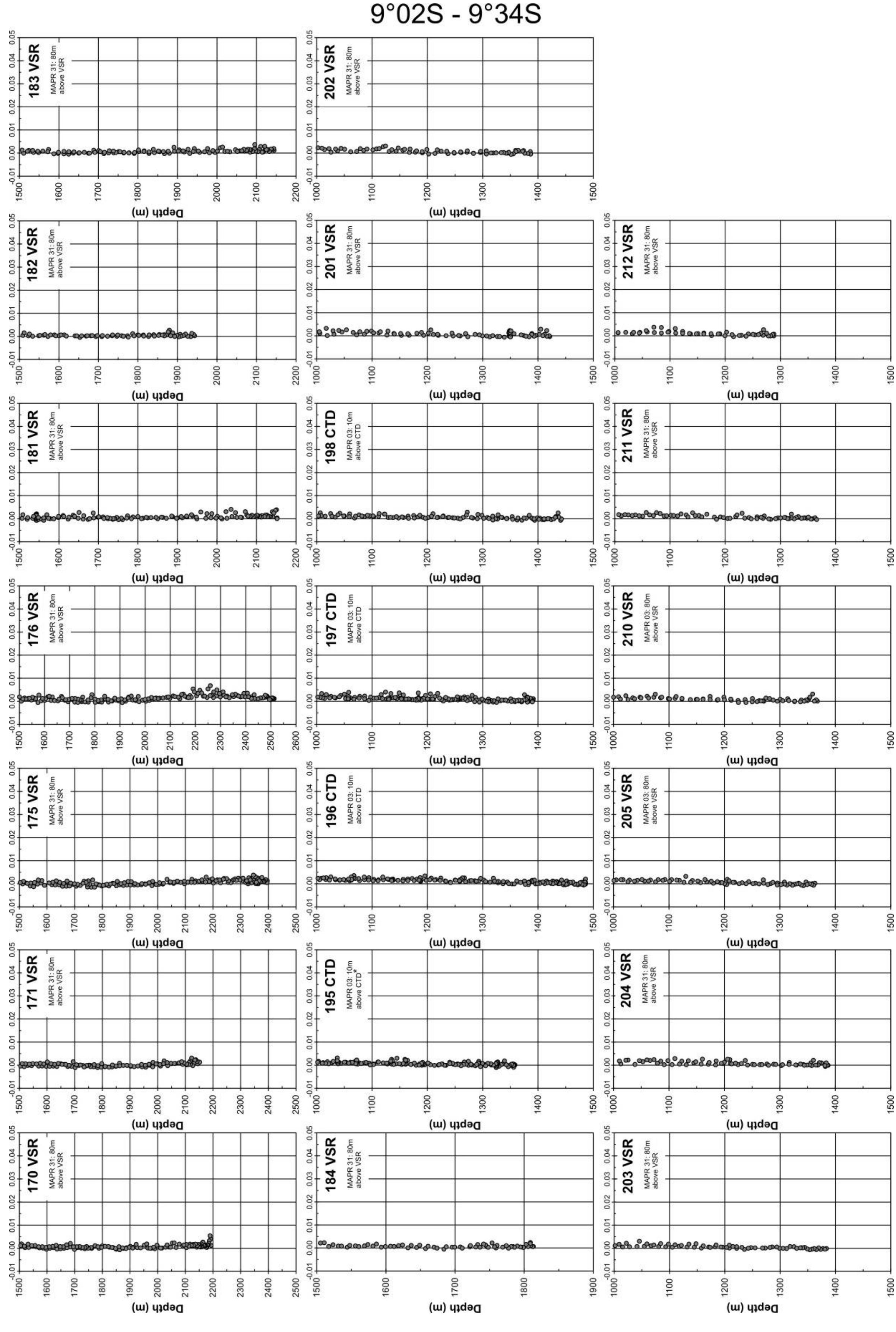

Fig. 1.10c: Backscatter profiles (□ NTU) from CTD and rock-corer stations in the area between 9°02 S - 9°34 S. *one example out of three MAPRs.

In order to map the distribution of the Turtle pits and Wideawake mussel field hydrothermal plumes five MAPRs were mounted 10m, 60m, 110m, 160m, and 210m above a DUMMY (several tyres) and were towed along 5 profiles. Temperature and light backscattering data have been collected during continuous lines of intersecting tow-yos in depth intervals of 2600 to 2900m. An exact x-y-z referencing of the recorded data was possible by using results from the GAPS transponder system. The data have been corrected and a three dimensional grid was constructed by using standard routines for gridding and interpolation in MATLAB onboard. The □□NTU profiles show that the hydrothermal plumes above the Turtle pits and Wideawake mussel fields (located at 4° 48.6' S, 12° 22.36' W) are minor compared to a plume signal/source located west of the studied hydrothermal areas (Fig. 1.11). The output of the Turtle pits and Wideawake mussel field vents seems to be highly variable as evident from the discontinuous □□□NTU anomalies above these sites.

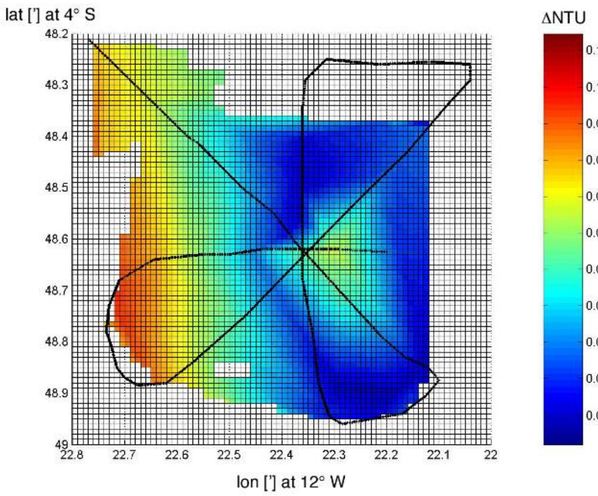

Fig. 1.11a Horizontal slice at 2830 m.

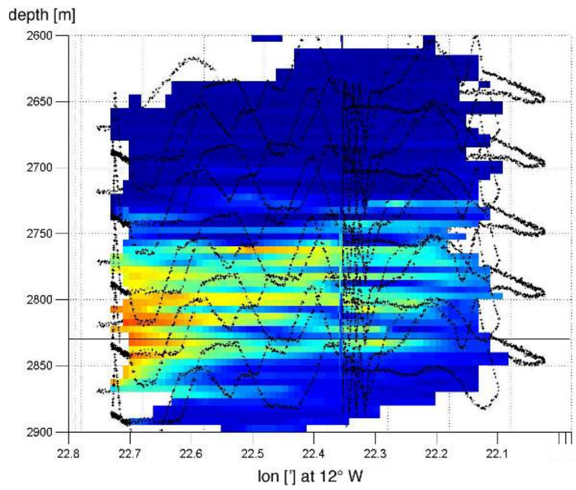

Fig. 1.11b Vertical slice at 4° 48.62' S.

In general, the recorded data in the area of Turtle pits, Wideawake mussel field and Red Lion show no sign of a temperature anomaly in the water column.

Further to the south, between 8°48S to 8°50S and 9°02S to 9°34S the light backscattering profiles show only straight lines, hence no signs of hydrothermal plumes in the water column even above the Lilliput vent field (Fig. 1.10b, c).

1.4.7. Zoology and Ecofaunistic Studies

(Jens Stecher, Olav Giere)

1.4.7.1. Goals

- to explore and to sample the recently found hydrothermal habitats at 5°S.
- to describe their variability and compare the faunas with that of hydrothermal vents of the northern MAR.
- to select suitable vent locations for faunistic long-term-studies on benthic assemblages, to interpret spatial and time inhomogeneous structures of vent sites.
- to search for new hydrothermal habitats at 9°S

1.4.7.2. Methods

Observations were conducted via the Remotely Operated Vehicle (ROV) Quest (University of Bremen, Marum) and the Ocean Floor Observation System (OFOS, IFM-GEOMAR, Kiel). The ROV observations were made using a LWL-cable with three video cameras and a high-resolution digital still camera. The angle of observation was 84° with a maximum view of 15 m. The OFOS observations were made with a PAL black and white video camera, via coaxial cable. For detailed faunal mapping, a 35 mm analog still camera equipped with an underwater housing and water-corrected lens was used. Pictures were taken for detailed mapping every 30s. These still photographs will be processed after the cruise, and are thus not included in the preliminary results. The fauna was sampled mainly by two kinds of nets with meshes of 100µm and 300µm in diameter. These tools were handled by the manipulator arm of the ROV. In order to get an overview of the dominant taxa the TV-grab was used for sampling. The grab sampled an area of 2m². For meiobenthic analysis sediments were taken and completely preserved with 4% seawater-buffered formalin. Additionally, the shells of mussels and clams which were dissected for genetic analysis were preserved in pure 72% Ethanol.

Within the first working area at 5°S samples were successfully taken at 9 of 13 stations. TV-grabs were only undertaken at Turtle Pits and Wideawake Mussel Field.

At the Lilliput hydrothermal field one dive with the ROV, two TV-graps and one OFOS station were driven (Table 1.3). The total bottom observation time at Turtle Pits was 31:44 [hh:mm], at Wideawake Mussel Field 10:20 [hh:mm], at Red Lion 18:24 [hh:mm], and at Lilliput 15:35 [hh:mm] hours. With a total seafloor observation time of 76:03 [hh:mm] hours combined with successfully sampling at 13 stations, the following description of the faunal assemblages will give a representative first overview.

Table 1.3: List of stations of biologically relevant surveys

Station/Tool	**field / Location**	**Date/Bio samples (Yes/No)**
108 ROV	Turtle Pits	08.04.2005 / No
114 ROV	Turtle Pits, samples taken at "Tower"	09.04.2005 / Yes
123 ROV	Turtle Pits , samples taken at "Tower"	11.04.2005 / Yes
125 ROV	Wideawake Mussel Field	12.04.2005 / Yes
130 ROV	Turtle Pits, sampled near marker M2	13.04.2005 / Yes
141 ROV	Turtle Pits	15.04.2005 / No
146 ROV	Red Lion, „Shrimps-Smoker" sampled	16.04.2005 / Yes
200 ROV	Lilliput Hydrothermal field	25.04.2005 / Yes
109 GTV-A	Wideawake Mussel Field	08.04.2005 / Yes
110 GTV-A	Wideawake Mussel Field	09.04.2005 / No
124 GTV-A	Turtle Pits	11.04.2005 / No
131 GTV-A	Turtle Pits, nearby „Stalagmite"	13.04.2005 / Yes
132 GTV-A	Wideawake Mussel Field	13.04.2005 / Yes
139 GTV-A	Turtle Pits, sediments between sulphides	14.04.2005 / Yes
213 GTV-A	Lilliput Hydrothermal field	27.04.2005 / Yes
214 GTV-A	Lilliput Hydrothermal field	27.04.2005 / Yes
215 OFOS	Lilliput Hydrothermal field	27.04.2005 / Yes

1.4.7.3. The vent site at 5°S

This site consists of three active hydrothermal habitats. The dominant taxa are decapode crustaceans such as Alvinocarididae, Mirocarididae, and Bythograeidae as well as mussels of the genus *Bathymodiolus*. Within the Wideawake Mussel field the grab samples showed that limpets and annelids are widely distributed, too. Additionally, sea anemones and scyphozoa occur in the different habitats. Besides these general structures each habitat shows own faunistic characteristics.

Decapoda

Generally, only *Rimicaris* and *Mirocaris* were found and no *Chorocaris* and *Alvinocaris* were observed. At the smokers of Turtle Pits, both species were sampled at two different smokers with *Rimicaris* being dominant. This stands in contrast to the distribution patterns in the Wideawake Mussel Field. There we sampled more *Mirocaris* than *Rimicaris*, it seemed to be that here *Mirocaris* is more abundant than *Rimicaris*.

At the Red Lion field, consisting of four active black smokers we found only *Rimicaris* in large abundance. At least two smokers, "Shrimps Smoker" and "Sugar Head", were covered by *Rimicaris* in such dense populations, that the chimneys appeared white. These *Rimicaris* were quite abundant and wide distributed in the vicinity of the field at pillow lava structures, up to 20 m away from the active smokers tending north.

The brachyurian crab likely is *Segonzacia mesatlantica*. It was collected at the chimneys of Turtle Pits and among *Bathymodiolus* specimen at Widewake Mussel Field. They are further abundant at the active chimneys of Red Lion.

Fig. 1.12 Decapod crustacean on the "Tower" of Turtle Pits. Specimens of *Rimicaris* c.f. *exoculata*, *Mirocaris*, and *Segonzacia* c.f. *mesatlantica*.

Bivalvia and Gastropoda

At Turtle Pits no dense patches of living Bathymodiolus were found. Only at the margins of the pits as well on the flanks we found some rare specimen. Most of them were dead like at the bottom of active smokers where only shells of dead Bathymodiolus could be seen. Neither snails like *Phymorhynchus* nor limpets were present.

In contrast, at the Wideawake Mussel Field living specimens dominated clearly over the dead ones. Within two TV- grabs (each of them covering about 2m²) more than 250 living specimen of Bathymodiolus were retrieved and no dead shells were among these samples. Additionally only few scavengers like *Phymorhynchus* were documented.

This picture changed in the southern part of the field. Here vesicomyid clams were found interspersed in *Bathymodiolus* beds. Although several of the vesicomyid clams were still alive, many of them were dead and not longer than 12 cm. Stecher et al. (2002) discussed the change of a natural ageing cycle of diffuse hydrothermal venting, in which clams were replaced by mussels. So a shift of the hydrothermal activity seemed to be visible here in the community structure, which was based on symbiontic microorganisms. Additionally, the scavenger *Phymorhynchus* was more abundant.

Remarkable were the different distribution patterns of limpets: Whereas limpets settled mostly on basalts within the central Wideawake Mussel Field, which is built of single patches of Bathymodiolus linked by bands of mussels, they were living on the shells of Bathymodiolus in the north-western periphery of the field. The mussels were obviously more patched than within the centre.

With only one exception we did not find any bivalves as well as gastropods at the active smokers of the Red Lion Field. In the northern part of the field we found no more than 60 specimens sitting near the bottom off an inactive smoker. This part of the massive sulphide block was coated by a small white band. If this band consists of bacteria, this might be a sign of slight hydrothermal activity.

Fig. 1.13 The *Bathymodiolus* – vesicomyid clam association in the southern part of Wideawake Mussel Field.

Annelids

We identified at least six forms: Terebellida (forms like Ampharetinae), Chaetopterida, some Phyllodocidae (Polynoidae, Spionida), Malanidae, and Archinomidae. These were all sampled in Wideawake Mussel Field mostly within the byssus filaments of Bathymodiolus. Only the spionids were attached with their tubes on basalt.

Cnidaria

Especially in the Wideawake Mussel Field small anemones and scyphozoa settled in dense aggregations on basalt blocks. Greater specimen of sea anemones were regularly observed on the active smokers of Turtle Pits as well as in between the *Bathymodiolus* patches of the Wideawake Field.

1.4.7.4. The vent site at 9°33'S – Lilliput

The Lilliput hydrothermal field is characterised by pillows which are coated with Fe- oxides so that the field appeared in red-orange colours. Shimmering water emerged out of cavities between pillow lavas. Young specimen of *Bathymodiolus* occurred in dense elongated populations along the cavities and along the pillow's cracks. Obviously, postlarval young mussels (0.5mm length) had settled this vent field recently whereas shells of adults were dissolved. Only their periostracum was found with juveniles attached to them by their byssus filaments. The only undissolved shells were found where no active venting was observed. Their length did not exceed 12cm. Shrimps and bythograeid crabs were subdominant, only a few specimen were observed directly at the source of shimmering water. Additionally, scavengers like Phymorhynchus were seen in the periphery. Grazers like limpets were not observed. In the vicinity of the mussel beds single gorgonians were sitting on the Fe-oxides coated pillows. These morphotypes of gorgonians are characteristic species of the hydrothermal periphery. All these facts stated that this assemblage is a reactivated diffuse venting source which was recently settled by a new generation of mussels.

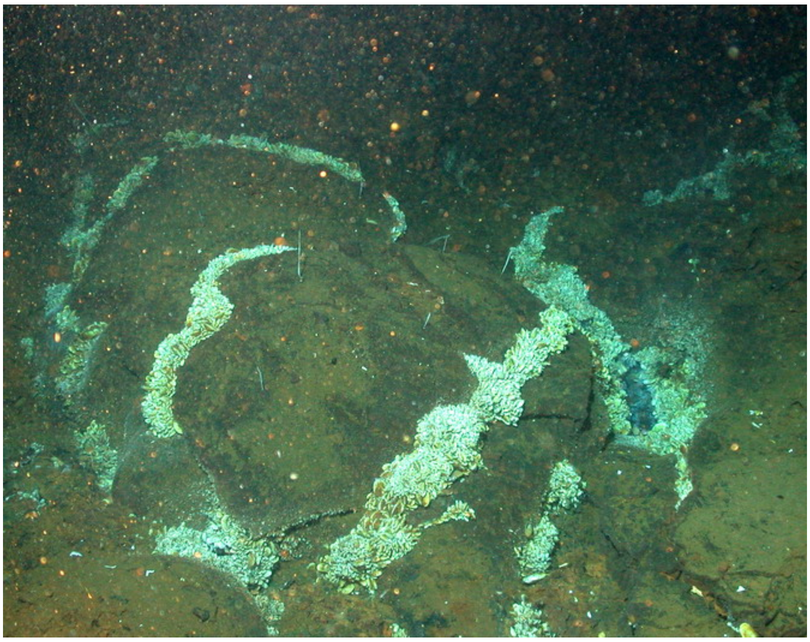

Fig. 1.14 The Bathymodiolus association at Lilliput.

Conclusions:

The identified taxa of the hydrothermal fields at 5°S and 9°33´S on the Mid-Atlantic Ridge resemble the northern Logatchev community (Gebruk et al. 2000) in most elements. Remarkable is the missing of following typical hydrothermal taxa within the new discovered fields:

Decapods of the families Alvinocaridae, like *Alvinocaris* and *Chorocaris*, and Galatheidae, echinoderms like Ophiuridae and Ventfishes of the family Zoarcidae.

Obviously, the St. Pauls and Romanche Fracture Zones act only partly as a physical barrier between vent fauna assemblages of the North and South Atlantic Oceans (see Shank 2004).

Therefore, the spatial environmental conditions seemed to be more responsible for faunal differences rather than geographic isolation mechanisms. This agrees with the results of Desbruyères et al. (2001), comparing different vent fields on the northern Mid-Atlantic Ridge. Therefore they suggested that future investigations should be focused on time series concerning the inter- and intraspecific competitions as well as the variability of microenvironments along gradients.

1.4.8. Molecular and structural analysis of symbioses

(Olav Giere)

Our studies followed several investigative lines:

- Molecular comparison of host tissue and symbiotic bacteria from various vents: Do the newly discovered vents south of the MAR fracture zone conform with those from the Logatchev vent field. Are there differences that could relate to a biogeographic separation? Host animals: *Bathymodiolus* cf. *puteoserpentis* (vent mussels) and *Rimicaris exoculata* (vent shrimps).
- Molecular analysis of genetic changes in both host and bacteria from various vent fields: is there a co-evolution between the symbiotic partners or do they evolve independently (cooperation with T. Shank, Woods Hole)?
- Molecular and ultrastructural comparison of the endobacterial consortium harboured in *Bathymodiolus* cf. *puteoserpentis*: does the relation of methanotrophic to thiotrophic bacteria vary at the different vent fields, possibly depending on the varying concentrations of methane and hydrogen sulphide (link to results from projects analysing the fluid chemistry)?
- Analysis of the establishment of the symbiosis: At what stage do the mussel hosts acquire their symbionts from the environment, i.e. contain the newly settled mussels (size 1 – 2 mm) already the complete set of bacteria? Is their distribution in the bacteriocysts identical to that in adult hosts (FISH and ultrastructural studies)?

The material retrieved at both vent fields sampled (4^{o}48 S and 9^{o}33 S) allows for answering all the different approaches outlined above. Results are to be expected after careful analyses in the home labs.

4^{o}48 S: From Wideawake Mussel Field all size ranges of *Bathymodiolus* c.f. *puteoserpentis* could be dissected and the parts fixed; even newly settled specimens in the mm-size class were retrieved. The new hot vent “Shrimp Smoker” yielded numerous *Rimicaris exoculata* of various size classes. The few specimens of Mirocaris fortunata sampled allow for the first molecular analysis of possible ectosymbionts on the mouth parts. In addition two specimens of *Calyptogena* sp. were sampled at another, yet unnamed hot smoker, and dissected for molecular analysis. This will enable us to analyse for the first time molecular biologically the symbiosis of an Atlantic species of *Calyptogena.*

9°33 S: Again *Bathymodiolus* c.f. *puteoserpentis* of all size classes

Some limpets populating preferably the mussel shells at Wideawake Mussel Field have been fixed for an exploratory molecular and ultrastructural inspection for symbiotic bacteria (in the gills?).

Compilation of material retrieved:

4°48 S: *Bathymodiolus* c.f. *puteoserpentis*: 30 specimens
Rimicaris exoculata: 46
Mirocaris fortunata: 8
Calyptogena sp.: 2
Limpets: 21

9°33 S: *Bathymodiolus* c.f. *puteoserpentis*: 50 specimens, from newly settled to juvenile; not all sizes allowed for dissection

1.4.9. Microbiology

1.4.9.1. Samples and methods

Basalts

(C. Flies)

During the cruise M64/1 different basaltic rocks should be collected

a) to determine the microbial diversity in cracks and pores of basaltic rocks of different age (started on board continued in the home laboratory). This will be done by several cultivation experiments to isolate aerobic/anaerobic, organo-/lithotrophic and/or heterotrophic/autotrophic microorganisms.
b) to investigate the microbial diversity of the samples in the home laboratory by molecular analysis like clone libraries of 16S rRNA genes (*Archaea* and *Bacteria*) in combination with amplified ribosomal rDNA restriction analysis – ARDRA and denaturing gradient gel electrophoresis – DGGE.
c) to study the community structure and morphology of *Bacteria* and *Archaea* in the basaltic rock by electron microscopy and fluorescence in situ hybridization – FISH
d) to calculate the microbial occurrence and abundance in basaltic rocks based on several geochemical techniques (extraction of organic substances and analysis of specific

biomarkers including isotopic analysis) in the home laboratory. Geochemical methods should also be used to analyze pure cultures to correlate the obtained data with single species or specific groups.

e) to determine sulfate and secondary mineralization products (iron and manganese) by anorganic extraction methods and isotopic analysis in the home laboratory. This products will also be analyzed by FTIR and powder-XRD. Furthermore, the correlation between the biological colonization and the precipitation of secondary minerals should be investigated.

To combine the results for a better understanding of the interactions between basaltic rocks and microbial activity all investigations will be done on identical samples.

Furthermore samples from sediment, deep sea water and surface water should be investigated by microbiological and molecular analysis to get the information about the microbial diversity outside basaltic rocks.

Hydrothermal systems - fluids, sediments and mineral phases

(J. Süling, M. Perner, J. Küver)

The aim of the cruise was the collection of material in order to perform

a) Molecular analyses of the microbial community structure of hydrothermal vent systems at 4°48 S and 9°33 S in comparison to the Logatchev vent field (in the home lab)
   - Construction of clone libraries using the 16S rRNA gene (Archaea and Bacteria); Qualitative analyses of present microorganisms.
   - 16S rRNA gene targeted DGGE (Archaea and Bacteria).
   - FISH (Fluorescence in situ Hybridization); Quantification of major phylogenetic groups.
   - Functional gene analyses based on *soxB* (sulfide oxidation), *aprAB* (sulfate reduction, sulfide oxidation), key enzymes of the reductive TCA- cycle, and other CO_2-fixation pathways.
b) Cultivation based experiments using specific media (started on board and continued in the home lab)
   - Selective media for autotrophic microorganisms using various electron donors (H_2, H_2S, S°, S_2O_3, Fe^{2+}, CH_4) as well as suitable electron acceptors (O_2, NO_3, Fe^{3+}, Mn^{4+}, S°, S_2O_3) in the presence of CO_2.
   - Selective media for aerobic and anaerobic heterotrophic microorganisms.
c) On board microscopic observations of microorganisms inhabiting freshly taken samples.

1.4.9.2. Results

Basalts

Basaltic rocks from different locations and different ages were taken using the TV grab or ROV. The samples were transferred into an anaerobic chamber which was filled with nitrogen. Macroscopic visible organisms like Actiniaria were collected and fixed with ethanol or other fixatives and stored at 4°C or at room temperature. The rock surfaces were sterilized with ethanol and the rock was broken in several pieces using a sterilized hammer and a chisel. Most of the pieces were stored at -20°C, air dried or fixed with glutardialdehyde and formaldehyde for further molecular and geochemical analyses in the home laboratory. Other fragments were separated on bord in different subsamples (crust, glass or basalt) and each zone was crushed with a sterile mortar. The splints were used for aerobic and anaerobic cultivation. For aerobic plates the splints were "suspended" in sterile seawater and this solution was used as inoculum. The cultures were incubated at room temperature and transferred to 4°C after several days. In the home laboratory further experiments will be done e.g. agar shakes to obtain pure cultures. Additionally both, splints and the "suspended" basalt were used as inocula for permanent cultures which were stored at -20°C.

Sediment and water samples:

Sediment samples as well as water samples from the deep sea taken by CTD and surface water were used for permanent cultures and aliquots were frozen for molecular analysis for further investigations in the home laboratory. On bord several cultivation experiments were carried out.

Hydrothermal systems - fluids, sediments and mineral phases

a) Molecular analyses of the microbial community structure of hydrothermal vent systems will be conducted in the home lab. Samples were taken via the fluid sampling system from diffusive vents as well as from fluids of black smokers during ROV cruises. Other samples represent hydrothermally influenced rocks and sediments which were retrieved via the TV-grab and the wax corer. The samples were frozen at -20°C and fixed for further treatment. Plume samples were taken using the CTD. These samples were filtered and immediately frozen at -20°C or fixed for further processing. Detailed information on single samples is shown in the extended version of the cruise report for each working group.

b) The samples mentioned above were also used for obtaining enrichment cultures. For this purpose selective media as indicated above were used. Growth was monitored by microscopic observation. Autotrophic as well as heterotrophic microorganisms in culture include various morphotypes. Further processing will be conducted in the home lab with the aim to obtain pure cultures.

c) Microscopic observations of microorganisms inhabiting freshly taken samples revealed heterogenous morphotypes in most samples. Interestingly enough on rock samples collected by the 132 TV-grab at the boarder of a *Bathymodiolus* sp. dominated mussle field two very obvious morphotypes containing sulfur globuli were observed. The white structures (0.5-2mm length) seen in Figure 1.15 consist of several filaments resembling the typical morphological features of *Thiotrix* sp. (non gliding, rosette formation and modified base cells for the attachment to hard substrates). The entire rock sample was irregularly covered by these structures. The filaments enclosed high numbers of sulfur globuli and had a width of up to 20µm.

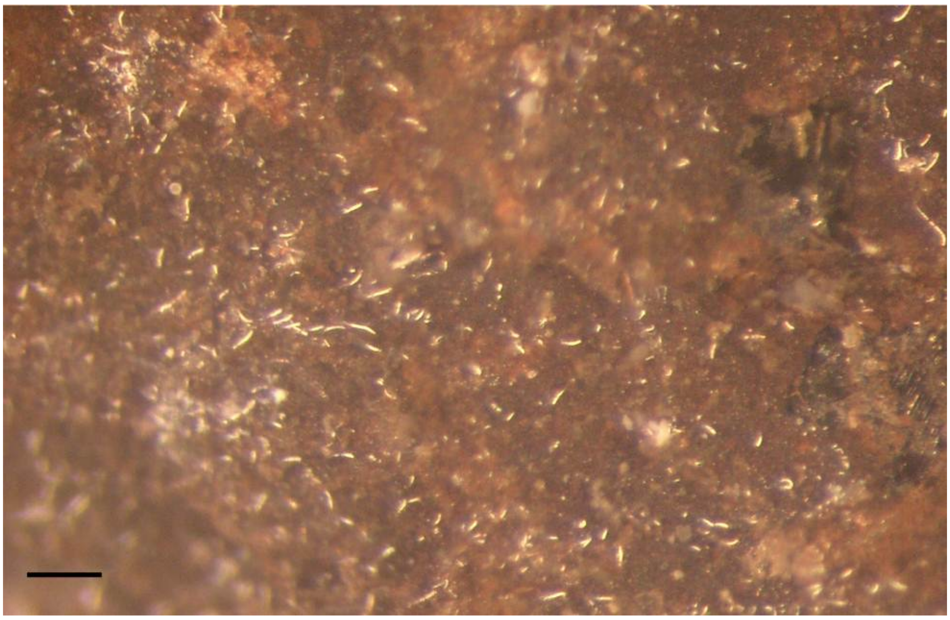

Fig. 1.15 Surface of a rock sample recovered by the 132 TV-grab. The white structures resemble *Thiotrix sp*. Scale bar 2mm. Photo by H. Paulick.

In addition to the sample mentioned above, a sample from 109 TV-grab also collected within the vicinity of a mussel field exhibited a coccoid organism containing numerous sulfur globuli with obvious similarity to *Achromatium* spp. (Fig. 1.16). Besides this large colourless sulfur bacterium which is non motile, several other highly motile small rods and vibrios were observed.

To our knowledge this is the first observation of these two microorganisms at deep sea hydrothermal vent systems. *Thiotrix* spp. have only been found in marine influenced cave systems and like *Achromatium* spp. are known from shallow water hydrothermal vent systems like the golf of Napoli or Paleochori Bay (Milos island).

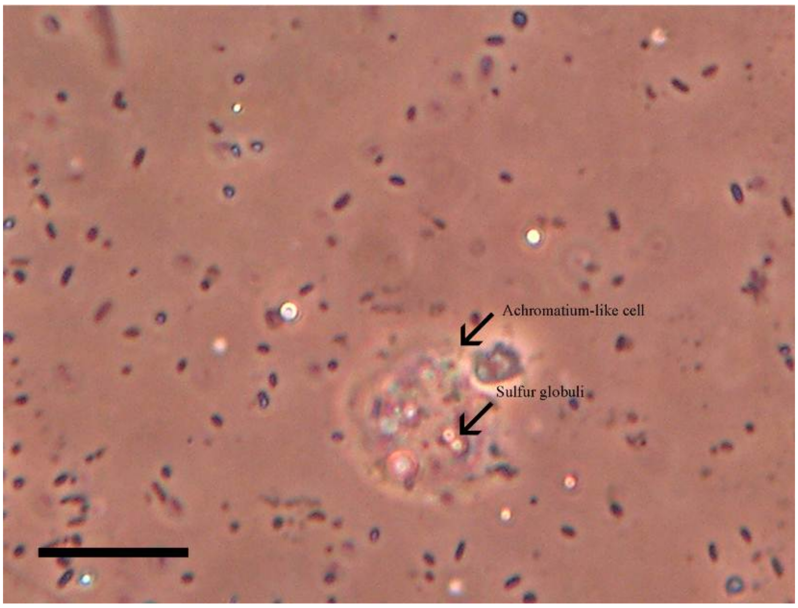

Fig. 1.16 Microscopic picture from an Achromatium-like organism (diameter 20µm) with enclosed sulfur globuli. Scale bar 20µm. Photo by H. Paulick.

1.4.10. QUEST Deepwater ROV

(V. Ratmeyer, A. Houk, S. Klar, P. Mason, N. Nowald, W. Schmidt, M. Schroeder, C. Seiter)

The deepwater ROV (remotely operated vehicle) "QUEST 4000m" used during M64-1, is operated by and installed at MARUM, Center for Marine Environmental Sciences at the University of Bremen, Germany. The QUEST is a commercially available, specially adapted for marine science, and 4000 m rated system designed and build by Schilling Robotics, Davis, USA. Aboard RV METEOR for the 5th cruise since installation in Mai 2003, the system is well adapted to the research vessel and could be handled during all stages of weather encountered during the cruise.

During M64-1, QUEST performed a total of 13 dives between depths of 1400 and 3100 m. 12 dives with al total of 98 hours bottom time allowed successful scientific sampling and observation at different sites along the Mid Atlantic Ridge.

The total QUEST system weighs 45 tons (including the vehicle, control van, workshop van, electric winch, 5000-m umbilical, and transportation vans) and can be transported in four 20-foot vans. Using a MacArtney Cormac electric driven storage winch to manage the 5000m of 17.6 mm NSW umbilical, no additional hydraulic connections are necessary to host the system.

The QUEST uses a Doppler velocity log (DVL, 1200kHz) to perform Stationkeep, Displacement, and other auto control functions. Designed and operated as a free-flying vehicle, QUEST system exerts such precise control over the electric propulsion system that the vehicle maintained positioning accuracy within centimeters and decimeters. In addition, absolute GPS positions are obtained using self-calibrating, acoustic IXSEA GAPS USBL positioning system. However, performance of the system was limited to an absolute accuracy below 20 m. For future cruises, absolute position accuracy will hopefully be substantially enhanced after a major upgrade of the GAPS acoustic array.

The combination of 60-kW power with DVL -based auto control functions provides exceptional positioning capabilities at depth. During many dives, QUEST was able to hold position at various depths between 1400 and 3100 m against all currents and cable movements. During dives at the hydrothermal vent fields, the DVL-based, automatically controlled 3D positioning capability allowed highly precise operations for close-up video filming and up to 1 hour continuous fluid sampling on vertical vent structures without vehicle seafloor contact.
The QUEST SeaNet telemetry and power system provides an extremely convenient way to interface all types of scientific equipment, with a current total capacity of 16 video channels and 60 RS-232 data channels. The SeaNet connector design allows easy interface to third-party equipment, particularly to prototype sensor and sampling devices, by combining power-, data-, video-distribution plus compensation fluid transport all through one single cable-connector setup . This ease of connection is especially important in scientific applications, where equipment suites and sensors must be quickly changed between dives. When devices are exchanged, existing cables can be kept in place, and are simply mapped to the new devices, which can consist of video, data, or power transmission equipment.

The substantial empty space inside the QUEST 5 frame allowes installation of mission-specific marine science tools and sensors. The initial vehicle setup includes two manipulators (7-function and 5-function), five video cameras, a digital still camera (SCORPIO, 3.3 Megapixel), a light suite (with various high-intensity discharge lights, HMI lights, lasers, and dimmable incandescent lights), a CTD, a tool skid with drawboxes, an acoustic beacon finder and a 675 kHz scanning sonar. Total lighting power is 5 kW, and additional auxiliary power capacity is 8 kW.
During M64-1, additional scientific equipment was installed:

- fluid pump system with remote sampling and temperature probe
- microbiological filtering system
- various "hand" tools including nets, scoops, markers, and an autonomous fluid sampler

For detailed video closeup filming, a near-bottom mounted broadcast quality (870 TVL) 3CCD video camera was used (ATLAS). Continuous video footage was recorded with the ATLAS camera and one additional color zoom video camera (PEGASUS or DSPL Seacam 6500). In order to gain a fast overview of the dive without the need of watching hours of video, one video feed is continuously frame-grabbed and digitized at 5sec intervals.

The QUEST control system provides transparent access to all RS-232 data and video channels. The scientific data system used at MARUM feeds all ROV- and ship-based science and logging channels into a commercial, adapted real-time database system (DAVIS-ROV).
During operation, data and video are distributed in realtime to minimize crowding in the control van. Using the existing ship's communications network, sensor data is distributed by the real-time database via TCP/IP from the control van into various client laboratories, regardless of the original raw-data format and hardware interface. This allows topside processing equipment to perform data interpretation and sensor control from any location on the host ship.

Additionally, the pilot's eight-channel video display is distributed to client stations in labs and bridge on the ship via CAT5 cable. This allows the simple setup of detailed, direct communication between the bridge and the ROV control van. Similarly, information from the pilot's display is distributed to a large number of scientists. During scientific dives where observed phenomena are often unpredictable, having scientists witness a "virtual dive" from a laboratory rather than from a crowded control van allows an efficient combination of scientific observation and vehicle control.

Post-cruise data archival will be hosted by the information system PANGAEA at the World Data Center for Marine Environmental Sciences (WDC-MARE), which is operated on a long-term base by MARUM and the Foundation Alfred Wegener Institute for Polar and Marine Research, Bremerhaven (AWI).

1.5. Weather Conditions during M64/1

(W. Ochsenhirt)

On April 02 forenoon MV METEOR left the port of Mindelo (Cape Verde Islands) heading south. The winds encountered were constant northeasterly tradewinds of Bft 4 or 5. On April 06 the reasearch vessel came to the intertropical convergence zone (ITCZ) near 8°N. When Passing the ITCZ the winds were calm and variable and during the following night an intensive tropical shower occured. On the next day near 02.30 North the ITCZ was already far north of the ships position. The Equator was crossed in the afternoon of April 06 and the tradewinds came from southeast with Bft 4 or 5.

In the evening of April 07 the first investigations started near 4.48°S, 12.24°W and were continued until 09.43°S, 13.06°W. During this time METEOR was situated at the edge of the subtropical high in the central South Atlantic. The southeasterly tradewind was mostly steady with 4 or 5, Bft, only for short periods Bft 6. Swell from south or southeast often occurred with a height of 2, sometimes up to 3 m.

In the afternoon of April 27 the investigations ended and METEOR headed for Fortaleza in a direct course. Under the influence of southeasterly to easterly following tradewinds of 3 to 5 Bft the transit voyage was no problem. METEOR arrived in Fortaleza in the early morning of May 03.

1.6. Station List M64/1

Station	Sample	Date	Lat. (S)	Long. (W)	Depth (m)	Rock description
M109 TV grab	109GTV-1	08.04.2005	04°48.64	12°22.36	2998	Fresh, glassy basalt; aphyric sheet flow.
	109GTV-2	08.04.2005	04°48.64	12°22.36	2998	Very fresh aphyric sheet flow, wrinkled surface.
	109GTV-3	08.04.2005	04°48.64	12°22.36	2998	basalt with 1 cm glass crust.
	109GTV-4	08.04.2005	04°48.64	12°22.36	2998	Piece of fresh, glassy sheet flow lava, wrinkled surface, aphyric.
	109GTV-5	08.04.2005	04°48.64	12°22.36	2998	Fresh, aphyric sheet lava with 1 cm glass rind on both sides.
M110 TV grab	110GTV-1	09.04.2005	04°48.55	12°22.36	2998	Fresh, aphyric sheet flow, 1 cm glassy rim.
	110GTV-2	09.04.2005	04°48.55	12°22.36	2998	Aphyric basalt glass.
	110GTV-3	09.04.2005	04°48.55	12°22.36	2998	Fresh aphyric basalt, glassy margins on both sides of sample.
M111 CTD	111CTD	09.04.2005	04°48.6	12°22.4	2998	
M112 VSR	112VSR-1	09.04.2005	04°48.75	12°22.28	2995	Small glass particles.
M113 VSR	113VSR-1	09.04.2005	04°48.77	12°21.76	2951	Fresh, aphyric basalt glass.
	113VSR-2	09.04.2005	04°48.77	12°21.76	2951	Fresh glassy ash with foram. sand.

M114 ROV	114ROV-4A*	10.04.2005	04°48.579	12°22.418	2993	Piece of black smoker chimney, zoned, interior consists of chalcopyrite (friable, porous). Outer rim: 1-2 cm of pyrite-marcasite, marcasite-rich outer crust coated with Fe-Oxihydroxides.
	114ROV-5A*	10.04.2005	04°48.579	12°22.418	2993	Zoned black smoker chimney. Outer 2 - 5 cm: pyrite-marcasite crust, interior; chalcopyrite-rich with abundant anhydrite and rare sphalerite. Prominent ribbon banding. Central conduit is open: 4 to 9 cm in diameter lined and filled by anhydrite (partially intergrown with fine- grained sulfide [sphalerite?]).
	114ROV-5B-F*	10.04.2005	04°48.579	12°22.418	2993	Several small pieces of pyrite-marcasite black smoker crustal material, behive-like layering.
	114ROV-5G-H*	10.04.2005	04°48.579	12°22.418	2993	Porous, friable chalcopyrite-rich material from black smoker interior.
	114ROV-5Bag*	10.04.2005	04°48.579	12°22.418	2993	Loose sulfide rubble, very porous, soft, collected in bionet.
	114ROV-6*	10.04.2005	04°48.579	12°22.418	2984	Sample of beehive structure, similar to sample 114-4; outer marcasite crust, interior is porous chalcopyrite showing behive layering.
	114ROV-7*	10.04.2005	04°48.579	12°22.418	2984	Piece adjacent to 114-6 but not behive structured (more like a layered knob); marcasite-rich outer crust; chalcopyrite-rich interior.
M115 VSR	115VSR-1	10.04.2005	04°48.77	12°22.61	3048	Basalt glass with large plagioclase phenocryst (10 mm in diameter).
	115VSR-2	10.04.2005	04°48.77	12°22.61	3048	Glass particles with plagioclase phenocrysts.
M116 CTD	116CTD	10.04.2005	04°48.8	12°22.7	2961	
M117 VSR	117VSR-1	10.04.2005	04°48.25	12°23	3033	Two small pieces of aphyric basalt glass.
M118 VSR	118VSR-1	10.04.2005	04°48.26	12°22.23	3000	Very fresh aphyric glass.
M119 VSR	119VSR-1	10.04.2005	04°48.26	12°21.48	2980	Fresh basaltic glass with plagioclase phenocrysts (max. 1 cm).
M120 VSR	120VSR-1	10.04.2005	04°47.79	12°22.97	3050	~1 cm thick glass crust, basalt with several plagioclase phenocrysts up to 1 cm.
M121 CTD	121CTD	11.04.2005	04°47.8	12°22.6	3022	
M122 CTD	122CTD	11.04.2005	04°48.5	12°22.4	2971	
M123 ROV	123ROV-4A*	11.04.2005	04°48.583	12°22.41	2986	Outer portion of active chimney consisting of numerous, friable microchimney structures (1 - 5 cm diameter). Marcasite crust. Interior is complex and zoned grading from anhydrite, sphalerite to pyrite-sphalerite to chalcopyrite. Exterior is partially oxidized and locally covered with white bacterial? dots.
	123ROV-4B*	11.04.2005	04°48.583	12°22.41	2986	Two fragments of chimney interior, chalcopyrite-anhyydrite association.
	123ROV-4C*	11.04.2005	04°48.583	12°22.41	2986	Various fragments of chimney exterior, marcasite-pyrite + Fe-oxihydroxide + white coatings. Finer rubble with chalcopyrite-rich material, anhydrite, microchimneys.
	123ROV-8	11.04.2005	04°48.58	12°22.4	2985	Aphyric basalt, lobate feature on surface of jumbled sheet flow. 3 mm thick glass on both sides. Interior is microcrystalline with large lensoidal cavities parallel to outer surfaces (drain-out feature?) lines with thin Mn-Oxide film.
	123ROV-9*	11.04.2005	04°48.559	12°22.413	2990	Piece of inactive sulfide chimney, recrystallized. Chalcopyrite-rich interior ca. 5 cm in diameter, partly oxidized (pigeon coloration). Outer zone is sphalerite-pyrite-marcasite. Crust is marcasite, outer crust is 1 mm thick Fe-oxihydroxide.

M124 TV grab	124GTV-1A*	11.04.2005	04°48.573	12°22.424	2998	Three pieces of approx. similar size, slabby blocks of aphyric basalt, 1-2 mm of glass crust on both sides and extensive Fe-oxihydroxide coating.
	124GTV-1B*	11.04.2005	04°48.573	12°22.424	2998	Similar to 124-1A but with prominent wrinkles on the surfaces.
	124GTV-2A*	11.04.2005	04°48.573	12°22.424	2998	Massive pyrite/marcasite; outer 5 mm biogenic(?) marcasite crust followed by 1 cm massive marcasite, interior pyrite: dendritic growth cross cutting beehive layering.
	124GTV-2B*	11.04.2005	04°48.573	12°22.424	2998	Same as 2A + small normal fractures lined with chalcopyrite. Zones of sphalerite enrichment.
	124GTV-2C*	11.04.2005	04°48.573	12°22.424	2998	Same as 2A but interior is with more chalcopyrite (Cu-rich end member of this type).
	124GTV-2 D - M*	11.04.2005	04°48.573	12°22.424	2998	Crustal material of black smoker chimney: pyrite + marcasite, rare to trace sphalerite + chalcopyrite in cavities and along fractures.
	124GTV-2G*	11.04.2005	04°48.573	12°22.424	2998	Similar to 2A but more black sphalerite, Zn- rich end member of this type.
	124GTV-3 A -C*	11.04.2005	04°48.573	12°22.424	2998	Massive pyrite-marcasite with strong beehive texture.
M125 ROV	125ROV-1A	12.04.2005	04°48.6111	12°22.327	3000	Glassy aphyric lava with large vesicle (max. diameter is 5 cm) and some spotty biological coating.
	125ROV-4	12.04.2005	04°48.6111	12°22.327	3000	Aphyric basalt crust, 4 cm thick, 3 mm glass crust with rough polyhedral joints. Interior is microcrystalline with small vesicles and 3 -4 cm thick lower surfaces showing complex plastic deformation and lava stalagtites.
	125ROV-6	12.04.2005	04°48.624	12°22.355	2986	Three pieces, basalt overgrown with scyphocytes, aphyric basalt, 2 mm thick glass crust, interior with large vesicles.
	125ROV-8	12.04.2005	04°48.635	12°22.345	2985	Aphyric basalt, 3 mm thick glass crust, interior is microcrystalline. Fracture surfaces normal to top of sample are coated with Fe-oxihydroxides.
	125ROV-9	12.04.2005	04°48.634	12°22.355	2986	Very fresh glass from flow carapace, abundant quench fractures, <1 vol% olivine phenocrysts, max. diameter ~ 1mm, locally with elongate to lensoidal vesicles up to 2 x 3 cm, no small vesicles.
	125ROV-10	12.04.2005	04°48.634	12°22.355	2986	Some more fragments of the same type and the same location as sample 125-9 (see above).
M126 CTD	126CTD	12.04.2005	04°46.8	12°23.2	3063	
M127 CTD	127CTD	13.04.2005	04°48.7	12°23.0	2959	
M128 CTD	128CTD	13.04.2005	04°48.8	12°22.4	2967	
M129 CTD	129CTD	13.04.2005	04°48.6	12°22.6	2982	
M130 ROV	130ROV-1*	13.04.2005	04°48.57	12°22.417	2985	There are two types of fragments: 1. Chimney interior consisting of anhydrite and chalcopyrite. 2. Chimney crust consisting of pyrite, chalcopyrite and marcasite, partially covered by Fe-oxihydroxides.
	130ROV-2*	13.04.2005	04°48.57	12°22.417	2985	Hollow chimney structure with 2 cm thick walls. Walls consist of cpy and marcasite and a 1- 5 mm marcasite crust. Interior of the vent (5 x 3 x 2 cm) is extensively lined by 1-3 mm thick pyrrotine crust with beautiful blade crystals up to 1 mm in diameter.
	130ROV-3*	13.04.2005	04°48.57	12°22.417	2985	Particles are 5 to <1mm, 75% pyrite particles including some collomorphic aggregates; 10% basalt glass chips (max. 5 mm); 10% anhydrite <1 mm, some larger particles are well-rounded due to resorption by seawater;<5% cpy (altered) and pyrite aggregates, <1% globugerina; rare goethite.

M131 TV grab	131GTV-1	13.04.2005	04°48.57	12°22.37	2999	Piece of aph yric basalt w ith 1 x 1 cm mafic xenolith. Wrinkled to bulbous crust of a sheet flow with 1 to 5 mm glassy upper surface (locally some Feox-hydrox. staining). L ower surface shows plastic deformation indicating that this is the roof o f a lav a lobe/tunnel. Xenoliths of gabbro (cp x to 8 m m and plag to 2 mm) up to 5 cm in diameter.
	131GTV-2	13.04.2005	04°48.57	12°22.37	2999	Similar to 131-1. Crust of drained lava tube. Top surface shows ropy texture; 2 t o 3 mm thick glass covered by F e-Oxihydroxides. Margins of piece are no rmal fractures co vered by Fe-Oxihydroxides and biology.
	131GTV-3	13.04.2005	04°48.57	12°22.37	2999	Similar to 131-1 and 2. Plat y slab repr esenting the roof of a drained sheet lava flow . Top is flat and covered b y <1 mm hy drothermal(?) crust. Glass is 10 mm thick and shows nice gradation over 3 mm into microcrystalline interior. Lo wer surface shows lava stalagtites.
	131GTV-4	13.04.2005	04°48.57	12°22.37	2999	Similar to 131-1, -2, and -3. Lava tongue (4 cm thick) with 1 to 5 mm thick glass on both sides. Top surface is ropy to wrinkled.
	131GTV-5	13.04.2005	04°48.57	12°22.37	2999	Aphyric lava with gabbroic xenoliths: clinopyroxene and plagioclase up to 8 mm.
M132 TV grab	132GTV-1	14.04.2005	04°48.62	12°22.34	2996	Fresh lava piece, bulbous, aphyric, 10 mm of glass on both sides.
	132GTV-2	14.04.2005	04°48.62	12°22.34	2996	Similar to 132-1, fresh surface w ith biological colonization.
	132GTV-3	14.04.2005	04°48.62	12°22.34	2996	Similar to 132-1.
M133 CTD	133CTD	14.04.2005	04°48.6	12°22.4	2966	
M134 VSR	134VSR-1	14.04.2005	04°49.01	12°23.05	3000	Basaltic glass with plagioclase phenocrysts.
M135 VSR	135VSR-1	14.04.2005	04°49.02	12°22.51	3001	Two pieces of aphyric basalt lava with 1 cm glass crust.
M136 VSR	136VSR-1	14.04.2005	04°48.26	12°21.86	2970	Aphyric basalt glass + some globigerina.
M137 VSR	137VSR-1	14.04.2005	04°48.23	12°21	2903	Foraminiferous sediment.
M138 CTD	138CTD	14.04.2005	04°47.8	12°22.6	2971	
M139 TV grab	139GTV-1 to 8	14.04.2005	04°48.57	12°22.417	2985	Diverse accociation of different types of sulfides: individual cpy-rich chimneys, pyrite-marcasite-chimneys, coalesced microchimneys, anhydrite-rich pieces w ith varying proportions of magnetite+chalcopyrite, cavities lined w ith euhedral gypsyum crystals, friable magnetite-rich samples, minor sphal erite; locally oxidation => hematite bands.
M140 CTD	140DUMMY	14.04.2005	04°48.2	12°22.9	3035	
M141 ROV	141ROV_AC-6	15.04.2005	04°48.56	12°22.41	2985	Pyrite-marcasite crust, chalocop yrite in the interior is ty pically altered (pigeon color). Redbrown outer surface: Fe-oxihydroxide coating. One piece w ith central vug (2 x 3 cm) line with pyrrotite + isocubanite (?). Some of the fragments contain 1-3 mm la yer of magnetite separating the chacop yrite and p yrite-marcasite zones.
M142 VSR	142VSR-1	15.04.2005	04°48.75	12°22.52	3004	Several aphyric basalt glass fragments.
M143 VSR	143VSR	16.04.2005	04°48.9	12°22.0	2983	empty
M144 VSR	144VSR	16.04.2005	04°48.0	12°22.6	3023	empty
M145 CTD	145CTD	16.04.2005	04°48.9	12°22.8	2974	
M146 ROV	146ROV-1	16.04.2005	04°48.88	12°22.93	2973	Altered, highly plagioclase-phyric basalt, 20 % plagioclase phenocrysts up to 12 mm in diameter. Sample of lava cr ust. Glass is completely altered (clay-Mn Oxide, Fe Oxihydroxide), abundant biological colonization.
	146ROV-2	16.04.2005	04°48.35	12°22.69	3024	Fresh glassy aphyric basalt; large elongat e cavities: long axis (>5 cm) parallel to the flow fold axis.

	146ROV-3	16.04.2005	04°47.902	12°22.618	3045	Sulfide knob o n inactive chimne y. Friable interior with irregular cavities lined by sphalerite and chalcopyrite (crystals <1 mm). Bulk of the piece consists of chalcopyrite-marcasite. Crust: 2 mm black Fe-oxihydrixide.
	146ROV-7	16.04.2005	04°47.824	12°22.595	3048	Sphalerite-rich fragment of a ctive smoker. Internal cavitiy (2 x 1.5 cm) lined b y pyrrotite (+isocubanite?). Crust of Fe-oxihydroxide is extensively coated by white material (sulfur?) and orange-brown globules coated by Fe-oxides .
M147 VSR	147VSR	18.04.2005	08°50.0	13°29.7	2224	empty
M148 VSR	148VSR-1	18.04.2005	08°49	13°29.8	2230	Small chips of gra y, microcrystalline aphyric basalt, trace of glass chips.
M149 VSR	149VSR	18.04.2005	08°48.0	13°31.0	2214	empty
M150 VSR	150VSR-1	18.04.2005	08°48.01	13°30.3	2211	Small amount of glass particles.
M151 VSR	151VSR-1	19.04.2005	08°47.99	13°30.1	2219	Basalt
M152 VSR	152VSR-1	19.04.2005	08°47.99	13°29.81	2223	Several glass pieces.
M153 VSR	153VSR-1	19.04.2005	08°47.99	13°29.29	2165	Shell fragments (sediment patch).
M155 ROV	155ROV-1	19.04.2005	08°48.98	13°30.5	2161	Glassy basalt from talus breccia, covered b y mud, rare <1mm olivine phenocrysts.
	155ROV-2	19.04.2005	08°48.99	13°30.44	2172	Microcrystalline basalt, ca. 5% vesicles up to 2 mm in diamter, <1% olivine phenocrysts up to 1 mm, top coated by Mn-Oxide crust, abundant microorganisms.
	155ROV-3	19.04.2005	08°49	13°30.3	2149	Four cm thick ro of of lava lobe. Top surface is glassy (2 mm thick), 5 % vesicles up to 5 mm in the microcrystalline basalt below the glass crust; lower surface with stalagtite texture; rare olivine phenocrysts <1mm.
	155ROV-4	19.04.2005	08°48.96	13°30.17	2195	Aphyric basalt, pillow section, microcrystalline with partially palagonitized glass crust (ca. 1 mm); 2 % vesicles up to 2 mm.
	155ROV-5	19.04.2005	08°48.99	13°30.06	2199	Altered aphyric basalt with <1% pyroxene and rare plagioclase (<1 mm). Piece consists of two individual lobes showing ductile deformation.
	155ROV-6	19.04.2005	08°48.99	13°30.04	2190	Piece of pillow crust with prominent striated top surface texture. Roof (3 cm thi ck) of partiall y drained pillow. Glass on both sid es (top: 2 to 4 mm; base < 1mm). Partial palagonitization. 1% olivine phenocrysts up to 5 mm.
	155ROV-7	19.04.2005	08°48.99	13°29.97	2221	Abundant aphyric basalt glas s chips of pillow crust. Partially palagonitized.
	155ROV-8	19.04.2005	08°49.04	13°29.85	2218	Single piece of microcrystalline basalt w ith 1% olivine phenocrysts (up to 1 mm); ca 1% vesicles (up to 2 mm). Glass cr ust is 1-3 mm thick and locally shows spherulitic textures.
M156 VSR	156VSR-1	19.04.2005	08°48.43	13°30.42	2208	Basalt glass.
M157 VSR	157VSR-1	19.04.2005	08°47.7	13°30.56	2190	Basalt glass.
M158 CTD	158DUMMY	20.04.2005	08°53.1	13°31.2	2198	
M159 ROV	159ROV-1	20.04.2005	08°48.18	13°30.12	2204	Glassy basalt with 1% olivine a nd plagioclase phenocrysts up to 1 mm, some palagonite.
	159ROV-2	20.04.2005	08°48.15	13°30.12	2201	Basalt with 3 mm glass crust, < 1% plagioclase phenocrysts 2% vesicles up to 2 mm, minor Fe staining.
	159ROV-3	20.04.2005	08°48.06	13°30.12	2198	Aphyric glassy basalt; flow fold quenched on both sides, slight palagonitization, microcrystalline groundmass surrounds elongate cavity (long axis >4 cm parallel to fold axis).
	159ROV-4	20.04.2005	08°47.99	13°30.12	2201	Aphyric glassy basalt, abundant shards <1 to 3 cm in foram./pteropod sand.

	159ROV-5	20.04.2005	08°47.96	13°30.16	2186	Piece of lava protrusion, plagioclase-phyric glassy basalt, 10 vol.% plagioclase phenocrysts up to 10 mm, surface with striation marks, glass crust partially palagonitized and covered by thin layer of black Mn-oxide.
	159ROV-6	20.04.2005	08°47.81	13°30.19	2151	Abundant fragments of aphyric basalt glass shards.
	159ROV-7	20.04.2005	08°47.75	13°30.21	2201	Plagioclase-phyric basalt with 2 mm glass crust, <1% plagioclase up to 1 mm, 3% vesicles up to 2 mm, several zones of shearing up to 1 cm wide oriented parallel to the surface spaced at 2-4 cm intervals. Slight Fe-Oxihydroxide staining.
	159ROV-8	20.04.2005	08°47.76	13°30.21	2202	Basalt with 1-2 mm glass crust, slightly palagonitized, few plagioclase phenocrysts (< 1mm), 1 vol. % vesicles up to 1 mm.
	159ROV-9	20.04.2005	08°47.5	13°30.21	2215	Pillow top is glassy (1-2 mm thick), slight palagonitization, <1% plagioclase and olivine, up to 1 mm, lower surface is ondulated, solidified lava droplets.
	159ROV-10	20.04.2005	08°47.46	13°30.18	2219	Small lava fold with glassy crust (1-2 mm), plagioclase-phyric basalt, 1% plagioclase up to 1 mm.
	159ROV-11	20.04.2005	08°47.46	13°30.18	2219	Lava lobe of 4 cm thickness with glassy crust on both sides, abundant palagonitization, 1% plagioclase phenocrysts up to 5 mm, rare olivine.
M160 VSR	160VSR-1	20.04.2005	08°46.93	13°30.39	2208	Basalt glass.
M161 VSR	161VSR-1	20.04.2005	08°46.7	13°30.57	2266	Basalt glass with plagioclase phenocrysts.
M162 VSR	162VSR-1	21.04.2005	08°46.22	13°30.64	2273	Basalt glass with plagioclase phenocrysts.
M163 VSR	163VSR-1	21.04.2005	08°45.43	13°30.74	2287	Basalt glass with plagioclase phenocrysts.
M164 CTD	164CTD	21.04.2005	08°54.0	13°29.2	2122	
M165 VSR	165VSR-1	21.04.2005	08°50	13°29.68	2225	Aphyric basalt glass.
M166 VSR	166VSR-1	21.04.2005	08°50.51	13°29.48	2188	Chips and fragments of microcrystalline and glassy basalt.
M167 CTD	167CTD	21.04.2005	09°00	13°29	1974	
M168 CTD	168CTD	21.04.2005	09°00	13°28	2153	
M169 CTD	169CTD	21.04.2005	09°00	13°27	2244	
M170 VSR	170VSR-1	21.04.2005	09°20	13°27	2313	Sediment in vaseline with a few glass particles.
M171 VSR	171VSR-1	21.04.2005	09°4.01	13°26.6	2320	Sediment patches.
M172 CTD	172CTD	22.04.2005	09°7.5	13°27.0	2530	
M173 CTD	173CTD	22.04.2005	09°7.5	13°26.0	2530	
M174 CTD	174CTD	22.04.2005	09°7.5	13°25.0	2530	
M175 VSR	175VSR-1	22.04.2005	09°7.5	13°25.86	2530	Olivine-phyric basalt (1% olivine phenocrysts up to 2 mm), glassy and microcrystalline fragments, moderate palagonitization.
M176 VSR	176VSR-1	22.04.2005	09°9.02	13°25.51	2640	Basalt glass.
M177 CTD	177CTD	22.04.2005	09°10.5	13°26.1	2654	
M178 CTD	178CTD	22.04.2005	09°10.4	13°25.0	2582	
M179 CTD	179CTD	22.04.2005	09°10.5	13°24.0	2284	
M180 CTD	180CTD	22.04.2005	09°10.5	13°23.0	2372	
M181 VSR	181VSR-1	22.04.2005	09°15.29	13°17.5	2285	Altered glass crust with sediment.
M182 VSR	182VSR-1	22.04.2005	09°17.02	13°17.02	2072	Very few glass chips.
M183 VSR	183VSR-1	22.04.2005	09°20.9	13°17.1	2261	empty
M184 VSR	184VSR-1	23.04.2005	09°22.49	13°15.53	1932	Few thin rock fragments.
M185 CTD	185CTD	23.04.2005	09°19.0	13°17.0	2370	
M186 CTD	186CTD	23.04.2005	09°19.0	13°16.0	1932	
M187 CTD	187CTD	23.04.2005	09°19.0	13°15.0	2059	

M188 ROV	188ROPV_P-1	23.04.2005	09°42.48	13°5.02	1772	Piece of aphyric basalt lava. Roof of lava lobe. Glassy crust with abundant palagonitization. Rare olivine phenocr ysts (< 1 mm), ca 1% vesicles up to 5 mm. E xtensive Mn-oxide coating.
	188ROPV_P-3	23.04.2005	09°42.49	13°4.96	1787	Piece of aph yric lava lobe. 1 to 2 mm glass y crust with intense palagonitization. Ca. 5 % tubular vesicles (1 mm x 10 mm) concentrated below crust. E xtensive Mn-oxide coating and biological colonization.
	188ROPV_P-4	23.04.2005	09°42.49	13°4.8	1857	Piece of aph yric basalt lava lobe with rare olivine phenocrysts. Glass crust (1 to 3 mm) is heavily palagonitized. Some Fe-oxih ydroxide alteration and a bundant worm tubes. Vesicles: <1%, < 1mm.
	188ROPV_P-5	23.04.2005	09°42.39	13°4.67	1864	Two pieces of small lava lobe. Glass crust (1 to 2 mm) is strongly palagonitized. Vesicles: < 1%, < 1 mm.
	188ROPV_P-7	23.04.2005	09°42.36	13°4.51	1882	Aphyric basalt pillow. Glass crust (1 to 2 mm) is strongly palagonitized. Coated by Mn-oxide and some biological colonization.
M189 CTD	189CTD	23.04.2005	09°27.0	13°14.0	1701	
M190 CTD	190CTD	23.04.2005	09°27.0	13°16.0	2083	
M191 CTD	191CTD	23.04.2005	09°27.0	13°12.0	1886	
M192 CTD	192CTD	24.04.2005	09°30.0	13°13.0	1653	
M193 CTD	193CTD	24.04.2005	09°32.5	13°12.9	1458	
M194 ROV	194ROPV_P-1	24.04.2005	09°34.37	13°12.95	1454	One piece of aphyric pillow basalt. Vesicles: 3% up to 3 mm. Palagonitized glass crust (1-3 mm); Mn-oxide and Fe-oxihydroxide coating and some biology.
	194ROPV_P-4	24.04.2005	09°34.37	13°12.86	1429	Section of aphyric pillow basalt. Vesicles: 5% up to 10 mm. Palagonitized glass crust. Extensive Mn-oxide coating. Bi ological colonization including trunk of gorgonaria.
	194ROPV_P-6	24.04.2005	09°34.37	13°12.77	1436	Aphyric basalt. Extensive palagoniti.zation and Mn-oxide coating.
	194ROPV_P-7	24.04.2005	09°34.37	13°12.67	1448	Roof of lava lo be; Top: wrinkled glass (ca. 5 cm), fresh. Aphyric. Vesicles: 3%, up to 1 mm.
	194ROPV_P-8	24.04.2005	09°34.41	13°14.53	1465	Section of pillow. Rare olivine phenocry sts (up to 1 mm). Vesicular central part (30% up to 20 mm, locally coalesced). Tubular vesicles (up to 4 cm long) oriented normal to the exterior in the outer 10 cm of t he section. Outermost 1-2 cm are vesicle-free. Some glassy patches preserved.
	194ROPV_P-9	24.04.2005	09°34.43	13°12.52	1465	Three pieces of aph yric basalt with 1 to 3 m m glass crust.
	194ROPV_P-10	24.04.2005	09°34.37	13°12.5	1470	Vesicular aphyric basalt. Vesicles: 10%, up to 5 mm, locally coa lesced. Outer zone (1 cm) is vesicle-free. Glass crust (1-2 m m) is slightly palagonititzed.
	194ROPV_P-11	24.04.2005	09°34.38	13°12.49	1470	Piece of aphyric lava fold with 1 mm glass crust on both sides. Central zone contains 20% vesicles up to 1 cm; abundan t tubular vesicles oriented normal to the exterio r. Outer 1 cm on both sides are vesicles-free.
	194ROPV_P-12	24.04.2005	09°34.38	13°12.34	1460	Crust of aph yric lava lobe w ith wrinkely lower surface. Slightly palagonitized glass crust (1 to 2 mm). Vesicles are tub ular, oriented normal to the surface (20%).
	194ROPV_P-13	24.04.2005	09°34.38	13°12.34	1468	Slab of aph yric sheet flow exposed in collapse pit. Roof of lava tunnel. Top surface is wrinkled on 10 cm sca le. Fresh glassy crust with prominent perlite texture. Lower surface with abundant lava droplets, thin-walled bubbles and linear lava stalagtites.
M195 CTD	195CTD	24.04.2005	09°34.5	13°12.5	1402	
M196 CTD	196CTD	24.04.2005	09°31.5	13°13.0	1550	

M197 CTD	197CTD	25.04.2005	09°33.9	13°12.7	1477	
M199 CTD	199CTD	25.04.2005	09°33.0	13°12.9	1473	
M200 ROV	200ROV_P-1	25.04.2005	09°32.99	13°12.92	1469	Aphyric pillow basalt. Vesicles: 5% up to 10 mm. Extensive Mn-Oxide coating. Patch of glassy crust, partially palagonitized.
	200ROV_P-2	25.04.2005	09°32.96	13°12.80	1523	Pillow basalt. Olivine phenocrysts: <1% up to 1 mm. Vesicles: 5 %, irregular shapes, up to 10 mm. Extensive Mn-oxide coating, 1 mm palagonitized glass crust.
	200ROV_P-3	25.04.2005	09°32.90	13°12.72	1505	Piece of lava lobe roof. Aphyric. Top surface shows mm-scale scretch marks (parallel to flow direction) and cm-scale flow folds (long axis normal to flow direction). Fresh glass crust (3 mm). Vesicles: 10% round and tubular. Lower surface: irregular stalagtite texture.
	200ROV_P-5	25.04.2005	09°32.93	13°12.51	1494	Bright orange Fe-oxihydroxide mud and few small pieces of semi-lithified material.
	200ROV_P-6	25.04.2005	09°32.92	13°12.53	1496	Piece of 6 cm thick aphyric lava crust. Glass crust (1-2 mm) with minor Mn-oxide coating. Upper layer is vesicle-free; lower 3 cm contain 20% tubular vesicles (up to 3 cm long and 0.5 cm wide) normal to surface with regular spacing.
	200ROV_P-7	25.04.2005	09°32.88	13°12.55	1495	Semi-lithified pieces of Fe-oxihydroxides; crude layering, no apparent Mn-oxides.
	200ROV_P-12	25.04.2005	09°32.71	13°12.55	1495	Section of aphyric pillow basalt. Vesicles: 10% round to irregular, locally coalesced (up to 2 cm). Glass crust (2 mm) with Mn-oxide coating and biological colonization.
M201 VSR	201VSR-1	25.04.2005	09°31.98	13°12.21	1551	Pelagic sediment.
M202 VSR	202VSR-1	25.04.2005	09°32.49	13°12.71	1512	Basalt glass.
M203 VSR	203VSR-1	26.04.2005	09°32.72	13°12.65	1509	Basalt glass.
M204 VSR	204VSR-1	26.04.2005	09°33.01	13°12.36	1518	Basalt glass.
M205 VSR	205VSR-1	26.04.2005	09°33.5	13°12.53	1497	One pillow fragment with glass crust and several glass chips.
M206 CTD	206CTD	26.04.2005	09°33.3	13°12.5	1469	
M207 ROV	207ROV	26.04.2005	09°32.9	13°12.5	1510	
M208 CTD	208CTD	26.04.2005	09°32.8	13°12.6	1501	
M209 TV grab	209GTV-1	26.04.2005	09°32.86	13°12.52	1511	Glassy volcanic crust; partially altered.
	209GTV-2	26.04.2005	09°32.86	13°12.52	1511	Orange to brown semi-lithified Fe-oxihydroxides; numerous pieces of fragile crusts up to 15 x 10 x 1 cm; fine grained.
M210 VSR	210VSR-1	26.04.2005	09°33.83	13°12.50	1482	Several pieces of aphyric basalt, abundant glass shards.
	211VSR-1	26.04.2005	09°34.13	13°12.55	1488	Fresh aphyric basalt glass.
M212 VSR	212VSR-1	26.04.2005	09°34.55	13°12.40	1413	Some glass chips.
M213 TV grab	213GTV-1	27.04.2005	09°32.83	13°12.55	1513	Basalt glass chips.
	213GTV-2	27.04.2005	09°32.83	13°12.55	1513	Fe-oxihydroxide crusts.
	213GTV-3	27.04.2005	09°32.83	13°12.55	1513	Thin (<1 mm) sheets of sulfides.
M214 TV grab	214GTV-1	27.04.2005	09°32.84	13°12.54	1511	Fresh aphyric basaltic glass chips.
	214GTV-2	27.04.2005	09°32.84	13°12.54	1511	Fe-oxihydroxide crusts.
	214GTV-3	27.04.2005	09°32.84	13°12.54	1511	Thin sheets (<1 mm) of sulfides.
M215 OFOS	215OFOS	27.04.2005	09°32.1	13°12.9	1550	
M216 CTD	216CTD	27.04.2005	09°32.8	13°12.9	1509	

*: Sample position accurate within +/- 1 to 2 m relative to the beacon set at 4°48,559'S; 12° 22,413'W
Abbreviations for sampling equipment: GTV-TV grab samples
ROV_AC-Accidentially sampled material during ROV dive due to seafloor contact
ROV_P-Sample taken on position with ROV manipulators
VSR-Vulkanit Stossrohr (wax-corer for volcanic rocks), ROV-PC - Particle Catcher deployed by ROV

1.7. Concluding Remarks

Cruise M64/1 was a very successful cruise without any major technological or logistical problems. The cooperation between the crew and the scientists resulted in a large number of successful sampling stations and numerous excellent geologic and biologic samples. Several outstanding results have been obtained like the sampling of the hottest vents known from the Mid-Atlantic Ridge, the finding of the southernmost vent field on the Mid-Atlantic Ridge, and the definition of several new targets for further exloration in this area. Consequently, M64/1 has made important new contribution to our understanding of the volcanic, hydrothermal and biologic processes on a slow-spreading axis and it also paved the way for further cruises during the lifetime of SPP 1144.

1.8. References

Baker, E.T. and Milburn, H.B., 1997. MAPR: a new instrument for hydrothermal plume mapping. RIDGE events, 8: 23-25.

Baker, E.T., Tennant, D.A., Feely, R.A., Lebon, G.T. and Walker, S.L., 2001. Field and laboratory studies on the effect of particle size and composition on optical backscattering measurements in hydrothermal plumes. Deep-Sea Research. Part I: Oceanographic Research Papers, 48(2): 593-604.

Charlou, J.L., Donval, J.P., Fouquet, Y., Jean-Baptiste, P., and Holm, N. (2002). Geochemistry of high H_2 and CH_4 vent fluids issuing from ultramafic rocks at the Rainbow hydrothermal field (36°14'N, MAR). Chem. Geol. 191, 345-359.

Desbruyères, D., Biscoito,M, Caprais, J.-C., Colaco, A., Comtet, T., Crassous, P., Fouquet, Y., Khripounoff, N., Le Bris, N., Olu, K., Riso, R., Sarradin, P.-M., Segonzac, M. and Vangriesheim, A. (2001): Variations in deep-sea hydrothermal vent communities an the Mid-Atlantc Ridge near the Azores plateau. – Deep-Sea Research I 48: 1325-1346.

Grasshoff, K., Kremling, K., Ehrhardt, M., 1999. Methods of Seawater Analysis. 3rd edition, 600 p., Wiley-VCH.

Kadko, D. C., Rosenberg, N. D., Lupton, J. E., Collier, R. W., and Lilley, M. D. (1990). Chemical reaction rates and entrainment within the Endeavour Ridge hydrothermal plume. Earth Planet. Sci. Lett. 99, 315-335.

Localli, C., Torsi, G., 2001. Voltammetric trace metal determinations by cathodic and anodic stripping voltammetry in environmental matrices in the presence of mutual interference. Journal of Electroanalytical Chemistry 509, 80-89.

Obata, H., van den Berg, C.M.G., 2001. Determination of picomolar levels of iron in seawater using catalytic stripping voltammetry. Analytical Chemistry 73, 2522- 2528.

Shank, T. (2004): The evolutionary puzzle of seafloor life. - Oceanus Magazine • Vol. 42, No.2 http://oceanusmag.whoi.edu/v42n2/shank.html.

van Damm, K.L., 2004. Evolution of the hydrothermal system at the East Pacific Rise 9°50'N: geochemical evidence for changes in the upper oceanic crust. In: Mid-Ocean Ridges: Hydrothermal Interactions between the Lithosphere and Oceans.

Seifert, R., Delling, N., Richnow, H.H., Kempe, S., Hefter, J., and Michaelis, W. (1991). Ethylene and methane in the upper water column of the subtropical Atlantic. Biogeochemistry 44, 73-91.

Meteor Berichte

Mid-Atlantic Expedition 2005

Cruise No. 64, Leg 2

Longterm study of hydrothermalism and biology at the Logatchev field, Mid-Atlantic Ridge at 14°45'N (revisit 2005; HYDROMAR II)

6 May – 6 June 2005, Fortaleza (Brazil) – Dakar (Senegal)

K.S. Lackschewitz, M. Armini, N. Augustin, N. Dubilier, D. Edge, G. Engemann, M. Fabian, J. Felden, P. Franke, A. Gärtner, D. Garbe-Schönberg, H.-H. Gennerich, D. Hüttig, H. Marbler, A. Meyerdierks, T. Pape, M. Perner, M. Reuter, G. Ruhland, K. Schmidt, T. Schott, M. Schroeder, G. Schroll, C. Seiter, J. Stecher, H. Strauss, M. Viehweger, S. Weber, F. Wenzhöfer, F. Zielinski

Project Leader: Heiner Villinger

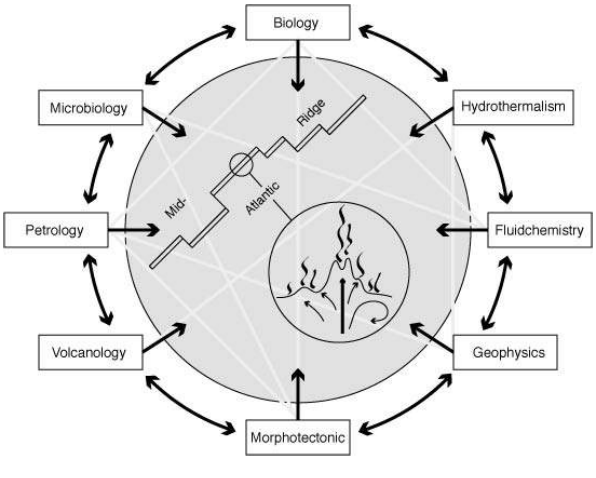

Table of Contents Part 2 (M64/2)

2. Leg M 64/2

2.1 Participants

	Name	Discipline	Institution
1.	Lackschewitz, Klas, Dr. / Chief Scientist	Mineralogy	IFM-GEOMAR
2.	Amini, Marghaleray	Fluid Chemistry	IFM-GEOMAR
3.	Augustin, Nico	Mineralogy	IFM-GEOMAR
4.	Dubilier, Nicole, Dr.	Microbiology	MPI Bremen
5.	Edge, Dave	ROV	SOC
6.	Engemann, Greg	ROV	ASR
7.	Fabian, Markus, Dr.	Geophysics	GeoB
8.	Felden, Janine	Microbiology	IFM-GEOMAR
9.	Franke, Philip	ROV	MARUM
10.	Gärtner, Andrea	Microbiology	IFM-GEOMAR
11.	Garbe-Schönberg, Dieter, Dr.	Fluid Chemistry	IfG Kiel
12.	Gennerich, Hans-Hermann, Dr.	Geophysics	GeoB
13.	Hüttig, Daniel	ROV	MARUM
14.	Marbler, Herwig, Dr.	Fluid Chemistry	IUB
15.	Meyerdierks, Anke, Dr.	Microbiology	MPI Bremen
16.	Pape, Thomas, Dr.	Gas Chemistry	IfBM Hamburg
17.	Perner, Mirjam	Microbiology	IFM-GEOMAR
18.	Reuter, Michael	ROV	MARUM
19.	Ruhland, Götz	ROV	MARUM
20.	Schmidt, Katja	Fluid Chemistry	IUB
21.	Schott, Thorsten	Technican	IFM-GEOMAR
22.	Schröder, Marcel	ROV	MARUM
23.	Schroll, Gunnar	Gas Chemistry	IfBM Hamburg
24.	Seiter, Christian	ROV	MARUM
25.	Stecher, Jens, Dr.	Zoology	Senckenberg
26.	Strauss, Harald, Prof. Dr.	Geochemistry	GPI Münster
27.	Viehweger, Marc	Microbiology	MPI Bremen
28.	Weber, Stefan	Gas Chemistry	IfBM Hamburg
29.	Wenzhöfer, Frank, Dr.	Microbiology	MPI Bremen
30.	Zielinski, Frank	Microbiology	MPI-Bremen

ASR	Alstom Schilling Robotics 201 Cousteau Place Davis, CA 95616 / USA
GeoB	Universität Bremen FB Geowissenschaften Postfach 330440 28334 Bremen / Germany
GPI	Geologisch-Paläontologisches Institut Westfälische Wilhelms-Universität Münster Correnssstraße 24 48149 Münster / Germany
IfBM	Universität Hamburg Institut für Biogeochemie und Meereschemie Bundesstr. 55

	D-20146 Hamburg / Germany
IfM-GEOMAR	Leibniz-Institut für Meereswissenschaften Düsternbrooker Weg 20 D-24105 Kiel / Germany Wischhofstr. 1-3 D-24148 Kiel / Germany
IfG	Universität Kiel Institut für Geowissenschaften Olshausenstr. 40 D-24098 Kiel / Germany
IUB	International University Bremen Geosciences and Astrophysics P.O. Box 750561 D-28725 Bremen / Germany
MARUM	Zentrum für Marine Umweltwissenschaften Universität Bremen Postfach 330440 D-28334 Bremen / Germany
MPI-Bremen	Max-Planck-Institut für Marine Mikrobiologie Celsiusstr. 1 D-28359 Bremen / Germany
Oktopus GmbH	Kieler Str. 51 D-24594 Hohenwestedt / Germany
RCOM	Forschungszentrum Ozeanränder an der Universität Bremen Postfach 330440 D-28334 Bremen / Germany
Senckenberg	Forschungsinstitut Senckenberg Senckenberganlage 25 D-60325 Frankfurt a. M. / Germany
SOC	Southampton Oceanography Centre, European Way, Southampton SO14 3ZH, U.K.

2.2 Research Program

(K. S. Lackschewitz, H. Villinger)

The investigations of this cruise are a continuation of the program started between 14°45'N and 15°05'N on the Mid-Atlantic Ridge in 2004 (cruise M60/3). While in the 2004 cruise basic geochemical and biological studies were carried out in the Logatchev hydrothermal field, the emphasis of the 2005 cruise lies on the temporal variability of fluid emanations, fluid temperature and chemistry, microbial activities and associated fauna at selected hydrothermal vent sites. The overall goal of the proposed cruise is to advance the integrated study of the 14°45'N hydrothermal sites further through multi-disciplinary characterization and sampling at several sites. Biological, mineralogical and hydrological samples are to be taken in a well-characterized thermal environment so that the results on the samples can be interpreted in terms of the influence of the important environmental parameter temperature.

Long-term monitoring of all relevant environmental parameters is essential to assess the temporal variability observed in the biogeochemistry of the hydrothermal field. The parameters are (a) temperature, (b) absolute pressure, (c) mean micro seismicity and (d) local sea floor tilt. We will observe correlation and coupling between hot fluid outflow, hydrothermal activity, tidal loading, micro seismicity and recent tectonic processes with high resolution of amplitudes and time. Additionally, a plume temperature profiler for mapping the extend of the hydrothermal plume, a distributed temperature sensing system for monitoring in particular biological communities at the sea floor, a ROV temperature lance with online data transfer over the ROV communication system up to the ship and a temperature calibration facility for the temperature sensors is provided. Temperature measurements, the use of sensors and the sampling of fluids to determine the chemical composition of the fluids, material fluxes and spatial and temporal gradients give the basic information to characterize the environment in which the ecosystem develops. Three groups are mainly interested in the characterization of free living microorganisms, which are involved in carbon and sulfur cycling in hydrothermal vent areas. Methane consuming communities are studied in hydrothermal fluids, sediments and crusts with a special focus on the process of anaerobic oxidation of methane and in close cooperation with the gas geochemistry group. Another group is predominantly interested in sulfur bacteria and in the influence of temperature on microbial communities, cooperating closely with the groups analyzing sulfur species and isotopes. Environmental genomics are applied to investigate the metabolic capabilities of these microbial communities, thereby focusing on the finding of new genes and unexpected metabolic properties. The development of symbiotic communities (bacteria and host fauna) is directly related to the chemical content and energy of the fluids. However, the pathway of interactions does not only involve influence of the fluids on the development of organism communities, but microorganisms and fauna also change the fluid chemistry due to their uptake and excretion of chemical compounds.

Samples for the biologists are chosen in cooperation with the geochemists measuring the different abiotic parameters. The samples are shared between the different groups, analyzed in close collaboration and the results will be finally evaluated in the context of all geochemical and microbiological findings with respect to the bio-geo coupling. The aim is to develop an overall model for the temporal and spatial development of the Logatchev hydrothermal ecosystem.

2.3 Narrative of the cruise

(K.S. Lackschewitz)

The final preparations for cruise M64/2 were completed onboard the R/V METEOR in the harbour of Fortaleza (Brazil) between May 3 and 6. All 22 scientists of Leg M64/2 boarded the ship on May 5. A test of the ROV in the harbour was successfully carried out at midday on May 6.

The R/V METEOR cleared port of Fortaleza in the afternoon of May 6 and began her transit to 13°30’N and 45°00’W. The scientists used the five-day transit to set up the laboratories and to test their sensors and water sampling equipment. Scientific work started in the afternoon of May 10 with a reference CTD hydrocast station at 13°30'N/45°00’W for sampling seawater from different waterdepths. Hydrosweep mapping along the ridge axis was carried out during the night. A 90 minute transit to our main working area, the Logatchev hydrothermal field (LHF-1; 14°45.20’N/44°58.80’S), was followed by a CTD hydrocast station to investigate the hydrothermal plume over the LHF-1.

In the morning of May 11 the first ROV station failed shortly after deployment due to communication problems between the ROV and the control container. Therefore, a hydrocast station was carried out SW of LHF-1 to investigate the hydrothermal plume dispersal in the water column. A TV-grab (222GTV) was taken about 300m SW of LHF-1 in order to sample the periphery. The samples comprised of serpentinized ultramafics, partly covered with Mn-crusts, and one rock with atacamite. The night of May 12 was filled with a MAPR (miniatur autonomous plume recorder) string jo-jo (5 MAPP's and 20 temperature loggers) to trace the turbidity anomalies of the hydrothermal plume in the area of LHF-1.4.

On May 12 another attempt of a ROV dive failed again due to communication problems. A TV-grab station taken ca. 50 m southwest of IRINA II sampled ultramafics and Mn crusts. In the afternoon we started our first successful ROV dive (224) during our cruise M64/2. After reaching the seafloor we obtained an acoustic signal from the homer beacon 12 which we set up as a reference station during the cruise M60/3 at the QUEST site. We set up another beacon (Nr. 14; 14°45,199'N/44°58,783'W) and an ocean bottom tilt meter (OBT) ca. 42 m southwest of beacon 12. Fluid samples and temperature measurements were taken at a small active black smoker close to the IRINA-II smoker complex.

We continued our geological program with a TV-sled track from the NE to the SW over the LHF-1 in order to find hydrothermal precipitates and map the distribution of ultramafics in this area. Another hydrocast station should further map the distribution of the hydrothermal plume in the water column, whereas a stationary MAPR string over this area should map the temporal variations of the proximal hydrothermal plume. During May 13 a ROV deployment was not possible due to a high sea swell.

The night to the May 14 was filled with two TV-grab stations and one hydrocast station. 229GTV was taken ca. 50 m west of ANNA LOUISE. The samples comprised of weakly indurated to higher indurated brownish sediment, dark grayish sediment with fine dispersed pyrite crystals, and several Mn-crusts. At station 230GTV south of site „A“ the samples consist of altered coarse-grained to pegmatoid orthopyroxenites. The hydrocast station (231CTD) sampled the hydrothermal plume ca. 200 m northwest of the QUEST site.

During dive 232ROV on May 14 biological and fluid samples were taken from a mussel field at the southern rim of the IRINA II compex. A special objective was a mussel transplant experiment. In this experiment we are investigating how the removal of the mussels from the vent fluids will influence them and their symbiotic bacteria. Before collecting the mussels, insitu measurements of several physico-chemical parameters were taken (oxygen, temperature, sulfide, hydrogen, pH) with a profiler module. In addition, fluid samples were taken.

Plume mapping with the CTD was carried out during the night of May 14 to 15. The northernmost CTD station detected three turbidity anomalies at 2700 m, 2900 m and 3050 m ca. 1.5 km NNW of the LHF-1 suggesting at least one other unknown hydrothermal source. A TV-grab (st. 239) was taken ca. 250 m northeast of IRINA-II in order to sample the periphery of the LHF-1. Beside much sediment, crusts covered with atacamite and several pieces of talc were detected. On the sediment surface we found several mussel shells of *Bathymodyolus* and *Phymorhynchus*.

Hydrosweep mapping along 5 profiles was carried out during the night of May 16 to 17. The objective was to map the upper ridge flank east of the Logatchev field.

During dive 244ROV on May 17 the OBT was set up on a plain place together with beacon 14 to the SW of IRINA II. In the following we have continued the mussel transplant experiments of 232ROV by taking 5 nets with mussels and puting them in the inactive area of the OBT. Temperature measurements in the mussel field produced readings ranging between 5 and 50°C. Four hydrocast stations (st. 245 to 248) were carried out in the N of LHF-1. The objective of these stations was to investigate the distribution of the turbidity anomalies in 2700 m, 2900 m and 3050 m.

On May 18 station 249ROV was reserved for fluid sampling of black smokers at ANNA LOUISE and IRINA I. At both sites temperature measurements with an 8-channel temperature probe produced values of 205°C and 188°C, respectively. A TV-grab (st. 250) between IRINA II and site „B“ sampled a thick sediment unit showing colors from yellowish brown, reddish brown and green. A temperature measurement in the sediment yielded still 43°C. In addition, samples consist of silicified crusts and highly altered peridotites and pyroxenites.

The dive 252ROV on May 19 aimed at detailed mapping the southernmost area of LHF-1 including site „A“ which was not discovered during M60/3. After the installation of beacon 11 at IRINA I site we started our mapping profiles south of ANNA LOUISE. On the second profile we found a 5m high active black smoker which is related to site „A“, first described by Gebruk et al. (1997). We named this smoker „Barad-Dûr“ after the black tower of Mordor in the book „Lord of the Rings“. The marker “MB” indicates this site as a reference sampling station. We sampled several sulfide fragments from the underlying mound of Barar-Dûr and another rock sample from the IRINA I site. In the following, we deposited the markers “M4” and “M5” at site ANNA LOUISE and IRINA I, respectively.

Four hydrocast stations (st. 253-256) during the night from May 19 to 20 mapped and sampled the plume in 2700 to 2800 m ca. 600 m to the northwest of LHF-1.

During the day of May 20 the dive ROV257 placed 10 temperature loggers in the mussel field at IRINA II for longterm monitoring. Another main target of this dive was to sample fluids, sulfides and bacteria mats at site „B“. The onboard analyses of the fluids have shown a pH of 3.9. The following night two TV grab stations east and northeast of QUEST and a hydrocast station to the NNW of LHF-1 were carried out. The first TV grab (st. 258) sampled a few shells of the hydrothermal mussel species *Calyptogena* and several small peridotite pieces. The second TV-grab (st. 259) was empty. The hydrocast (st. 260) sampled 11 water samples from different water depth ca. 1.5 km NNW from LHF-1.

Station 261ROV on May 21 concentrated on fluid sampling at Site „A“ and IRINA I (indicated by marker “MD”). In addition, sulfides were sampled at both sites. During the night Hydrosweep mapping was continued on the upper ridge flank to the east.

During dive 263ROV on May 22 a special objective was a sampling program in the area of the Russian marker ANYA. We sampled two push cores for bacterial studies and mussels with a net. In addition, we set up a beacon (#11) to provide a precise site location because the original position according to Gebruk et al. (2000) appeared to be northwest of IRINA II.

We continued our program with two hydrocast stations west of LHF-1. Both stations showed no turbidity anomalies, but water samples between 2700-2800 m have still minor methan anomalies.

During ROV station 266 on May 23 fluid parameters were measured directly above five places in a diffuse venting mussel field of IRINA II by the profiler module. After the investigation of this site we picked up beacon 11 near the marker „ANJA“ and placed it 10 m east of site „B“. In the following, we took fluid samples at a black smoker which is close to the sampled smoker of 257ROV. Temperature measurements at both sites show values of 350°C and 300°C..

Four hydrocast stations (st. 267-270) ca. 0.5-1 sm south and southeast of LHF-1 did not show a turbidity signal of the plume. However, we have still identified the plume by a slight increase of CH_4 in water samples between 2700-2800 m

On May 24 we started with a deployment of a 25 m longterm temperature mooring from the ship (st. 271). During the following ROV station 272 we repositioned this mooring in the region between IRINA I and ANNA LOUISE. Another target was the precise horizontal placement (angle of < 2°) of the OBT at beacon 14. In addition, we placed two push cores in the mussel field of IRINA II for microbial experiments and we took some samples from an inactive smoker ENE of IRINA II.

Another four hydrocast stations (st. 273-276) have indicated that the eastern ridge flank acts as a boundary for the distribution of hydrothermal plume to the east and northeast.

During dive 277ROV on May 25 we placed again the profiler module in the diffuse venting mussel field at IRINA II. Temperature measurements showed values up to 140°C. In addition, a baited trap was deployed on the mussel bed close to the chimney complex. Detailed video images were recorded along two horizontal profiles of the eastern part of the chimney complex for constructing a photomosaic of this whole structure. Diffusely venting fluids were sampled at the chimney complex close to the area which was already sampled during M60-3 (st. 38ROV). Hydrothermal fauna were collected here also. At the end of the dive we mapped the area east of IRINA II along two profiles.

A TV-sled track (st. 278) was carried out 2 sm north of LHF-1 in order to find indications of an active vent field creating the hydrothermal plume in 3050 m water depth. Due to an electric failure this station was aborted shortly after the first profile. In following two hydrocast station were carried out above the QUEST vent site and ca. 3 sm NW of LHF-1.

The main target of dive 281ROV was a sampling program at the QUEST site. First we placed a benthic chamber on a mussel bed at IRINA II to measure H_2 and S^{2-} for several hours. At QUEST site we sampled fluids and a net of hydrothermal fauna at a diffuse venting mussel bed. At this site we placed also 9 longterm temperature monitoring loggers. In addition, we took fluid samples, temperatures and sulfide samples from a hot venting black smoker (indicated by marker "MC"). During the following night Hydrosweep mapping was continued on the upper eastern ridge flank.

At dive 283ROV on May 27 we continued our work at QUEST site. We deployed two 8-channel temperature loggers in the main mussel bed and sampled diffuse fluids with 3 Niskin bottles. A camera survey over the mussel bed was made to produce a photomosaic. Next we placed the OPT on more stable ground and took the last net for the mussel bed experiment. In the following we finished our sampling program in IRINA II taking another fluid samples, temperatures at two vents and a net with shrimps. At the end of the dive we picked up the beacon 13 and the baited trap. The night to May 28 was filled with another TV-sled station (st. 284) which investigated the area northwest of LHF-1 along several profiles searching unknown hydrothermal sites.

After this TV-sled track our last ROV station (285ROV) explored and mapped the area northwest of QUEST site in order to find an unknown vent site. After several profiles we found a new diffuse venting site with several highly altered crusts ca. 150 m northwest of QUEST site.

Station work of cruise M64/2 was finished after this station and R/V Meteor started her transit to Dakar. R/V Meteor arrived the port of Dakar on June 4, at 06:00 am. All containers were brought to the pier and loaded there by the scientific and technical crew. The scientists of cruise M64/2 disembarked until the early evening of June 6, 2005.

2.4 Preliminary Results

2.4.1 Detailed geological studies of the Logatchev-1 hydrothermal field
(K.S. Lackschewitz, N. Augustin)

The geological setting and structure of the Logatchev-1 hydrothermal field (LHF-1), situated on a small plateau on the eastern flank of the inner rift valley at 14°45' N, has been described by several workers (e.g., Krasnov et al. 1995; Gebruk et al., 1997). Extensive bathymetric and video mapping of the LHF during the first RV Meteor cruise M60/3 have revealed the main factors of its tectonic control (Kuhn et al., 2004). Detailed sampling has allowed study of the interrelationship of geological, geochemical and biological processes of an ultramafic-hosted hydrothermal system.

The present detailed work carried out during the second RV Meteor cruise M64/2 resulted in a further mapping and sampling as well as the first deployments of long term monitoring stations (Fig. 2.1).

The LHF-1 extends at least 800 m in a NW-SE and probably more than 400 m in a SW-NE direction as previously described by Kuhn et al. (2004). At the southeastern end of LHF-1 we discovered the 5m high black smoker of Site“ A“ which was previously identified by Gebruk et al. (1997). We gave this smoker the name „Barad-Dûr“ after the black tower of Mordor in the book „Lord of the Rings“. Barad-Dûr is sitting on a 3 m-high mound of chimney talus. There were no mussel beds at this site, and hydrothermal fauna was restricted to shrimps and crabs on the upper part of the smoker. A photographic and video survey obtained by the ROV proved to be adequate for preparing a photomosaic of the structure (Fig. 2.2A).

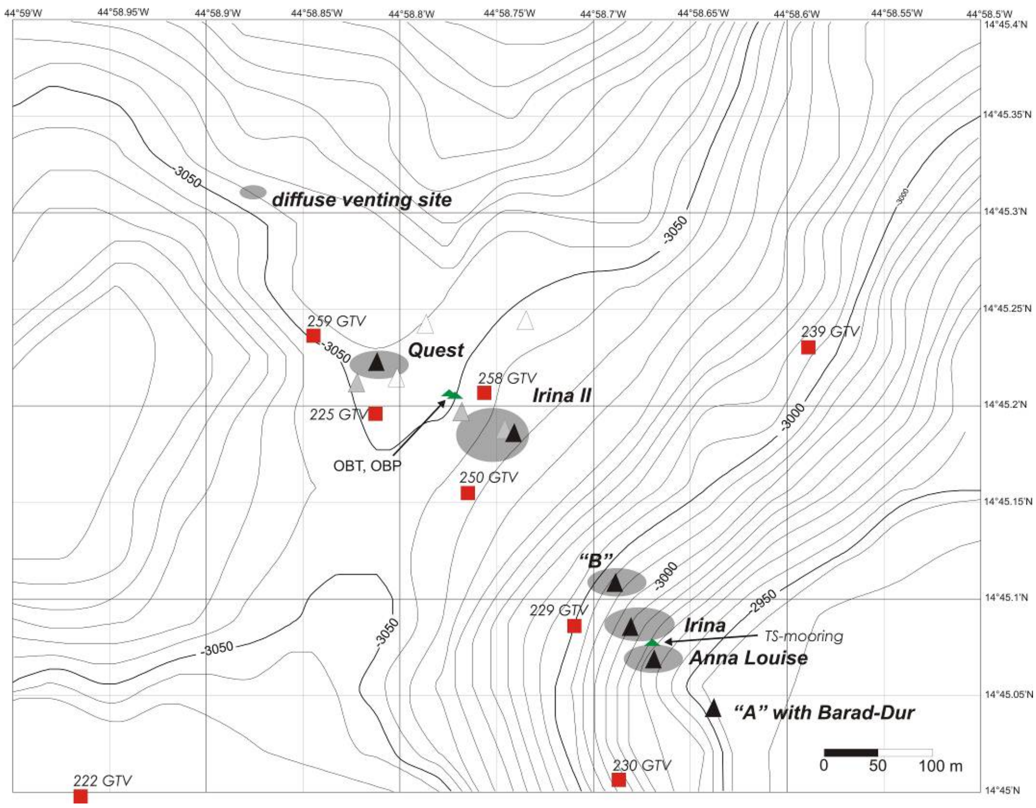

Fig. 2.1 Logatchev-1 hydrothermal field with long-term monitoring and TV-Grab stations carried out during M64/2. A new diffuse venting-site is indicated NW of QUEST.

Hydrothermal fluids were sampled here for the first time. The marker „MB“ indicates this site as a reference fluid sampling station. In addition, several chimney fragments were sampled at the base of Barad-Dûr.

The area northwest of site „A“ is characterised by the three hydrothermal sites ANNA LOUISE, IRINA und „B“ consisting of smoking craters. At ANNA LOUISE black smoke was intensely venting from the chimneys on the crater rim and from holes in the ground within the crater. Strong bottom currents resulted in almost horizontal plume dispersal to the south. Therefore, the so-called „Candelabrum“ chimney on the southern rim of the crater (Kuhn et al., 2004) was hidden from view during most of our observations. A 25 m-long temperature sensor mooring, which we have set up between ANNA LOUISE and IRINA, should measure the temperature variations of the plume dispersal over several months. Hot fluids and chimney fragments were sampled from a black smoker on the norther crater rim of ANNA LOUISE. Other fluid and rock samples were taken also at IRINA and „B“.We deposited a marker „MA“ at the sampled smoker of site „B“ and a marker „MD“ at the sampled smoker of site IRINA. Temperature measurements of the fluids have shown values of 205°C for ANNA LOUISE, 177°C for IRINA (at marker „MD“) and 350°C for site „B“ (at marker „MA“). Another small smoker at site „B“ has revealed a temperature of 300°C.

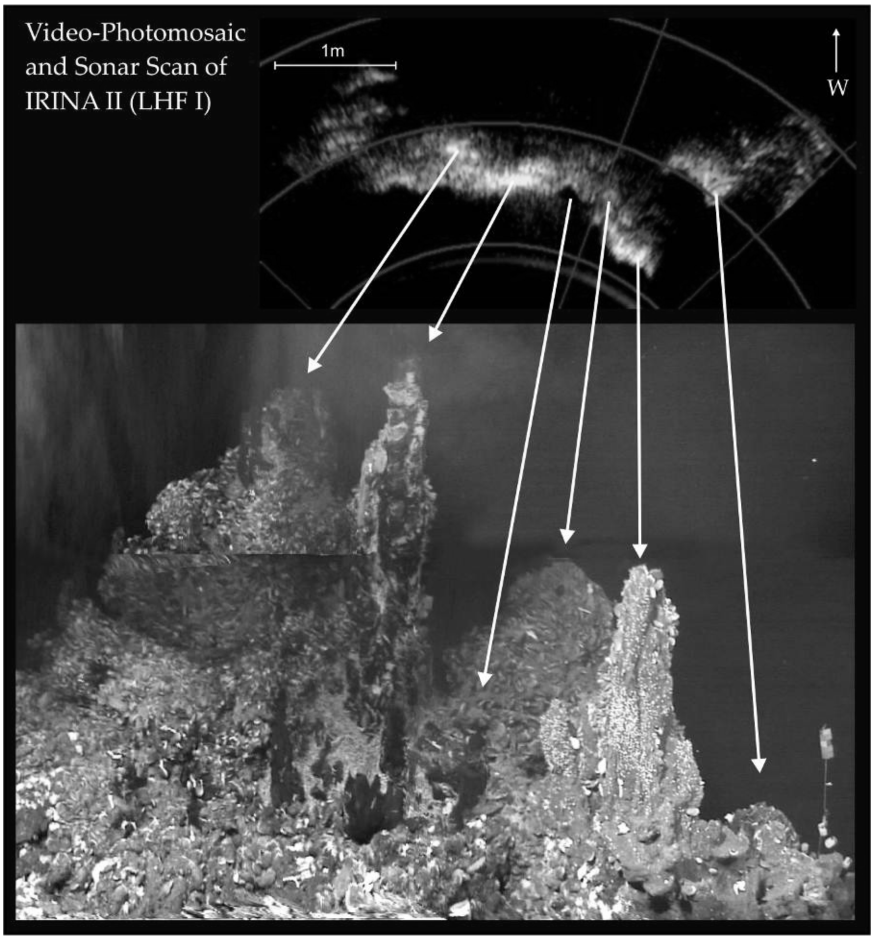

Fig. 2.2 A Photomosaic of Barad-Dûr (Site “A”). B: Photomosaic and Sonar Scan of the eastern IRINA II chimney complex.

The largest site in the LHF-1 is IRINA II which was one of main targets of our biological studies. IRINA II consists of a mound with steep slopes rising about 15 m above the surrounding seafloor. A chimney complex, ca. 2 m high, marks the top of the mound. Based on a video and photographic survey we were able to create a photomosaic of this smoker complex (Fig. 2.2B). A sonar scan shows clearly the different chimney structures.

Most of the chimneys are densely overgrown with mussels (*Bathymodiolus*). Shrimps are (*Rimicaris exoculata*) highly concentrated over low-temperature fluids along the sides of the chimneys. The chimney complex is surrounded by densely populated mussel beds and by small active and inactive chimneys. Temperature measurements at a small active chimney on the northwestern side yielded values of up to 170°C, whereas a small chimney in between the complex revealed values of up to 225°C. These chimneys were also sampled for hot fluids. The mussel beds around the chimney complex are characterized by diffuse venting fluids. The temperatures of these emanating fluids, which were measured by a profiler module have shown a temperature range of 2.6° to 8°C (see chapter 2.4.10). We placed ten temperature loggers on a mussel bed at the southeastern side of the smoker complex to monitore the diffuse venting fluids for several months. A special objective was a mussel transplant experiment. In this experiment we are investigating how the removal of the mussels from the vent fluids will influence them and their symbiotic bacteria (see chapter 2.4.9).

As already described by Kuhn et al. (2004) the area around the Russian marker ANJA is located at a slope approximately 30 m northwest of the IRINA II-complex. This marker identifies a site called ANJA'S GARDEN in Gebruk et al. (2000) and these authors described that it occurs a 100 m northwest of IRINA-II. Based on our precise DVL navigation, we assume that the Gebruk et al. (2000) description of the ANJA marker location is incorrect. At the ANJA marker we found clusters of living and dead *Bathymodiolus* shells together with shimmering water. Visual observations during our dives in this area indicated that vesicomyid clams might be present. However, a ROV sample taken from the area of an old marker „C“, which is located close to the ANJA marker, revealed only *Bathymodiolus* shells.

Just north of the IRINA II mound we placed an Ocean Bottom Tiltmeter (OBT) and an Ocean Bottom Pressuremeter (OBP) as longterm monitoring stations (see chapter 2.4.4) close to the new LHF-1 reference beacon 14 (14°45.199' N/44°58.783' W).

The QUEST site, which was newly discovered during our first Meteor cruise M60/3 (Kuhn et al., 2004), is situated ca. 130 m WNW of the chimney complex of IRINA II. It is characterized by a smoking crater surrounded by several small active chimneys. Fluids and chimney fragments were sampled from a small black smoker on the northeastern side of the crater indicated by the marker „MC“. We have measured here fluid temperatures up to 285°C. Elongated clusters of mussels occur southeast of the smoking crater. ROV samples revealed that the mussels consists of abundant juvenile forms which is in contrast to the high abundance of adult forms at IRINA II. A temperature logger (#3), which we deployed here on the M60/3 cruise, showed values of up to 12°C. Therefore, we placed here nine 1-channel temperature loggers and two 8-channel temperature loggers for longterm measurements.

Mapping the area north of QUEST site with the ROV revealed sediments with ripple marks intercalated by several ultramafic outcrops. At ca. 150 m northwest of the QUEST site we found a diffuse venting site with highly altered ultramafics confirming a larger extent of LHF-1 similar to the observation made by Kuhn et al. (2004).

2.4.2 ROV deployments

(G. Ruhland and ROV-Team)

The remotely operated deep diving robot QUEST is an electrical 4000 m rated, work class ROV, which is operated by MARUM, University of Bremen, since May 2003. The vehicle has been manufactured by Schilling Robotics, Davis, USA. The total QUEST system weights 45 tons (including the vehicle, control van, workshop van, winch, 5000 m umbilical, launch-and-recovery-frame, and two transportation vans, all 20-feet-size). The 5000 m of 17.6mm NSW umbilical is stored and managed by an electrical MacArtney Cormac winch. No hydraulic connections have to be installed during mobilisation.

QUEST's first use within SPP1144 took place during Rv METEOR leg M60/3 in January 2004. The leg M64/2 is the second task of QUEST in the Logachev Hydrothermal Vent Field. The technical innovations of the ROV provided a flexible and highly adaptable platform for scientific sampling and observation tasks and therefore played a major role to the scientific success aboard Rv METEOR. Since the previous leg new features have been additionally installed including the highly integrated USBL positioning system, based on the french IXSEA-GAPS Inertial Navigation and Positioning system. However, due to a malfunction of the GAPS system Inertial Navigation and Positioning could be used only very limited. In addition, QUEST uses a Doppler velocity log (DVL) to perform StationKeep or Displacement mode, automatically controlled 3D positioning, and other auto control functions. Navigational purposes were supported by an array of Sonardyne HF beacons set in the vent field. An additional frame installed in the ship's A-frame enables much smoother and safe handling of the ROV during launch and recovery.

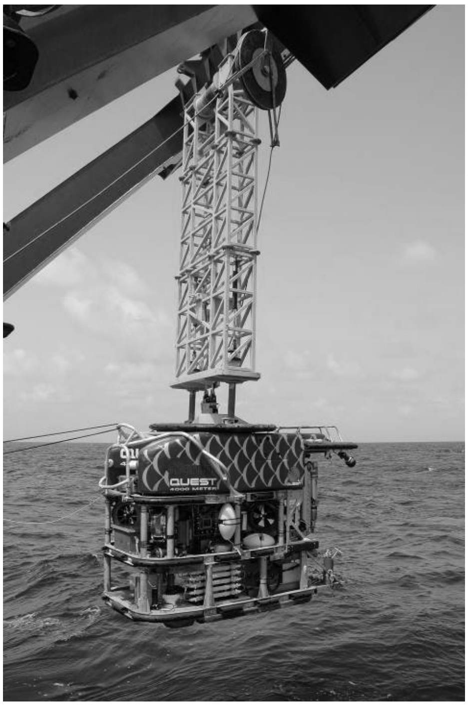

Fig. 2.3 Launching of the ROV with an additional frame at the aft (Photo: D. Garbe-Schönberg).

The QUEST system can be precisely controlled with its 60 kW electric propulsion system and is operated as free-flying vehicle. No tether management system (TMS) has to be operated at the same time the ROV is working. The collection of biological and geological samples and the pumping of fluids could be done with two installed robotic arms. While the RIGMASTER manipulator can lift and handle devices or samples up to 250 kg, the ORION manipulator is used to handle probes or work on delicate tasks.

A set of video and still picture cameras together with a 2.4 kW light suite provides possibilities for video mapping and photo mosaicing. Therefore two green lasers which are installed parallel to each other can be used as size relation. Due to a water leak the Insite Pacific ATLAS camera could be used on the first four dives only.

Besides cameras and manipulators, the scientific equipment installed during leg M64/2 constisted of a CTD with turbidity and high-temperature sensors, which could be used only on three dives due to a water intrusion in the housing. A set of niskin bottles, a 675 kHz scanning sonar, a sample drawbox and several different sampling tools such as “hand” nets and grabbing devices complete the installed equipment.

The scientific data base system used at MARUM feeds all ROV- and ship-based science and logging channels into an adapted real-time database system (DAVIS-ROV). The QUEST control system provides transparent access to all RS-232 data and video channels. During operation data and video has be distributed by the real-time database via the ship’s network system in different laboratories and supply the scientists with data from their own devices. Dive summaries containing all data of interest including video and digital still photographs were compiled after each dive. Using the database's export capabilities in combination with the software product "ADELIE" developed at IFREMER, GIS based plots, data graphs and divetrack maps containing time and position-referenced scientific data, video and images were available shortly after or even during the dives.

Post-cruise data archival will be hosted by the information system PANGAEA (www.pangaea.de) at the World Data Center for Marine Environmental Sciences (WDC-MARE), which is operated on a long-term base by MARUM, University of Bremen, and the Foundation Alfred Wegener Institute for Polar and Marine Research, Bremerhaven (AWI).

During leg M64/2 QUEST could be successfully deployed 15 times while 14 of these dives reached the bottom. Launch and recovery has been done at sea states up to 2.5 m and winds of up to 6 bft.. Total bottom time of 110 hours could be achieved at depths of 2950 to 3050m. The planned scientific program could be finished completely during the leg. Beneath scientific sampling and photo mosaicing the current working map could be improved and completed in some parts. Two scientific devices, an ocean bottom tiltmeter (OBT) and an ocean bottom pressure sensor (OBP) had been transported with the ROV to the bottom and installed during the dives. 24 temperature loggers for a yearly monitoring program were also distributed in mussel fields. A profiler frame and a benthic chamber had been successfully transported and set with the ROV several times for a daily monitoring.

During all operations, the crew of Rv METEOR provided a very successful and smooth handling on deck, excellent navigation and professional technical support to fulfill the scientific tasks required.

2.4.3 OFOS deployments

(N. Augustin, H.-H. Gennerich, K.S. Lackschewitz, H. Marbler, T. Pape, S. Weber, G. Schroll)

A total of 3 TV-sled stations were carried out in the vicinity of LHF-1. The objectives of the OFOS (Ocean Floor Observation System) stations were to find signs of unknown hydrothermal activity.

The IFM-GEOMAR TV-sled was equipped with a BENTHOS photo camera and flash, a SONY digital camcorder and a FSI 3’’ memory CTD probe. During our first OFOS-station 226 we have mapped a NW-SE profile between 14°45.4’ N/44°58.35’ W and 14°44.85’ N/44°59.1’ W crossing site „B“ of LHF-1. The beginning of the profile is characterized by a talus field followed by sediments, where we found four temperature anomalies with an increase of 0.03°C. One of this anomalies is close to 239GTV-station showing a temperature of the sampled sediments of 43°C onboard. When we crossed site „B“ no sign of hydothermal activity was visible. However, we have measured a temperature anomaly of 0.06°C. The area southeast of LHF-1 is characterized by sediments, some talus and an ultramafic outcrop showing a temperature anomaly of 0.025°C.

Station 278OFOS was carried out to investigate observations during M64/2 stations 238CTD; 253CTD and 273CTD, where physico-chemical parameters in the water column suggested a yet undiscovered fluid source different from the known black smokers of the LHF. The OFOS was equipped with one MTL (Miniature Temperature Logger; see chapter 2.4.5) and one MAPR (Miniature Autonomous Plume Recorder; see chapter 2.4.6.2). Due to cable problems station 278OFOS was interrupted early after 1.5 hrs.

Consequently the area between LHF and the water chemical anomaly in it’s north west was the target of the next OFOS survey, station 284OFOS. This time OFOS, bottom control weight and deep sea cable were equipped with a dense array of 5 MAPRs, 20 MTLs and 1 CTD between the sea floor and up to 100 m above it, with singular extra sensors in 125 m and 170 m height.

Same as station 226OFOS, also stations 278OFOS and 284OFOS did not show any hints to hydrothermal activities by visual observations. The CTD results of these stations are presented and discussed in chapter 2.4.6.2.

2.4.4 Description of rocks and hydrothermal precipitates

(N. Augustin, H. Strauss)

During cruise M64/2 a total of 14 ROV dives and 8 TV-grab stations recovered geological samples from the seafloor. Information on all sampling stations is given in Table 2.1.

Table 2.1 List of geological samples with geographical positions of individual stations.

Lat	Long	Station	Sample types
14°44.99´N	44°58.97´W	222 GTV	serpentinized pyroxenites
14°45.19´N	44°58.82´W	225 GTV	serpentinized pyroxenites, Mn-crusts
14°45.08´N	44°58.72`W	229 GTV	silicified crusts, consolidated sediments, sulfidic muds
14°45.01´N	44°58.68´W	230 GTV	Mn-coated pyroxenites, weakly weathered
14°45.23´N	44°58.58´W	239 GTV	atacamite and silicified crusts
14°45.18’N	44°58.73’W	244 ROV	altered sulfide breccia
14°45.16´N	44°58.77´W	250 GTV	strongly altered peridotites and pyroxenites, quartz-veins
14°45.04’N	44°58.63’W	252 ROV	sulfides chimney-pieces
14°45.12’N	44°58.70’W	257 ROV	Fe-oxide-hydroxide crusts, sulfides
14°45.21´N	44°58.76´W	258 GTV	some Mn-Coated serpentinite pebbles

14°45.24´N	44°58.84´W	259 GTV	GTV empty
14°45.06'N	44°58.64'W	261 ROV	sulfide chimney
14°45,10'N	44°58,67'W	266 ROV	sulfides
14°45.20'N	44°58.74'W	272 ROV	iron-oxide and -hydroxide crusts
14°45.20'N	44°58.74'W	277 ROV	sulfides
14°45.21'N	44°58.81'W	281 ROV	sulfides
14°45,32'N,	44°58,84'W	285 ROV	Fe-oxide, -hydroxide crusts and mud

In general, serpentinized peridotites represent the host rocks of the Logatchev field. Remarkable are samples of coarse grained orthopyroxenites, which are interpreted as magmatic cumulates from the crust/mantle transition zone. Apart from these host rocks, a large variety of hydrothermal samples were collected, confirming the observations made in 2004 during Meteor cruise M60/3. Samples include pieces of active and inactive chimneys, massive sulfides, silicified breccias and crusts, hydrothermal sediments, abundant secondary Cu-sulfides, hematite impregnated serpentinites, abundant Fe-Mn-oxyhydroxides as well as atacamite and Mn-oxides.
Several TV grabs (222GTV, 225GTV, 239GTV, 250GTV and 258GTV) recovered variably altered serpentinized pyroxenites (Fig. 2.4), some of which were coated with a thin Mn-oxide layer. Of these, 250GTV recovered strongly altered peridotites and pyroxenites (a 25cm thick layer). In situ temperatures measured in the unconsolidated material onboard yielded

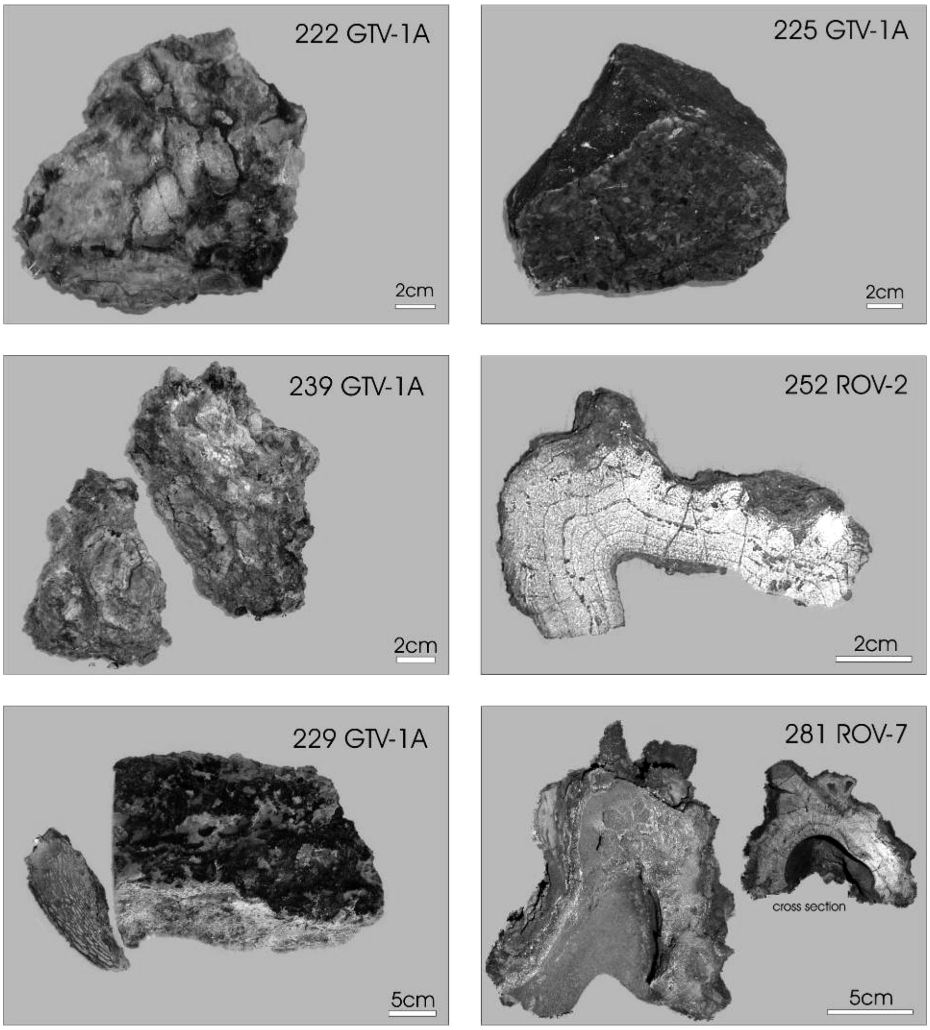

Fig. 2.4 Geological samples recovered during GTV and ROV stations: 222GTV-1A: altered serpentinized pyroxenite; 225GTV-1A: serpentinzed pyroxenite; 239GTV-1A: atacamite crust; 252ROV-2: chimney piece, collected at IRINA I, composed of layers of chalcopyrite; 229GTV-1A: reddish silicified Mn-oxide coating; 281ROV-7: chimney piece, collected at QUEST site, composed of chalcopyrite with Cu-sulphide rich outer layers.

temperatures up to 43°C. This shows that hot fluids circulate beneath the sediment without necessarily venting at the seafloor. 239GTV recovered similar material (this time a 10cm thin and cold layer), with thick atacamite-crusts, hematite impregnated serpentinites, talc and serpentine-breeze. This suggests the presence of an old inactive fluid-pathway. 258GTV contained reddish pelagic sediment, some Mn-coated serpentinite pebbles and empty *Calyptogena* shells. 259GTV grabbed a large boulder, was opened again, and returned empty.

Geological sampling during the various ROV dives recovered mainly sulphide samples, either from active or inactive chimneys and/or sulphide talus samples. Most massive sulphide pieces were composed of chalcopyrite, sometimes displaying a distinctive layering. Other samples comprise more porous chalcopyrite rich interior portions and clearly layered parts towards the outer rim. Occasionally, different fluid conduits could be recognized. The outer rim of all sulphide pieces was generally covered with a thin Fe-oxide coating. 252ROV recovered a large number of pieces which, apart from chalcopyrite as major sulphide, contain abundant colourful copper-rich sulphide minerals (Fig. 2.4). During 261ROV, a fresh sulphide piece comprising largely chalcopyrite was collected from the Barad-Dur chimney at Site A. Further chimney pieces, composed mainly of chalcopyrite and showing individual orifices (Fig. 2.4), were recovered from IRINA II (277ROV) and the QUEST Site (281ROV).

2.4.5 Environmental parameters and longterm monitoring

(M. Fabian, H.-H. Gennerich)

During M64/2 we have deployed two long term monitoring instruments, an ocean bottom tiltmeter (OBT) and an ocean bottom pressure meter (OBP). The OBT is a platform tiltmeter with two perpendicular axis, X, Y. It has also a high performance MEMS (Micro-Electro-Mechanical-System) accelerometer whose axis is aligned parallel to the OBTs vertical axis and measures total gravity g. The OBT uses a biaxial bubble tilt sensor of type Applied Geomechanics Inc. 756. The single-axis accelerometer is of type Kistler Servo K-Beam 8330A2.5 . The OBT will record local sea floor tilt caused by e.g. tectonics, tidal loading, changes in hydrothermal and deeper magma-plume activity and soil movements like landslides with 1 micro radiant resolution and 6 second sampling interval. Acceleration caused by e.g. micro seismicity, earthquakes or tremors will be measured with $10^{-5} m/s^2$ resolution at 0.75 seconds sampling rate. The aluminium frame consists of a rectangular triangle base plate with a tripod and a frame for handling. The larger titanium pressure tube houses batteries, data logger and electronics. The smaller aluminium tube is fixed to the base plate and contains the sensors. The OBT has a deep sea spirit level for levelling the instrument. A good coupling of the instrument to the ground is necessary. The OBT was deployed (14°,45.201' N, 44°,58.784' W, 3053m depth; see Fig. 2.5) in the LHF south east of "QUEST" site and west of site "IRINA II". For navigation purposes and to facilitate revisiting an acoustic beacon (No. 14) was placed at this station (see chapter 2.4.1). The OBT was installed on the hilltop of a rock pile by firmly and carefully pressing and moving the legs of the instrument. Orientation of the +Y-axis with respect to the directions of the compass is 295°±3°. The place of the OBT is apart vent sites that measurements are not influenced by hot fluids.

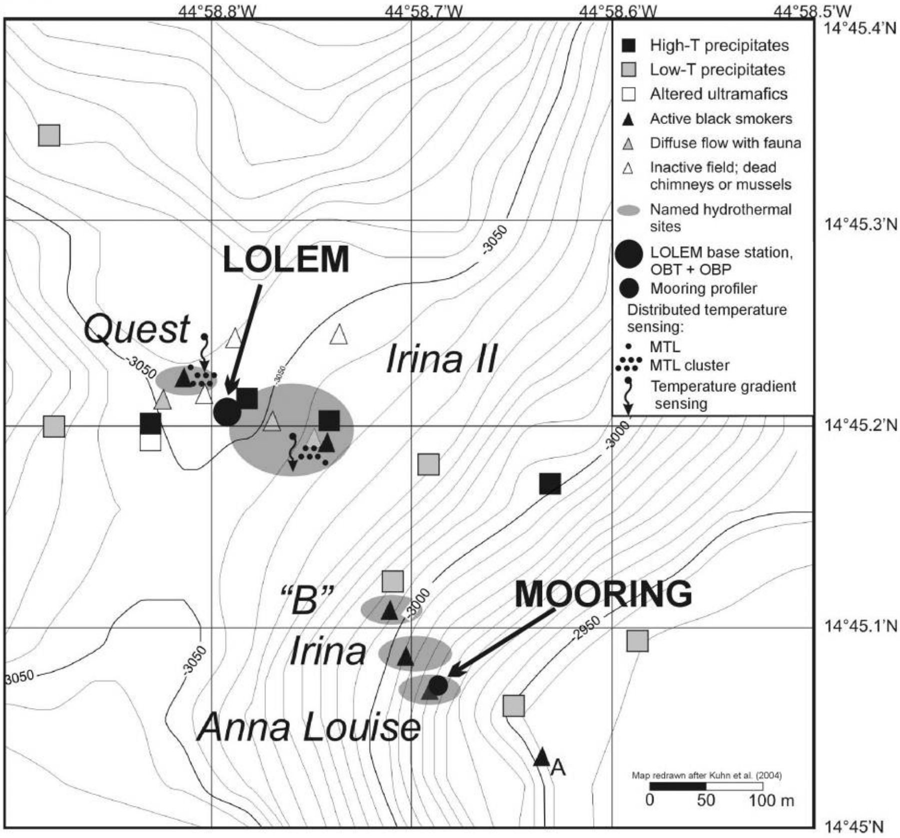

Fig. 2.5 The map shows the location where monitoring systems were installed. QUEST and IRINA II were equipped with temperature loggers, OBT and OBP and MOORING with the bottom water monitoring profiler.

The Ocean Bottom Pressuremeter (OBP), which was deployed close to the OPT (Fig. 2.6), measures changes in the water pressure at the sea floor very precisely to get exact local information about tides and level changes due to subsidence or uplift of the seafloor, indicating tectonic magmatic or hydrothermal activities. The OBP was designed very robust with a strong frame on three short legs and the pressure cases installed with clambs inside. The instrumentation consists of 3 pressure cases with a Brancker XR-420 data logger with built-in temperature sensor, a lithium battery pack (10,5 V, 56 Ah) and a Paroscientific Digiquarz pressure gauge. This base station was configured to sample pressure and temperature in 2 min intervalls. A 30 s pressure integration time was chosen providing a pressure resolution > 1 mm water column. This base station was brought to the sea floor (19.05.05, station 244ROV dive 52) and repositioned to it's final position (22.05.05, station 263ROV; dive 57).

The distributed temperature sensing instrumentation monitors temperature variations in the biological communities as an indicator for changes in their living environment due to variations in hydrothermal activity. The set of instruments consists of 20 1-channel temperature loggers (MTL) inserted into 40 cm long T-shaped steel tubes for easy ROV-deployments and four units each of a 8-channel temperature lance connected to a data logger with a 1 m cable. The temperature resolution is < 1 mK at an absolute accuracy < 5 mK. The 1- channel loggers were

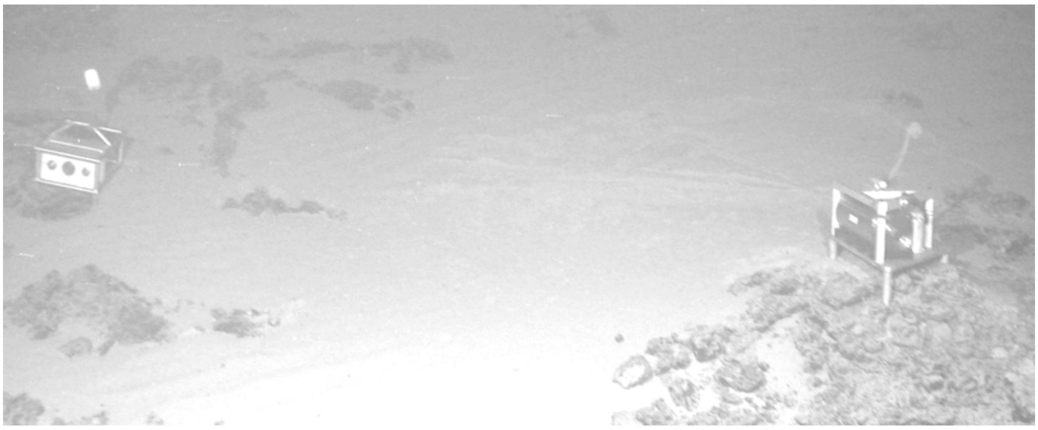

Fig. 2.6 OBP (left) and OBT (right) deployed at their final positions west of IRINA II.

set up to sample at 6 min intervals, the 8-channel loggers at 2 min intervals.

The first set of instruments consisting of 10 1-channel loggers sequentially numbered from #1854200 to #1854209 was labeled with 10 cm buoyant cylinders #0 to #9. It was deployed (20.05.05, station 257ROV, dive 55) in the IRINA II mussel field. The arrangement was installed in two parallel lines of 5 loggers each perpendicular to the mussel field's length axis until the rim of the mussel covered area. Shimmering water indicates elevated water temperature above the mussel field.

The second set of 10 MTLs (#1854210 to #1854219) labelled as #10 to #19 was deployed (30.05.05 station 281ROV, dive 61)) in the QUEST mussel field which has an extension of about 0.6 x 3 m . The loggers were arranged along the field's length axis spaced < 0.5 m with an additional cross profile and one extra logger 1 m beside in a bacteria mat.

Two 8-channel loggers (#10295, #10298) were placed (31.05.05, station 283ROV, dive 62) horizontally and vertically in the same location where the mussel field shows maximum thickness. An other set of two 8-channel loggers (#10296, #10297) was placed in the same configuration in the IRINA II mussel field, ca. 4 m beside the 1-channel logger array.

Two MTLs deployed during cruise M60/3 were recovered from the IRINA II and QUEST site mussel fields. Data show in a 1 week time series periodic changes in temperature up to 6°C resp 12°C with a periodicity which seems to be related to the ocean tides or multipliers of it.

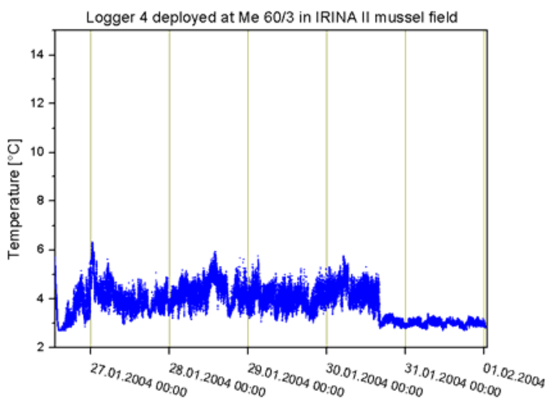

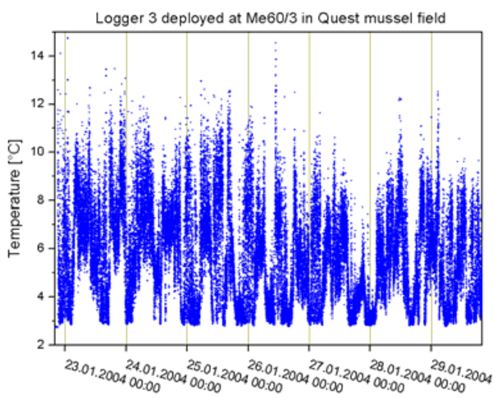

Fig. 2.7 Temperature time series in IRINA II (left) and QUEST (right) mussel field.

The Bottom Water Profile Monitor (BWPM) will register the variation of the bottom water temperature caused by changes in hydrothermal activity and water currents. The BWPM is constructed as a mooring where two 17' glass balloons with a total buoyancy of 56 kg are connected by a 25 m long rope to a bottom weight of 100 kg. A 25 m long sensor cable with 24 temperature sensors 1 m spaced and a Brancker XR-420-T24 24 channel data logger are attached to it. Acoustic beacon #15 was also attached to the mooring 20 m above the sea floor for easy finding and general navigation purposes in the Logatchev hydrothermal field. The logger is configured to register the temperature in 1 min time intervals at 24 equidistant positions equally spaced by 1 m at a temperature resolution of better than 1 mK and an absolute accuracy of 5 mK. The BWPM was lowered to the sea floor with the oceanographic wire, an additional weight of 300 kg and an acoustic releaser. The ROV collected the mooring from the sea floor by grabbing into a prepared loop of buoyant rope attached to the bottom weight and transported it to the final position between the black smokers and smoking craters of ANNA LOUISE and IRINA I (st. 272ROV-1).

The ROV temperature lance is intended to measure real time temperature at spots of interest as well as the gradient and width of the temperature anomalies. It is designed as a 0.5 m long lance with 8 evenly (4 cm) spaced temperature sensors inside and connected to a 8-channel logger. The logger provides a RS-232 data stream, which is transmitted in real time through the ROV-cable to the ship. The lance measured temperatures of up to 210 °C in a black smoker at ANNA LOUISE.

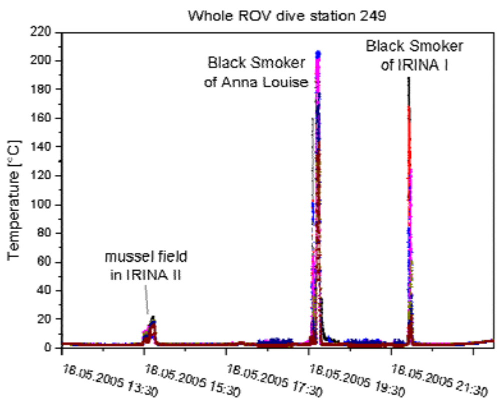

Fig. 2.8 Results of 8-channel ROV-temperature measurements of black smokers at ANNA LOUISE and IRINA I.

With the plume temperature profiler the water column is scanned for signs of a hydrothermal plume. For this purpose a set of MAPRs and 20 miniature temperature loggers (MTL) were attached to the oceanographic wire and towed through the water column while the ship was steaming slowly at 0.5 knts.

During station 223 a grid of 4 equally spaced parallel profiles covering an area of about 4 km^2 above the Logatchev hydrothermal vent field was surveyed. MAPRs and MTLs were attached over a length of 600 m. The TowYo array oscillated with an amplitude of 200m hereby approaching the seafloor to within 50 to 100m. During station 228 the variation of temperature and turbidity were recorded in the center location of station 223.

All surveys revealed that the upper plume between 2700 m and 3000 m is very clearly visible by increased turbidity in MAPR and CTD data. At the same time a sudden decrease in temperature gradient compared to the normal gradient is observed. The signal in the temperature is less obvious than the one in the turbidity.

At station 284 the OFOS was used to follow the seafloor with a constant distance of 2 m, while observing the seafloor for indicators of hydrothermal activity. A set of 20 MTLs and 5 MAPRs were attached to the wire and to the bottom distance control weight below the OFOS. This way the bottom water column of 100 m was surveyed in detail on three parallel tracks evenly spaced by 100 m.

Different from the upper plume, a bottom water plume could be identified in the interval between 2-10 m above the sea floor. This bottom plume is seldom visible by increased turbidity, but can be easily identified by temperature signals of 30 mK to 50 mK. The bottom plume seems to indicate hydrothermal activity from diffuse venting sites, which don't produce big amounts of particles like the black smokers do. Thus future cruise could be guided by observing the temperature anomalies in that depth interval to find diffuse venting sites. Results from station 226 suggest to have a closer look to an area 500 - 1000 m to the NW of the Logatchev vent area for diffuse venting sites.

2.4.6 Physico-chemical characterization of the Logatchev hydrothermal field (LHF)

2.4.6.1 Gas chemistry

(T. Pape, G. Schroll)

During M64/2 34 CTD stations were conducted for measurements of conductivity, temperature, salinity and light transmission of the water column. A map illustrating the positions of the stations is given in figure 2.11 (see chapter 2.4.6.2). CTD data were recorded for the entire water column using a SEABIRD CTD Type 911 equipped with a light transmission sensor. At 19 stations water samples were taken with a rosette of 23 10 L Niskin bottles for on board analysis of concentrations of H_2 and CH_4. Fluid and near-bottom water samples were obtained by a fluid sampling system or Niskin bottles during 12 ROV dives. Subsamples were stored for onshore measurements of stable carbon isotopic compositions of CH_4 and H/D ratios. In total, 146 samples from the water column and 35 vent associated water and fluid samples were recovered for analyses of dissolved gases (Table 2.2).

Table 2.2: Water sample list for CTD- and ROV-stations.
HC = CH_4 and C_2- to C_4-hydrocarbons.

Station	Long. N	Lat. W	No. of samples	HC	H_2	$\delta^{13}C$ CH_4	δ^2H_2
CTD							
217	13°30,0´	45°0,0´	12	12	11		
219	14°45,2´	44°58,8´	12	12	11		
221	14°45,1´	44°58,9´	12	12	12		
227	14°45,1´	44°58,7´	10	9	8		
231	14°45,3´	44°58,9´	11	11	11	10	
242	14°46,0´	44°58,8´	5	5	3	3	
248	14°46,0´	44°59,0´	11	11	9	10	
253	14°46,1´	44°59,2´	10	10	8	8	
260	14°46,0´	44°59,1´	11	11	9	10	
264	14°45,2´	45°01,0´	6	6	6	5	
267	14°44,0´	44°59,0´	4	4	2	4	
268	14°44,0´	44°58,0´	4	4	4	4	
269	14°44,4´	44°57,0´	3	4	1	2	
270	14°44,5´	44°57,5´	4	4	3	4	
273	14°46,0´	44°59,2´	10	10	10	10	
274	14°45,1´	44°58,1´	4	3	3	3	
275	14°44,4´	44°57,2´	3	3	2	1	
276	14°45,7´	44°57,5´	4	3	3	3	
279	14°45,4´	44°58,9´	10	10	10	10	
total:			**146**	**144**	**126**	**87**	

Station	Long. N	Lat. W	No. of samples	HC	H_2	$\delta^{13}C\ CH_4$	δ^2H_2
19							
ROV							
224			2	1	2	2	
232			4	2	4	2	
249			4	2	4	4	2
257			2	1	2	2	
261			7	5	7	4	
263			1	1	1	1	
266			4	2	4	4	
272			1	1	1		
277			2	1	2	2	
281			4	2	4	3	
283			2	2	2	2	
285			2	2	2	2	
total: 12			**35**	**22**	**35**	**28**	**2**

The methods used for preparation and on board analysis of dissolved gases and storage of gas and water samples are described in the cruise report of M64/1 in detail. Briefly, volatile dissolved hydrocarbons (C_1 to C_4) were extracted and concentrated deploying a purge and trap technique (Seifert et al., 1999). The trapped gases are released to a gaschromatograph (CARLO ERBA GC 6000) equipped with a packed stainless steel column and a flame ionisation detector (FID) to separate, detect and quantify individual compounds.

Dissolved hydrogen was extracted by applying a high grade vaccum in an ultrasonic bath and heating until boiling. Subsamples of the released gas were transferred from the degassing unit into the analytical system using a syringe. The analytical procedure was performed using a gaschromatograph (THERMO TRACEGC ultra) equipped with a packed stainless steel column and a pulse discharge detector (PDD). All analytical procedures were calibrated daily with commercial gas standards (LINDE).

For onshore analysis of stable carbon isotopes ($\partial^{13}C$) of dissolved light hydrocarbons aliquots of gas samples obtained by the vaccum-ultrasonic technique were transferred through a septum into gastight glass ampoules filled with NaCl-saturated water. For selected water samples aliquots of the vacuum-extracted gas were frozen on molecular sieve 4Å under nitrogen in a pre-vacuated glass vial for onshore measurements of stable hydrogen isotopes.

Based on results obtained during previous water column investigations at the Logatchev hydrothermal field (LHF) CTD surveys were deployed above vent sites and at adjacent (max. about 3 sm) non-vent areas. Signatures of hydrothermal activity within the water column were monitored by anomalies in the transmission profiles and ST diagrams (salinity vs. potential temperature). Generally, in the working area the anomalies are located at a waterdepth range between 2700 and 2900 m (Fig. 2.9).

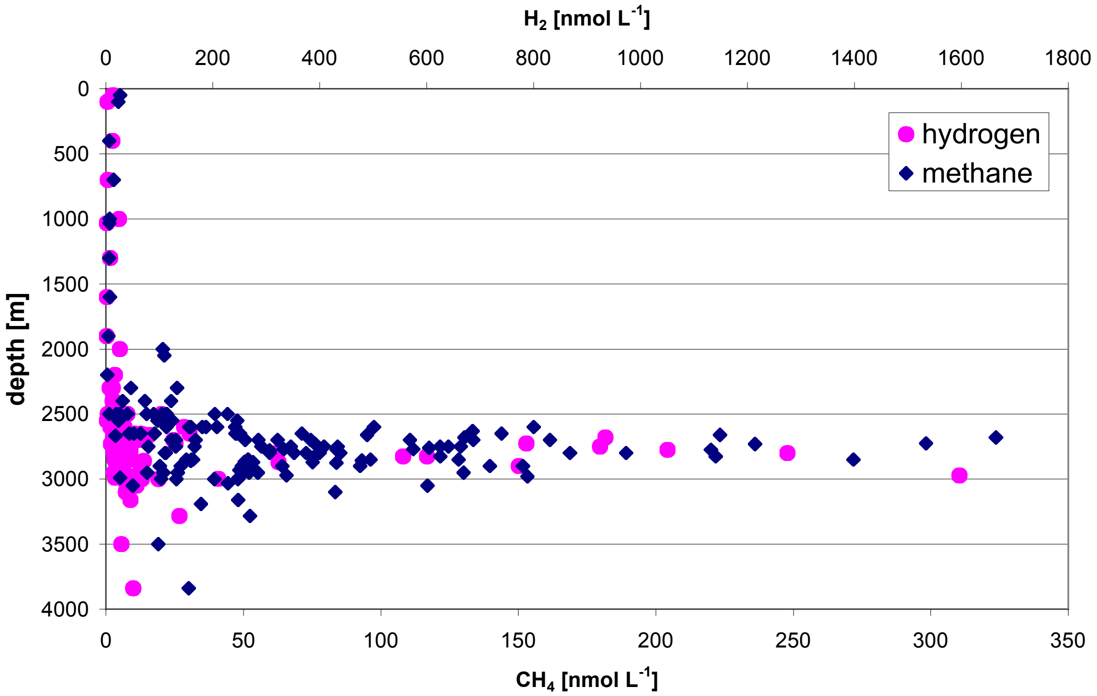

Fig. 2.9 Concentrations of H_2 and CH_4 in water samples of all CTD stations.

The ST plots indicate that the intrusions are derived from fluids relatively depleted in salinity generating distinct water bodies of elevated temperatures. At CTD station 231, which was performed about 0.15 nm NW of the black smoker site 'QUEST', the hydrothermal plume peaked at 2.787 m.

Furthermore, a good correlation between transmission anomalies and the concentration profiles of hydrogen and methane was found (Fig. 2.10) at station CTD231. However, at some other CTD stations we found lesser similarities between profiles of these physico-chemical parameters.

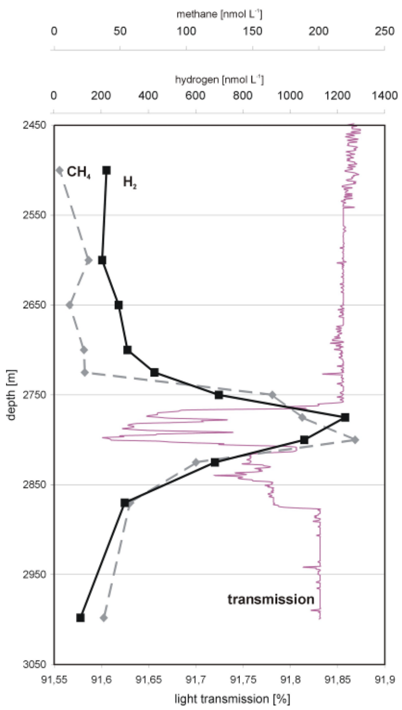

Fig. 2.10 Concentrations of H_2 and CH_4 and light transmission anomaly at station CTD231.

During M64/2 concentrations of dissolved gases obtained from CTD/rosette water samples revealed a considerable hydrothermal signature over a wide distribution area. A map illustrating the area where distinct anomalies in the turbidity profiles were observed is given in chapter 2.4.6.2. Highest concentrations of dissolved hydrogen and dissolved methane were observed for station CTD227 showing about 1.60 µmol L^{-1} H_2 (2.972 m depth) and about 0.3 µmol L^{-1} (2.680 m), respectively. This station was positioned equidistant to the hot fluid emanation sites 'IRINA' and 'Site A' and, as far as we know, these are the highest H_2 concentrations measured in the water column above the LHF field. Moreover, a slight transmission anomaly at station 238 at 3.030 to 3.080 m accompanied by elevated concentrations of hydrogen in near bottom waters at the nearby station 273 were observed. Since both stations were located more than 2 nm far from the LHF, these observations might be related to an fluid emanation site in the NW edge of the working area undiscovered so far. However, during ocean bottom observation tracks conducted with an OFOS system no hints for effusive or even diffusive vents were recognized (see chapter 2.4.3).

Water and fluid samples taken with 5 L Niskin bottles or a fluid sampling device directly at fluid emanation sites during ROV dives commonly showed very high concentrations of dissolved gases. In fluids obtained by putting the tip of the fluid sampling system directly into the outlet of black smokers, maximum concentrations measured were 167 µmol L^{-1} and 397 µmol L^{-1} of hydrogen (at IRINA II, ROV283) and methane (at Site "B", ROV249), respectively. Highest concentrations of dissolved gases in water samples taken with the ROV-based Niskins were found at the same sites and accounted for 136 µmol L^{-1} hydrogen (ROV257) and 67.5 µmol L^{-1} methane (ROV261). A considerable variety was observed for the H_2/CH_4 ratios of the fluid and near-bottom water sample set. The maximum ratio determined for fluids of IRINA (ROV261) accounted for 8.7 which is very similar to that observed during a the previous cruise M60/3 (H_2/CH_4 = 6.4; station 73ROV). Further insights into the variability in the gas chemistry of fluids at the LHF will be obtained by stable isotopes analysis of the comprehensive sample set in the laboratory at home.

2.4.6.2 Spatial distribution of the hydrothermal signature in the water column

(H. Marbler, T. Pape, H.-H. Gennerich, G. Schroll, S. Weber)

In order to determine the horizontal expansion and vertical structure of the hydrothermal plume at the Logatchev hydrothermal field (LHF) a plume-mapping was carried out.

During selected hydrocasts with CTD/rosette water sampler 25 measurements of the water column were conducted as one-point on-line measurements with CTD combined with light transmissiometer, associated MAPR (Miniature Autonomous Plume Recorder with turbidity, density and temperature sensors) and MTL (Miniature Temperature Logger). Time series measurements were also carried out with five MAPR and 20 MTL in different depths. A so-called "towyo-mapping" with MAPR and MTL was performed in four parallel S-N profiles over the vent field.

For seafloor observations combined with the determination of geophysical parameters of the near bottom plume an OFOS (Ocean Floor Observation System) combined with MAPR and temperature logger in defined levels were used (see Chapter 2.4.3).

Table 2.3: Station numbers with coordinates and the number of CTDs, MAPRs and temperature loggers.

Station No.	Long. N	Lat. W	CTD	MAPR	Temperature-Logger
217 CTD	13°30,0´	45°0,0´	1	1	1
219 CTD	14°45,2´	44°58,8´	1	1	1
221 CTD	14°45,1´	44°58,9´	1	1	1
223 Logger	Track			5	20
226 OFOS			1		
227 CTD	14°45,1´	44°58,7´	1	1	1
228 Logger	14°45,1´	44°58,7´		5	20
233 CTD	14°45,3´	44°58,8´	1	1	1
242 CTD	14°46,0´	44°58,8´	1	1	1
245 CTD	14°45,9´	44°59,3´	1	1	1
246 CTD	14°46,4´	44°59,5´	1	1	1
253 CTD	14°46,1´	44°59,2´	1	1	1
254 CTD	14°45,9´	44°59,2´	1	1	1
255 CTD	14°45,7´	44°59,3´	1	1	1
256 CTD	14°45,4´	44°59,5´	1	1	1
260 CTD	14°46,0´	44°59,1´	1	1	1
264 CTD	14°45,2´	45°01,0´	1	1	1
265 CTD	14°44,0´	45°00,0´	1	1	1
267 CTD	14°44,0´	44°59,0´	1	1	1
268 CTD	14°44,0´	44°58,0´	1	1	1
269 CTD	14°44,4´	44°57,0´	1	1	1
270 CTD	14°44,5´	44°57,5´	1	1	1
273 CTD	14°46,0´	44°59,2´	1	1	1
274 CTD	14°45,1´	44°58,1´	1	1	1
275 CTD	14°44,4´	44°57,2´	1	1	1
276 CTD	14°45,7´	44°57,5´	1	1	1
278 OFOS			1		
279 CTD	14°45,4´	44°58,9´	1	1	1
280 CTD	14°47,0´	45°00,0´	1	1	1
284 OFOS	Track		1	5	20

With an array of 25 CTD stations with associated MAPR (10 meters above the CTD) the extension of the turbidity plumes was mapped (Tab. 2.3). A CTD reference station was conducted some km west of the studying area. In the map (Fig. 2.11) the lateral extent of the upper plume in the area of LHF-1 is illustrated by a strong dashed line.

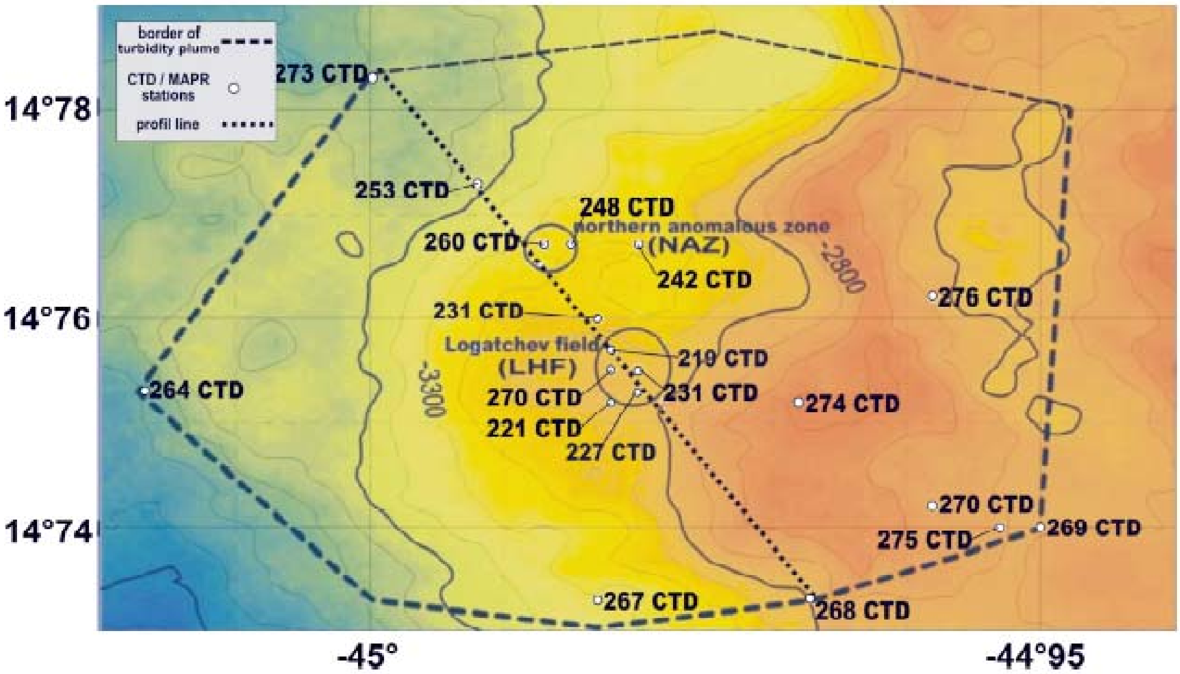

Fig. 2.11 Map of the CTD stations (white dots) in the area of the Logatchev vent field and the northern anomalous zone. The dashed line around the area marks the zone of sites where a turbidity anomaly could be recognized. It links CTD stations with strongly reduced turbidity anomalies. The circles show zones, where near bottom turbidity was observed.

Above LHF we observed turbidity plumes in two depths. One plume intrudes the water column between 2620m to 2800 m water depth and a second one was found between 2920 m and 2980 m (for example CTD219; Fig: 2.11). The latter is only observed in the close vicinity of LHF.

2 km northwest of LHF a continuation of the upper plume can be stated, while in the lower lewel a new strong turbidity plume was located between 2750 m and 3000 m (CTD 260; Fig. 2.12). This anomaly was observed in three CTD and MAPR stations. Between this northern anomalous zone (NAZ) and LHF the lower plume could not be detected, indicating that a different, while still unknown vent site as source exists. The near bottom plumes at NAZ and LHF consist of turbidity anomalies and very high CH_4 and H_2 values indicating individual hydrothermal sources at both locations.

With an array of CTD stations and associated MAPR the extension of the turbidity plumes was mapped. A CTD reference station was conducted some km west of the studying area

The strongest turbidity signal gennerally is observed in the upper plume at 2700 m to 2900 m depth. The disappearance of the turbidity plume in a distance of some km from the vent is explained by the sinking of Fe-oxides, Fe-oxihydroxides and Mn-oxides not too far from their origin.

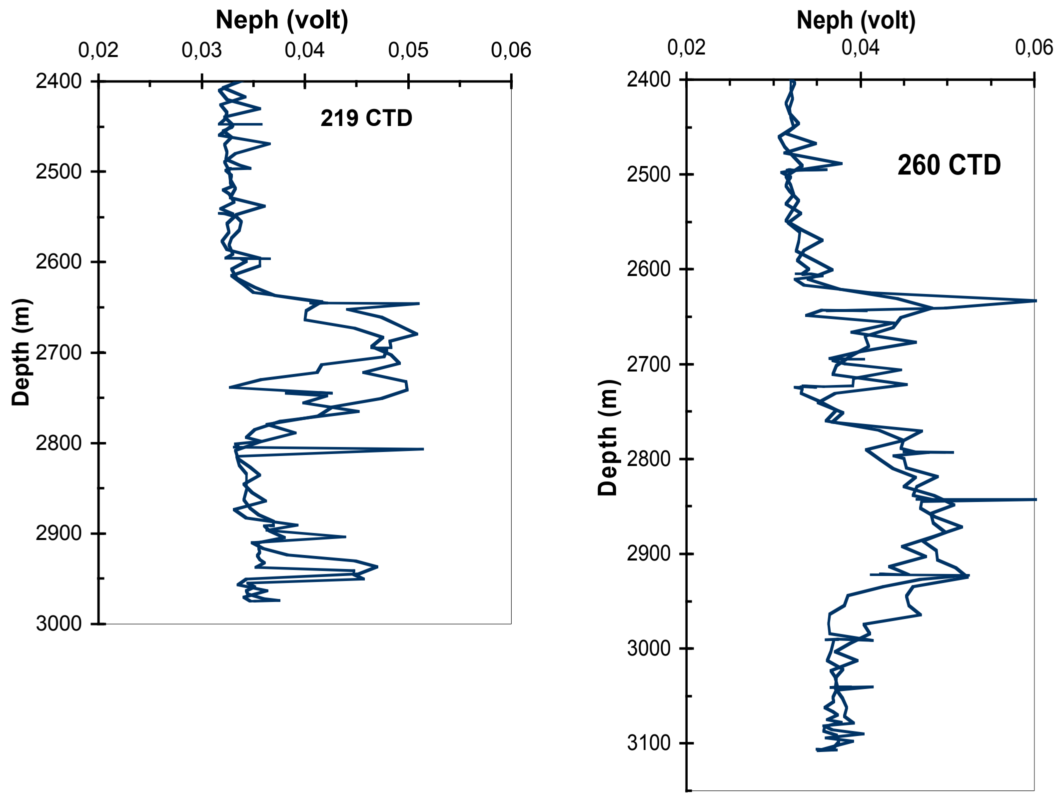

Fig. 2.12 Turbidity (Nephelometer volts) vs. water depth from MAPR-data at CTD stations above the Logatchev vent field (219CTD) and at the northern anomalous zone (260CTD).

To record the time variations within different plume levels in the water column a station with five MAPR and 20 MTL was carried out above the LHF during an eight hour station. Large time variations were observed especially in the lower part of the plume, like 75 and 175 m above the seafloor. Within the water depth between 2700 m to 2625 m (250 and 325 m above the seafloor) the turbidity level is less variable, which indicates a homogenous distribution of hydrothermal fluid in this level of the water column. In this buoyant plume the turbidity spreads within a distinct depths range.

2.4.7 Fluid chemistry

(M. Amini, D. Garbe-Schönberg, H. Marbler, K. Schmidt, H. Strauss)

One of the major objectives for cruise M64/2 was the detailed investigation of spatial and temporal variations in fluid composition within the Logatchev hydrothermal field. Re-sampling of all sites visited during M60/3 in 2004 and complete coverage of all known Logatchev vent sites could be accomplished during this leg.

Three different types of samples were collected for chemical and isotopic analyses: (1) water column samples from the CTD/Rosette, equipped with 24 Niskin flasks à 10 l volume; (2) samples from discharging vent sites collected with three Niskin flasks (5 l volume), mounted at the front of the MARUM ROV QUEST; (3) in situ-vent fluid samples collected with the new Kiel Pumping System (KIPS: 15 bottles à 675 ml).

For in situ-sampling of hydrothermal fluids directly from inside the vent orifices a pumped flow-through system (Kiel Pumping System, KIPS) mounted on the ROV's starboard back side was used.

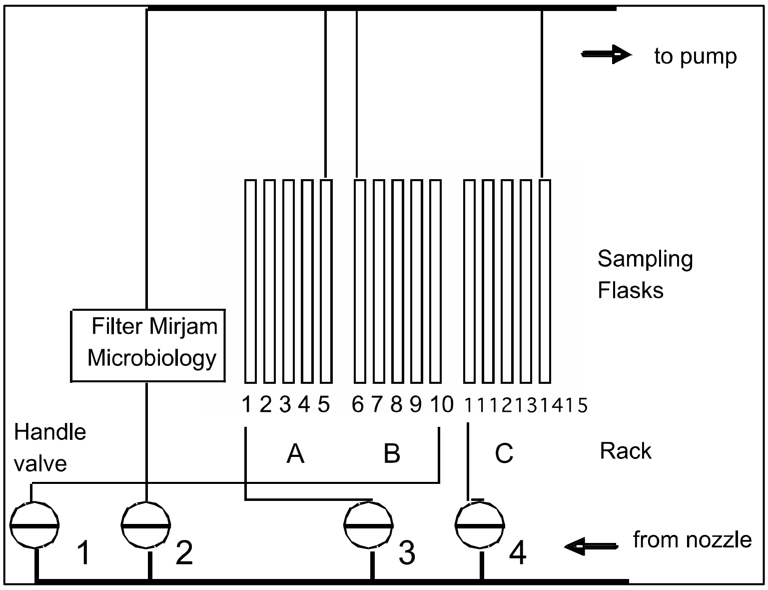

Fig. 2.13 Schematic configuration of the KIPS fluid sampling system.

The system is newly constructed and entirely made of inert materials (Teflon, titanium). Samples are collected via bent titanium nozzle of 50 cm length which can be directly inserted into the vent orifice by the ROV`s manipulator arm. Parallel to the nozzle is an on-line temperature probe monitoring the *in situ*-temperature at the point of sampling. Coiled PFA tubing connects the nozzle to 4 handle-operated open-close valves (Fig. 2.13) allowing the distribution of the vent fluids directly to either a series of PFA sampling flasks or an in-line filter holder for microbiological studies or a remotely controlled multiport valve (PETP/ PTFE) driven by a ROV actuator (Schilling, U.S.A). The valve control software is fully integrated in the ROV control system (MARUM, Bremen). The multiport valve in its current design has 18 ports which can be connected to 15 single PFA Teflon flasks (675 ml volume each, Nalgene, USA). A deep sea pump with nominal 3 l/min is mounted downstream to the sampling flasks with the outlet tube ending on the porch at the front-size of the ROV so that outflowing shimmering water could be observed during pumping. The flasks are mounted in three racks A-C, with every rack containing five horizontally positioned bottles, allowing an easy transfer of the racks to the laboratory where sub-sampling was done. Each bottle can be equipped with check valves at the inlet and outlet. An additional multiport valve for a series of microbiology filter units can be connected as a slave valve to one of the free positions (#16-18) of the first multiport valve.

A total of 90 water column samples, 15 fluid samples obtained with the ROV fluid sampling system, and 5 ROV Niskin samples were collected.

Based on the depth profiles for temperature, salinity and light transmission, samples were collected at different depths with the CTD/Rosette system, covering the vertical distribution of the hydrothermal plume. Sampling of these waters was performed directly after recovery of the CTD/Rosette system. Immediately after sampling, pH and Eh were measured. Subsequently, and depending upon future chemical analyses, non-filtered subsamples (with aliquots either non-acidified or acidified to a pH of 2 with suprapure HCl) were stored at 4°C. Barium sulphate was precipitated from sample aliquots (addition of barium chloride solution at pH 2) for measuring the sulphur and oxygen isotopic compositions of dissolved sulphate. For selected CTD stations, untreated water samples were collected for measuring the oxygen and hydrogen isotopic composition of these waters. For the CTD stations in the vicinity of active vents, samples have been collected for the analysis of amino acids in the dissolved and particulate organic material. Water samples were filtered through GF/F glass fibre filters and the filters wrapped in aluminium foil and frozen at -20°C. The organic compounds in the filtrate were concentrated by means of solid phase extraction onto C18 and SCX phases and subsequently stored at -20°C. For selected profiles throughout the water column an aliquot of the samples has been frozen at -20°C for later analysis of the ammonium concentration and its nitrogen isotopic composition.

Immediately after recovery of the ROV, all three Niskin flasks (N1, N2, N3) and all bottles from the KIPS were sub-sampled. Aliquots were sub-sampled for the following chemical and isotopic analyses: free gas and dissolved gases (CH_4, H_2, abundance and isotopic composition, approx. 1000 ml), total dissolved and particulate major and trace elements (2x 50ml), isotopic composition of Ca (25 ml), high precision alkalinity (250 ml), selected anions (50 ml), sulphate (1 ml) and sulphide (abundance and isotope geochemistry, 400 ml), dissolved inorganic carbon (abundance and isotopic composition, 30 ml), amino acids (2x 75 ml), ammonium (abundance and nitrogen isotopes, 60 ml), and aliquots for subsequent filtration (500-1000ml) and microbiological cultivation work.

On small unfiltered aliquots (30 ml), ph, Eh, total Fe and Fe-II, S^{2-}, and dissolved silica were measured directly after sampling for all samples. For all other chemical analyses, fluid samples were pressure-filtrated with Nitrogen (99.999%) at 1 bar through pre-cleaned 0.2 µm Nuclepore PC membrane filters by means of polycarbonate filtration units (Sartorius, Germany). The filtrates were separated into aliquots for voltammetric and ICP analyses and acidified to pH 1 with 100 µl subboiled concentrated nitric acid per 50 ml (ICP) and with suprapure HCl to pH 2 (voltammetry), respectively. Procedural blanks were processed in regular intervals. All work was done in a class 100 clean bench (Slee, Germany) using only all-plastic labware (polypropylene, polycarbonate, PFA Teflon). Rinse water was ultrapure (>18.2 Mohm), dispensed from a Millipore Milli-Q system.

For selected samples, about 200 ml of fluid were filled into specially pre-cleaned bottles and immediately deep-frozen at -20°C. These samples are shipped in frozen state for the determination of organic metal complexation in the home laboratory of the project partner Dr. Sylvia Sander (University of Otago, New Zealand). Some representative samples were deep-frozen or poisoned with $HgCl_2$, respectively, as conservation for organic analyses in the home laboratory.

On-board analyses

For all samples collected with either the CTD/Rosette, the Niskin flasks or the Kiel Fluid Pumping System (KIPS), pH and Eh measurements were performed on unfiltered sample aliquots immediately after sampling. Measurements were carried out with WTW electrodes (Ag/AgCl reference electrode).

Chloride Titration

In order to determine whether or not phase separation affected the chemical composition of the hydrothermal fluids, fluid samples from hot vents collected during ROV dives, either with Niskin bottles or with the Kiel Fluid Sampling System, were subjected to chloride concentration analysis. Measurements were performed as titration with 0.1 mM $AgNO_3$-solution, using fluorescene-sodium as the indicator. For reference, samples from a water column profile were also analyzed.

Photometric Determination of Dissolved Inorganic Silica

Silica tends to be enriched in hydrothermal fluids (e.g., van Damm, 2004). Hence, fluid samples and selected CDT/Rosette water column samples were analyzed for their abundance of dissolved silica. The analysis of dissolved silicon compounds in seawater and hydrothermal fluids is based on the formation of α-silicomolybdic acid via complexation of the dissolved silica with ammoniumheptamolybdate (e.g., Grasshoff et al., 1999). Concentration measurements were performed with a biochrom Libra S12 spectral photometer at an extinction of 810 nm. Silica contents in water column samples were measured both in filtered and non-filtered samples. No significant difference was detected.

Photometric Determination of Iron Concentrations

The principle of this method is the determination of an orange-red ferroin complex, which is formed by Fe(II) ions in the fluid sample with 1,10-phenantroline in a pH range of 3-5. In addition to a quantification of Fe(II), it is also possible to measure the Fe_{tot} fraction in the sample by reducing all Fe with ascorbic acid. Fe(III) is determined as difference between Fe_{tot} and Fe(II). Analyses were carried out with a biochrom Libra S12 spectral photometer and the absorption was measured at 511 nm. Fe concentrations were measured only in filtered samples of hydrothermal fluids. The detection limit is about 0.1 ppm. Samples with concentrations above 100 ppm were measured in diluted samples.

Voltammetric Determination of Trace Element Concentrations

For onboard sulfide and trace metal concentration analyses, the electrochemical method of voltammetry was used. Voltammetry is able to differentiate between different redox species and (in combination with UV digestion of the water samples) free and complexed forms of ions in solution and is highly sensitive. All the voltammetric measurements were performed using a Metrohm system comprising a 757 VA Computrace run with a standard PC, an 813 Compact Autosampler and two 765 Dosimats. The three-electrode configuration consisted of the multi-mode electrode (MME) as the working electrode, an Ag/AgCl reference electrode (3 mol l^{-1} KCl), and a platinum wire as the auxiliary electrode.

Immediately after recovery, the unfiltered fluid samples were analysed for total dissolved sulfide in alkaline solution using the method after Metrohm Application Bulletin 199/3e. Filtered aliquots were submitted to a digestion process in a UV Digestor (Model 705, Metrohm), which contains a high pressure mercury lamp (500 W), decomposing organic metal complexes. After 1 hour UV irradiation, the total content of Mn, Zn, Cu, Cd, and Pb in all fluid samples and Fe in selected water column samples were determined by the standard addition method. For Fe, the highly sensitive cathodic stripping voltammetric method of Obata and van den Berg (2001) using 2,3-dihydroxinaphthalene as complexing agent was applied in samples with low Fe concentrations, while photometry was used for samples with high Fe concentrations (>0.1 ppm). Mn concentrations were determined using anodic stripping voltammetry in an alkaline ammonia buffer solution (Locatelle and Torsi, 2001). For Cu, Pb, Cd, and Zn analyses samples were buffered at pH 4.6 with 1 M acetate buffer solution and measured by ASV (Application Bulletin Metrohm 231/2).

Titration of Alkalinity

Alkalinity was determined onboard for samples of very less amounts and for a cross check with later analyses due to potential modifications by H_2S oxidation and/or $CaCO_3$ precipitation.

The measurements are carried out by a titration device after Galina Pavlova. 1 ml of sample was added to 4 ml of Millipore water and 0.02 ml of the indicator (mixture of methylorange and methylenblue). The mixture was titrated by 0.01M HCl until a stable redish colour appears. The released CO_2 and H_2S respectively was outgassed/displaced by N_2. The results are averages of at least three replicated measurements. Analytical uncertainties are in the range of less than 0.7 %.

Results from On-Board Analyses

The chemical and isotopic characterization of hydrothermal vent fluids is strongly dependent upon the sampling procedure and the sampling location inside the orifice. Dilution of the emanating hydrothermal fluid by turbulent mixing with ambient seawater within the vent orifice is always likely. In order to qualitatively assess the contribution from seawater, a number of

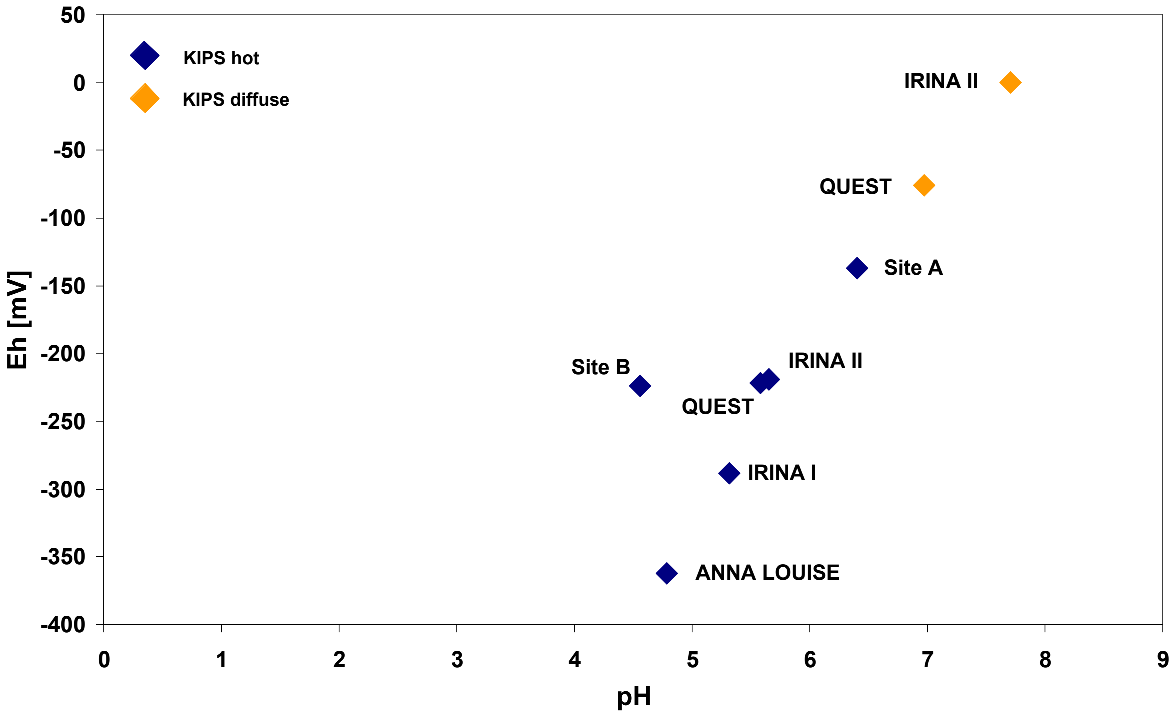

Fig. 2.14 Plot of pH and Eh for fluid samples obtained with the fluid sampling system (KIPS).

analytical parameters, such as Eh, pH and chloride have been measured on-board. A final quantification of the fluid contribution from a hydrothermal source will be performed by using Mg concentrations (hydrothermal endmember Mg = 0, seawater endmember Mg = 55 mM). Mg will be measured in the home laboratories.

The sampled vent fluids are highly reducing and acidic (Fig. 2.14), indicating a low proportion of intermixed oxic seawater. Lowest values obtained for fluid samples were 3.89 for pH and –370 mV for Eh. The highest in-situ temperature measured during this cruise was 350°C (Site "B"), which is nearly identical to the published value from Douville et al. (2002).

Sulfide. The measured dissolved sulfide concentration ranges between 0,5 mM and 2,5 mM for samples directly collected at the vent sites. The published values for ultramafic-hosted hydrothermal fields range between 0,8 mM and 1 mM for the Logatchev Field and Rainbow, respectively (Douville et al., 2002).

Chlorinity. Measured chloride concentrations are slightly lowered compared to seawater (max. 10%). This may indicate phase separation, which must happen in the supercritical region (water depth >3000 m, critical point: 405°C/300bar).

Silica. The silica concentrations range between 0,8 mM und 4 mM and show significant differences between individual sites (Fig. 2.15). Higher concentrations seem to be reflected in more complex vent architectures (IRINA II and possibly Site "A"). The variations between individual sites confirm the trend observed for the samples collected during the M60/3 cruise.

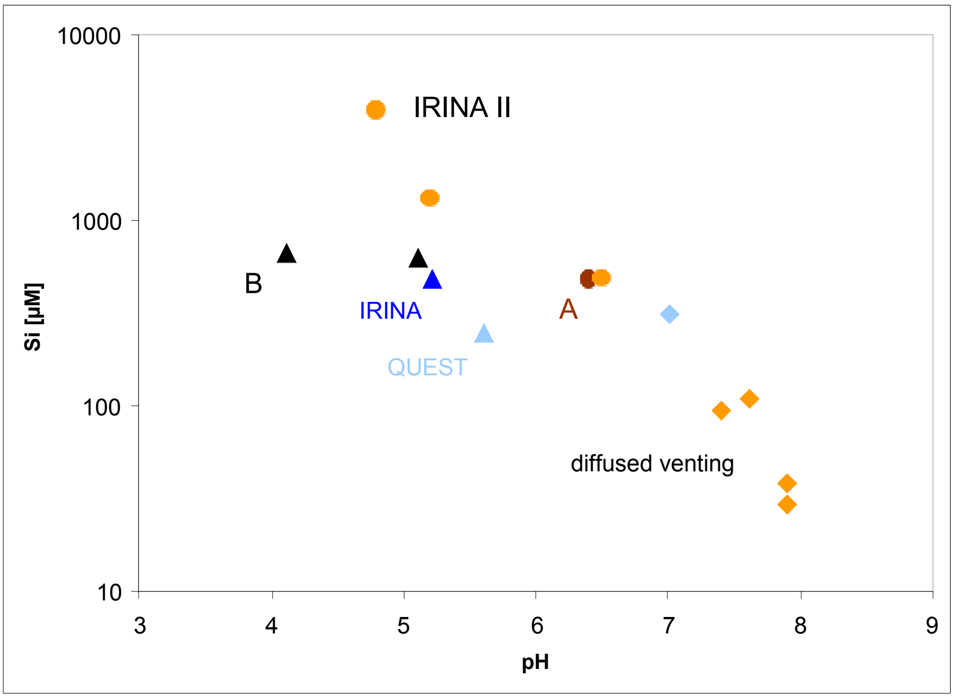

Fig. 2.15 Plot of Si vs pH for KIPS fluid samples. Fluid samples from IRINA II and Site A are characterized by elevated Si concentrations.

Trace metals. Spatial variations can also be seen in the concentrations of Zn and Cu. The highest concentrations were measured at IRINA II (Zn: 4 µM; Cu: 5,1 µM), the lowest at IRINA I and QUEST (less than 1 µM). The low concentrations compared to published data are probably caused by the strong bounding of these chalcophile elements in the precipitating sulfide particles before and during the sampling.

Fe/Mn ratios differ also between the individual sites. For Site "B" and QUEST the highest ever reported values for the MAR were found (Fe/Mn=18, Fig. 2.16), resulting from very high total dissolved Fe concentrations up to 2,5 mM (more than 90% as reduced Fe^{2+}). These not yet endmember-corrected Fe data are in the same range as the calculated endmember concentration for the M60/3 fluids.

Diffuse vent fluids sampled at IRINA II and QUEST show intermediate compositions between hot fluids and seawater. They were partly significantly reducing (Eh of –200 mV) and slightly acidic (pH of 6.5). The silica enrichment at IRINA II (see above) can also be seen in the diffuse fluids. Measured sulfide concentrations range between 0,5 µM and 6 µM.

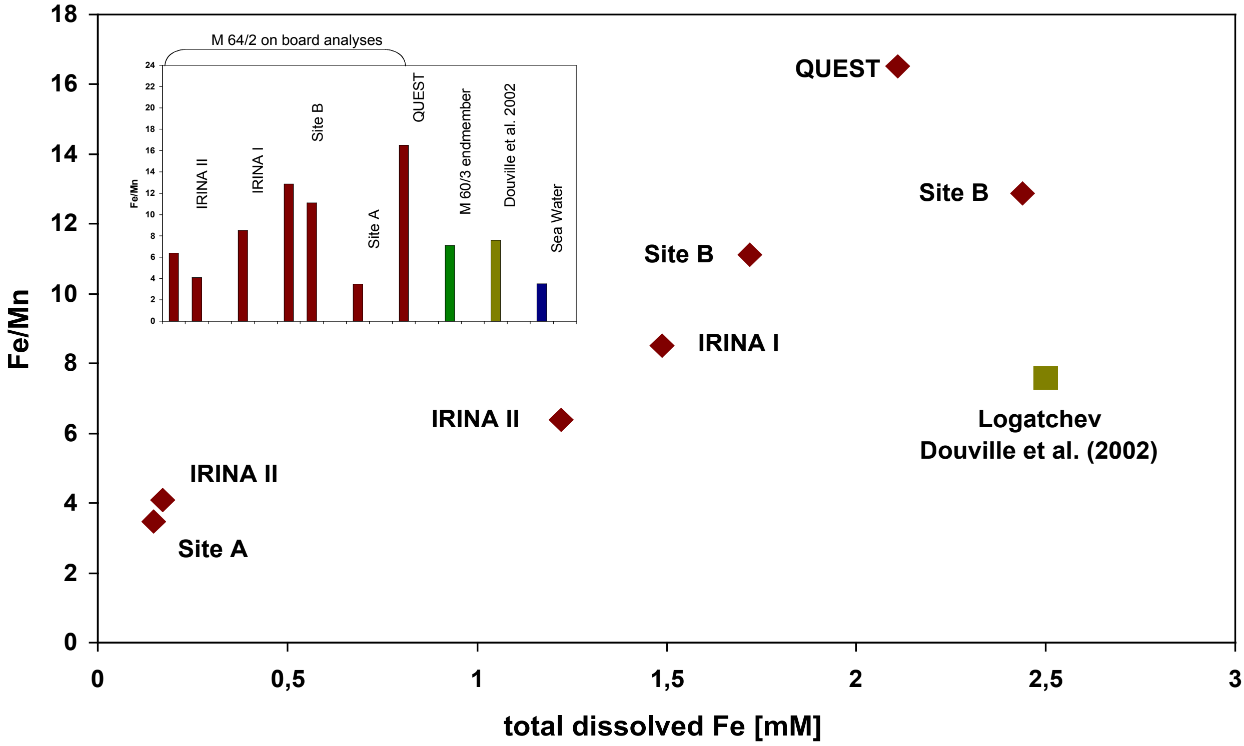

Fig. 2.16 Plot of Fe/Mn vs total dissolved Fe. Insert shows Fe/Mn ratios in comparison to data from M60/3 and Douville et al. (2002).

Alkalinity: The results are listed in table. As expected the alkalinity of the CTD samples as well as of the diffuse vent samples range between 2.0 and 2.3, which is in accordance with the value of 2.33 yielded for IAPSO and the averaged CTD samples.

Samples taken from smoking vent sites are decreased to more than a quarter of the reference value varying from 0.5 to 1 mM. These values have to be checked and elaborated by potentiometric titration afterwards. Furthermore contributions of carbonate and borate/silicate have to be identified.

2.4.8 Marine microbiology
(A. Gärtner, M. Perner)

The aim of the cruise was the collection of microbial communities from the Logatchev-I hydrothermal vent field (LHF I) at 14°45 N in order to perform molecular analyses of the microbial community structure (in the home lab) and cultivation based experiments using specific media (started on board and continued in the home laboratory). In addition, we started with on board microscopic observations of microorganisms inhabiting freshly taken samples and with in situ cultivation experiments.

Therefore, two nets of porous substrate were positioned above a mussel field with shimmering water at IRINA II and collected after 48 hours. One net was positioned directly above a site of diffusive fluid emanations of the mussel field. The other served as a reference and was placed over a part that had been cleared of mussels within the vicinity of shimmering water. Cultivation experiments using this porous material have begun on board (see b). Molecular analyses of the microbial community that was absorbed by the porous material will be conducted in the laboratory at home.

Five substrate nets were placed along the temperature sensor mooring positioned between IRINA I and ANNA LOUISE. The nets are located at a height of 2.5m, 5m, 7.5m, 10m and 20m depth above the seafloor. They will be collected in 2006 and treated as the 2 day deployments were.

Further samples were taken via the fluid sampling system from diffusive vents as well as from fluids of black smokers during ROV cruises. Other samples represent hydrothermally influenced rocks and sediments which were retrieved via the TV-grab and the ROV. The samples were frozen at -20°C and fixed for further treatment. Plume samples were taken using the CTD. These samples were filtered and immediately frozen at -20°C or fixed for further processing

The samples mentioned above were also used for obtaining enrichment cultures. For these purposes selective media as indicated above were used. Growth was monitored by microscopic observation. Autotrophic as well as heterotrophic microorganisms in culture include various morphotypes. Further processing will be conducted in the home lab with the aim to obtain pure cultures. In cultures that were enriched with hot hydrothermal vent fluid hyperthermophilic microorganisms were observed. They grew at 92°C on acetate with hydrogen and iron(III).

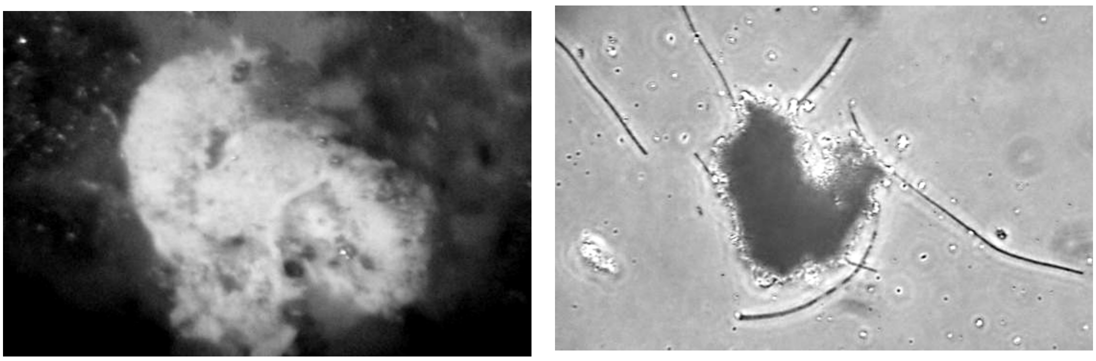

Fig. 2.17 Pictures showing the "microbial mat" positioned between IRINA II and site "B" (257 ROV). (A) Stereo microscopic picture of white "microbial mat" (scale bar 2mm) and (B) showing the attachment of filaments to the white floc (scale bar 10µm).

Microscopic observations of microorganisms inhabiting freshly taken samples revealed heterogenous morphotypes. A white "microbial mat" (Fig. 2.17A) with shimmering water was discovered between IRINA II and site "B" (257ROV). Microscopic observations revealed that the white flocs observed are not microorganisms but substrate to which filamentous bacteria are attached to (Fig. 2.17B).

Further microscopic analysis revealed that these filaments consist of single bacteria chained together (Fig. 2.18). This sample generally exhibited heterogenous morphotypes of microorganisms such as cocci, rods, or spiril shaped ones. Grey sediment collected from the border of the IRINA I crater (252ROV-4) showed amongst rods and cocci also morphotypes resembling spirochaetes.

Fig. 2.18 Microscopic picture from the "microbial mat" showing filaments comprising single bacteria chained together (scale bar 10µm).

2.4.9 Hydrothermal symbioses
(N. Dubilier, F. Zielinski)

Our main goal for this cruise was to investigate the transfer of energy from vent fluids to the dominant members of the faunal community at Logatchev, the mussels *Bathymodiolus puteoserpentis*. These mussels have greatly reduced guts, and their main source of nutrition are symbiotic bacteria that live in their gills. Two types of symbionts coexist in the gill cells: thiotrophic bacteria that use reduced sulfur compounds such as sulfide as an energy source and fix CO_2 as a carbon source, and methanotrophic bacteria that use methane as both an energy and carbon source. The energy sources for the mussel symbioses are delivered by the hydrothermal fluids that carry high concentrations of sulfide, methane, and other reduced compounds. The dilution of these effluents with ambient seawater leads to gradients in sulfide and methane concentrations that vary over time and space. These gradients play a major role in determining the biomass, activity and productivity of the vent community. We have defined these interactions between hydrothermal and biological processes as the geobiological coupling between vent fluids and symbiotic primary producers.

During this cruise, we contributed to our ongoing studies of geobiological coupling at MAR vents by identifying and characterizing gradients in vent fluids in mussel beds, and collecting mussels along these gradients for analysis of the biomass and activity of the bacterial symbionts. To collect geochemical data at a scale relevant to the mussel community, we worked in close collaboration with the fluid chemistry group, temperature logger group, and in situ group on mussel beds from three sites at Logatchev, two sites at IRINA II and one at QUEST. Site 1 at IRINA II was located relatively high on the IRINA II mound, close to the active black smokers on top of the IRINA II complex. This site was completely dominated by *Bathymodiolus* mussels that formed a dense bed of several layers thickness with no empty shells visible. Site 2 was lower on the IRINA mound, south of the large chimney complex, and close to the small active black chimney. At this site, 2 mussel beds separated by only a few meters were sampled: the mussel bed at Site 2A appeared less active with many empty mussel shells and high abundances of gastropod snails and ophiurid sea stars covering the mussels, which were rusty brown in color. In contrast, the mussels at Site 2B appeared to be thriving, with little coverage by other animals, and the mussel shells shiny dark-brown to black in color. Site 3 at QUEST was a mussel bed located southeast of the active smoker at QUEST. This site was characterized by high abundances of juvenile mussels. Shimmering water was observed at all collection sites, and shrimp were regularly observed at the bottom layers of the mussel beds. A summary of collections sites and geochemical data is provided in Table 2.5.

Table 2.5 Mussel collection sites and corresponding in situ, temperature, and fluid data.

site	location	purpose	mussel sample	Profiler data	temperature data		fluid data				
				station number	station number	logger #	station number	$[CH_4]$ [μM]	$[H_2]$ [μM]	$[S^{2-}]$ [μM]	[pH]
1	**IRINA II mussel bed**	mussel transplantation experiment	**252 ROV/6** (0 days) **244 ROV/7** (1 day) **244 ROV/6** (2 days) **244 ROV/8** (5 days) **244 ROV/9** (7 days) **244 ROV/10** (10 days)	232 ROV/4(a) 244 ROV/1	249 ROV/1 249 ROV/2 249 ROV/3 249 ROV/4 249 ROV/6 257 ROV/1	online online online online 4143 0-9	232 ROV/7	**3,06**	**5,44**	max. 0,4	7,86
2A	**IRINA II mussel bed**	mussel collection	**232 ROV/5**	232 ROV/1	232 ROV/4 232 ROV/6	online 4144	232 ROV/3	**1,63**	**1,36**	max. 0,16	7,92
2B	**IRINA II mussel bed**	mussel collection	**266 ROV/7**	266 ROV/1 266 ROV/2 266 ROV/3 266 ROV/4 266 ROV/5 277 ROV/?	None		266 ROV/6	**15,04**	**5,89**	6	7,63
3	**QUEST mussel bed**	mussel collection	**281 ROV/3**	None	281 ROV/4	10-19	281 ROV/2	**63,68**	**4,20**	70	6,97
-	**IRINA II near dome structure**	shrimp collection	**272 ROV/6**	None	None		None				
-	**IRINA II near dome structure**	shrimp collection	**283 ROV/7**	None	None		None				

A further major goal during our cruise was to study how the removal of mussels from fluid gradients affects the symbiosis. In a so-called transplant experiment, we collected mussels at Site 1 on the IRINA II complex and placed them at a site far removed from any obvious vent fluids (beacon #14, Fig. 2.19).

Fig. 2.19 Site at beacon 14 where mussels were transplanted from Site 1 on the IRINA II complex to remove them from hydrothermal activity.

Mussels were collected using the ROV manipulator arm in nets (40 cm length with a 20 cm diameter opening, mesh size 1000 µm) with a net-covered lid that could be closed after collecting the mussels, to prevent predators such as vent crabs from entering the nets or mussels from escaping from the nets. Nets were recovered from the beacon 14 site 1, 2, 5, 7, and 10 days after collection at Site 1 and prepared on board for morphological and molecular analysis in the home laboratory. For on board analysis of methane oxidation rates, gill tissues were incubated in radioactive methane for up to 8 hours and the decrease in methane in the incubation over time determined in collaboration with Janine Felden (MPI Bremen) from the in situ group (Fig. 2.20). No significant decrease in methane oxidation rates occurred for up to 2 days after removal of the mussels from vent fluids, but after 5 days, methane oxidation rates decreased by at least 60%. This indicates that the symbionts are not digested by the mussels and remain fully active during the early stages of starvation, but become less active during the later stages of starvation, possibly because of partial digestion by their hosts. Our home laboratory analyses will show if this assumption is supported by morphological and molecular data.

In addition to our studies on the *Bathymodiolus* mussels, shrimp were collected from the IRINA II chimney complex, using the nets described above and the ROV manipulator arm. After recovery, the shrimp were stored in chilled seawater for up to 4 hours before specimens belonging to the genus *Rimicaris* were dissected and fixed on board for analysis in the home laboratory.

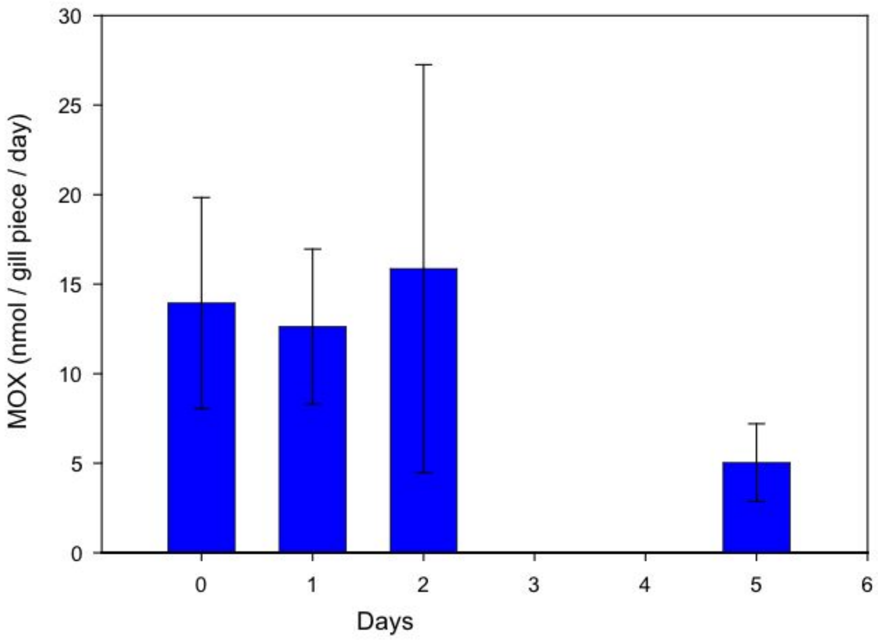

Fig. 2.20 Oxidation rates of methane in gills of *Bathymodiolus puteoserpentis* mussels removed from vent fluids for up to 5 days. Data for 7 and 10 days is currently being analysed.

The symbionts of these shrimp, that are abundant on their appendages and in their gill chamber, will be investigated using morphological and molecular techniques. Attempts to collect live vesicomyid clams that reportedly occur in the vicinity of the ANYA marker were not successful, and only empty *Bathymodiolus* shells were found in our collection nets. Live thyasirid clams, of which only a few specimens were found in the ANYA area during the last HYDROMAR I cruise M60/3, were not observed during this cruise.

2.4.10 Fluid dynamic and microbial processes

(F. Wenzhöfer, J. Felden, M. Viehweger)

The main goal of this study was the investigation of physico-chemical gradients at water-substrate interphases and microbial processes at selected habitats. *In-situ* micro sensor measurements of O_2, pH, H_2S, T and, for the first time, H_2 were used to investigate the links between the geochemical energy supply from hydrothermal fluids and hydrothermal vent communities. These high-resolution micro profiles allow determining the variability of hydrothermal fluid emission in space and time and its influences on vent communities. With the aid of such fluid analyses (together with fluid sampling), habitats were selected for studying microbial turnover rates of methane, CO_2 fixation and thymidine incorporation.

Profiler and benthic chamber deployments

To investigate the small-scale fluid dynamics at vent mussel fields two benthic lander modules, a profiler and a chamber, have been constructed to be deployed and operated by the ROV. The autonomous profiler module (Fig. 2.21; Wenzhöfer et al., 2000) hosted 2 O_2, 1 temperature

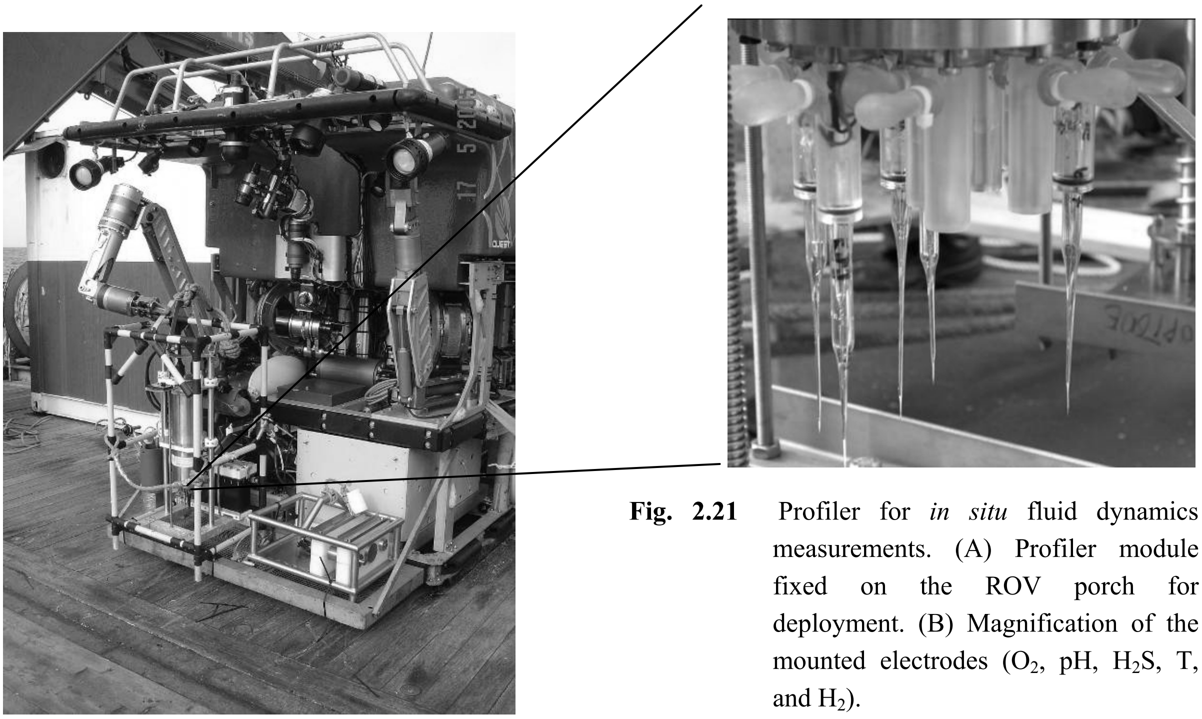

Fig. 2.21 Profiler for *in situ* fluid dynamics measurements. (A) Profiler module fixed on the ROV porch for deployment. (B) Magnification of the mounted electrodes (O_2, pH, H_2S, T, and H_2).

(Pt100, UST Umweltsensortechnik GmbH, Geschwenda, Germany), 2 pH, 3 H_2S and for the first time 1 H_2 microelectrodes (UNISENSE, Denmark). If not specifically mentioned all electrodes have been constructed in our laboratory in Bremen. During the deployments measurements were taken every second to study the short-time variations within diffuse fluid fluxes above a mussel bed.

The benthic chamber module is a modified version of the free-falling chamber lander previously used to study benthic processes in the deep-sea (Wenzhöfer and Glud, 2002). This small benthic module consists of a circular chamber, an electronic cylinder, a water sampling system and a battery, which can be operated by the ROV. The chamber encloses an area of ca. 285 cm^2 together with 15 cm of overlying bottom water. Two microelectrodes (1 H_2S and 1 H_2) mounted in the chamber lid monitor the concentration change in the enclosed water body while at pre-programmed time intervals 5 water samples (each 50 ml) were retrieved for later analyses of O_2, DIC and other elements.

All in-situ measurements were performed at IRINA II along a gradient of different diffuse fluid flows (Tab. 2.6).

Microbial activity measurements

Rates of aerobic methane oxidation, chemoautotrophic production (CO_2 fixation) and bacterial growth (Thymidine incorporation) were measured on hot and diffuse fluid samples taken by the ROV (Niskin bottles mounted on the tool sledge and fluid sampling system) and CTD-Rosette (Tab. 2.6). Samples were processed directly after the recovery of the sampling devices or stored shortly at 4°C. After adding the tracer, all samples were incubated for 6 hours to 5 days at 4, 20, 60 and 80ºC, respectively. Activity was counted in degassed samples on a liquid scintillation counter. Rates of aerobic methane oxidation, CO_2 fixation and Thymidine incorporation will be calculated back home after determining the dry weight of the incubated biomass, the dissolved inorganic carbon concentration in the fluids and the tracer activity.

Additionally microbial rate measurements and incubation experiments were carried out on mussel gills, sediments and rock particles.

Preliminary results

All electrode signals showed a highly fluctuating signal over time when placed on a diffuse venting mussel bed. However, the maximum signal change varied within the same mussel field on a distance of a few decimeters. As an example temperature signals from 4 different sites from a mussel bed at IRINA II are shown in figure 2.22. The ambient temperature of the bottom water was 2.6ºC while the maximum temperature above a mussel bed with visually shimmering water was 6.5ºC. At occasions where warmer fluids pour out electrode signals of H_2S and H_2 increased while O_2 electrodes showed a distinct reduction. The exact concentration changes will be calculated back home, after analyzing the calibration solutions. All electrode signal readings, however, revealed a highly dynamic diffuse fluid venting with space and time.

Table 2.6 Overview of sampled stations for Profiler and benthic chamber deployments, aerobic methane oxidation (MOx), chemoautotrophic production (CO_2 fixation) and bacterial growth rates.

Station	Profiler	Chamber	MOx	CO_2 fixation	Thymidine incorporation
217 CTD			X	X	X
232 ROV	X (2 sites)				
242 CTD			X		
244 ROV	X				
249 ROV			X		
257 ROV			X	X	X
266 ROV	X (5 sites)		X		
270 CTD			X	X	X
272 ROV			X	X	X
277 ROV	X		X		
281 ROV		X	X		
283 ROV			X		

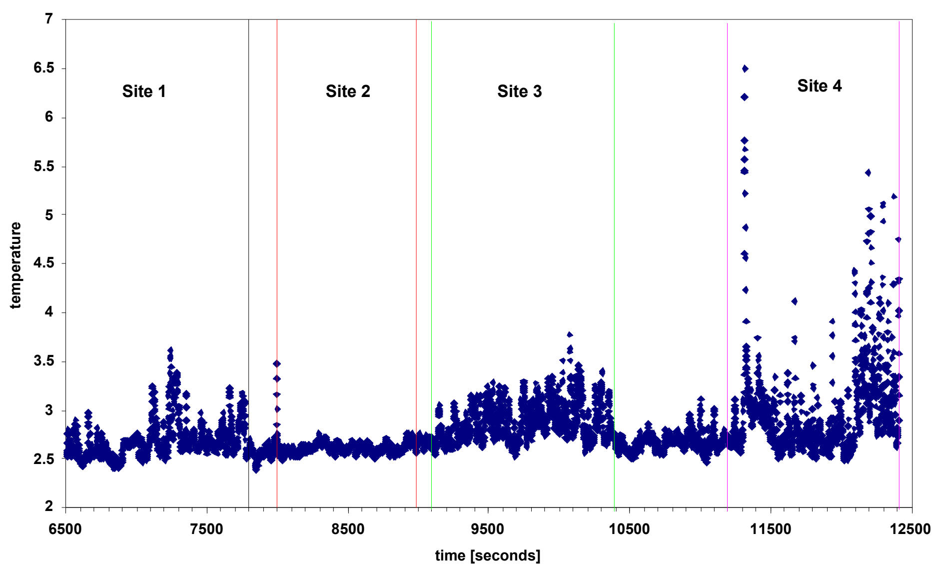

Fig. 2.22 In situ temperature at 4 different sites above a mussel field at IRINA II.

2.4.11 Metagenomics
(A. Meyerdierks)

The aim of the participation in cruise M64/2 to the Logatchev hydrothermal field was the sampling of free living microbial communities at few characteristic hydrothermally influenced sites with high biomass for metagenome analyses. Preferred samples were sediments and microbial mats as several grams of a microbial mat or several hundred grams of sediment contain generally sufficient cells for a metagenome study. The samples should be taken in a targeted way, e.g. by the ROV, at well characterised sites.

Methods

Upon retrieval, each sample was divided in several parts. Sediment cores were sectioned into 1 cm or 2 cm slices prior to further treatment. Sediment samples were fixed with 60% ethanol in phosphate buffered saline (PBS) and 2-3% formaldehyde (FA)/PBS, respectively, for cell count determination, and community structure analysis. The major part of the sample was deep frozen for DNA extraction (-20°C) in the home laboratory. Small parts of rocks, crusts and sulfide samples were fixed with 1% FA/PBS for community structure analysis, and the other part of the sample was again deep frozen for DNA extraction. Microorganisms in fluid and plume samples were fixed with 1% FA/PBS or left untreated prior to a concentration of the cells on polycarbonate membrane filters (0.22 µm) or in a Sartobran 300 filter unit.

Samples and Preliminary Results

Samples were taken at different characteristic sites by the ROV, the CTD-rosette sampler, and the TV-grab, and included the following material:

1) Two sediment cores were taken in an area exhibiting a white surface, close to the “marker Anya” (263ROV, Fig. 2.23a and b). Temperature measurement by the environmental parameters group (3.4.5) revealed 52°C at a depth of about 25 cm below seafloor. The analysis of fluid, taken with Niskin bottles above this site, by the gas chromatography group (3.4.6), indicated elevated methane and hydrogen values. The sediment had a sulfidic smell.
   Additionally, a sediment core (20 cm) was taken close to the mussel bed found in the QUEST area at a side also covered with a white film (283ROV).
2) Other sediment samples (5 stations) were taken by the TV-grab (229GTV, 239GTV and 250 GTV), or sampled, together with mussels, in a net taken at QUEST (281ROV). One sediment sample was collected 88 m south of IRINA II at a field, again covered with a white film, using a shovel with lid (252ROV, Fig. 2.23c). Here, the temperature on top of the sediment was about 27°C, determined by the environmental parameters group (3.4.5). Shimmering water was observed, and microscopic analysis by the microbiology group revealed a diverse microbial community supposedly associated with the white matrix (see chapter 3.4.8).

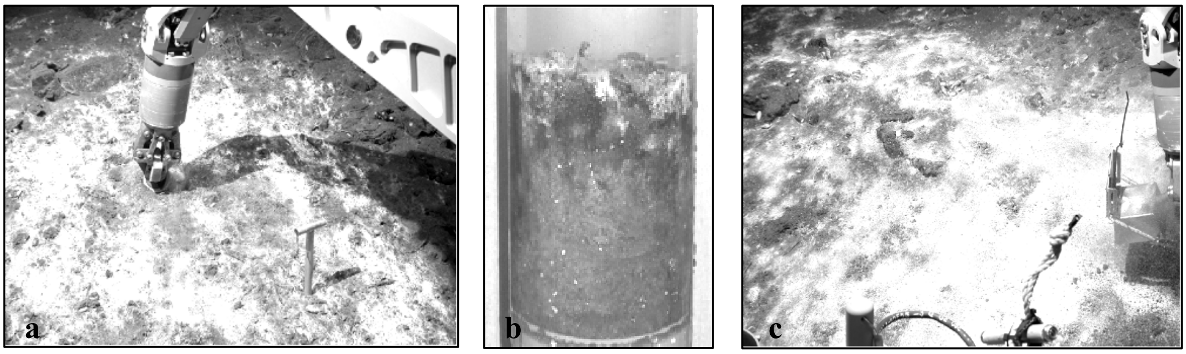

Fig. 2.23 a) Sampling of sediment cores with a push corer and temperature measurement at a field exhibiting a white surface layer close to the marker "Anya". b) Sediment core before sectioning. c) Sampling of sediment with the shovel, south of IRINA II.

3) Sulfide structures, crust and rock samples (8 stations) were collected by the gripper of the ROV, and found in TV-grab contents and nets after mussel sampling.
4) Hydrothermal fluids were obtained using Niskin bottles (6 stations) or by participating in the fluid sampling system (chapter 3.4.7; 4 stations). Up to 6 l diffuse flow, sampled with Niskin bottles, and up to 1.4 l derived from the fluid sampling system were filtered for DNA extraction. Two samples were derived from a black smoker (261ROV).
5) Hydrothermal plume (2 stations) was collected using the CTD-rosette sampler. About 42 l of hydrothermal plume from 242CTD (water depth 2770 m) and about 79 l of plume sampled during CTD270 (water depth 2800) were filtered for DNA extraction.
6) Finally, mussel byssus and its associated microbial community (2 stations) were sampled by scraping byssus from mussel shells (232ROV, 281ROV).

2.4.12 Marine zoology

(J. Stecher)

Zoological samples were taken at 36 stations, representing 7 hydrothermal active sites and 8 non-hydrothermal active locations.

The Smoker-Complex and Chimney Habitat

The highest biodiversity was observed at the IRINA II site. Three of the chimneys, characterised by shimmering water, were covered by *Bathymodiolus puteoserpents*, whereas only one was dominated by dense shrimps-aggregations of *Rimicaris* cf. *exoculatus*. Additionally *Chorocaris* and *Mirocaris* were observed here. At this chimney the fluids showed maximum temperatures of 170°C (277ROV, 283ROV). Obviously those shrimps were clearly less abundant at the small separate smoker on the southern end of the smoker-complex. Here the fluids showed maximum temperature of 225°C (224ROV).

Concerning the distinct patched settlement of different species at chimneys one remarkable feature is worthwhile to mention. The northern chimney was clearly separated into two sections, the side, facing to active venting was covered by dense aggregation of *Bathymodiolus puteoserpents* whereas the far side was only overcast with clutches of gastropods.

In the western forefront of the smoker-complex we found a well-established *Bathymodiolus puteoserpentis*- association. Its length-width dimension was approximately 4m x 3m. In comparison with the mussel association of the smoker-complex this assemblage showed own characteristics based on its accompanied fauna. The brittle starfish *Ophioctenlla acies* and the snail *Phymorhynchus* cf. *moskalevi* were clearly more abundant in the forefront assemblage as thus at the smoker-complex itself. Dense aggregation of shrimps, comparable to those of the smoker-complex were absent. Specimen of *Alcinocaris* and *Mirocaris* were more frequently observed here. They inhabited the mussel field in slightly abundances between the mussels. Additionally chaetopterid, and terebellid annelidsas well as *Archinome* c.f. *rosacea* lived within the byssus of *Bathymodiolus puteoserpentis*. The vent endemic fish *Pachyara thermophilus* was only seen here in the IRINA II site of LHF I. Two more typical species, which belong to the accompanied fauna were the decapod crustaceans *Segonzacia mesatlantica* and the squat lobster *Munidopsis crassa*. Whereas *Segonzacia mesatlantica* was widely distributed at the smoker-complex as well on the mussel field, *Munidopsis crassa* was clearly patched. *Munidopsis crassa* was manly observed in inactive regions at the northeast side of the smoker-complex, where an extinct field of dead mussels was located. In contrast *Segonzacia mesatlantica* was observed in the vicinity of shimmering water with temperatures ranging from 3°C to 8°C.

The fauna became impoverished at site "A". Live specimens were only seen at the single active chimney Barad-Dûr. Single shrimps inhabited the tip region of the chimney where black fluids emerged. Additionally see-anemones (actinaria) were sitting here. Right in the vicinity of emerging fluids specimens of the gastropod *Peltospira smaragdina* were sampled. Those snails were also found at black smokers of IRINA II. Furthermore the vent crab *Segonzacia mesatlantica* was seen on flanges in 4-5m height as well at the bottom of the chimney. An expanded mussel field with live *Bathymodiolus* specimens, comparable to this of IRINA II was not found. At the bottom only several actinians were seen.

The "Smoking-Crater"-Habitat

With the exception of the "QUEST" site the biodiversity at the smoking craters was very low, comparable with that of the smoker Barad-Dûr. Only at the little smokers of the crater rim we found a vent fauna, consisting the shrimp *Rimicaris exoculata* and the bythograeid crab *Segonzacia mesatlantica*. In the periphery of the smokers actinaria were regularly observed as well as fishes of the family Bythitidae, mainly *Cataetyx* c.f. *laticeps*. The less abundances of crustaceans were documented at site "B", were we measured the highest fluid temperatures with 300°C up to 350°C.

At "IRINA I", where the temperatures of fluids were significantly lower (177°C) shrimps and crabs were more abundant. On the other hand actinians were obviously more abundant in the vicinity of smokers at site "B".

Live *Bathymodiolus puteoserpentis* mussels patches we found only in the "QUEST" site. One major patch, which was accurate investigated, covered an area of 3m x 1m. This assemblage was characterised by juvenile's mussels. They covered not only the float of at the temperature logger No3, which was left back on Meteor cruise M60/3; additionally we found them living among adults within the mussel field. This indicated that recruitment processes were successful during the last one and a half year. The accompanied fauna was similar with those of the "IRINA II" mussel field. Only *Phymorhynchus mosalevi* was less abundant at the "QUEST" site. The temperature of its diffuse fluids exceeds not over 12 °C. Therefore the diffuse fluids were slightly wormer than those of the mussel field of "IRINA II". Whereas the major mussel patch was approximately 3m away from the cater rim, several much smaller mussel patches (20-30cm in diameter) were located in the vicinity of little active smokers directly at the crater's rim. Comparable distribution patterns of patched mussels we also found in "IRINA I". Unfortunately the *Bathymodiolus*-population was dead, only some live specimens were noticed at the bottom of the active smokers at the crater's rim.

Size-Frequency Distributions of Bathymodiolus puteoserpentis

During the transplantation experiment 6 nets were collected, laid beside the mussel field and recovered after a fixed time schedule (see chapter 2.4.9). One more net was excluded for the experiment, because its recovery exceeded the time schedule. All *Bathymodiolus* specimens were shipboard measured and length was used for size-frequency analysis. Hence to the transplantation experiment 243 *Bathymodiolus puteoserpentis* specimens were measured. Additionally 61 specimens were retrieved from the same mussel field by two samples (232ROV-5, 266ROV-7), 5m away from the transplantation experiment spot, nearby the T-logger No4 from the Meteor cruise M60/3 (Tab. 2.7, Figs. 2.24 and 2.25). These samples are comparable with the station 38ROV-4, taken on M60/3.

Table 2.7 Samples used for size-frequency analysis of *Bathymodiolus* puteoserpentis, retrieved from the mussel-field IRINA II.

Station	total number of *Bathymodiolus puteoserpentis*	Location
244 ROV# 6, Net No 6	54	"IRINA II" mussel-site 2 (transplantation-experiment), northern end of the field
244 ROV# 7, Net No 4	37	
244 ROV# 8, Net No 2	34	
244 ROV# 9, Net No 8	38	
244 ROV#10, Net No 10	22	
252 ROV# 6, Net No 9	66	
232 ROV# 5	18	"IRINA II", mussel-site 1, southern end of the field
266 ROV# 7	43	
Total number	304	

Additionally four more nets of *Bathymodiolus* were taken. One at the E-wall of the smoker-complex (277ROV-6), and three at the "QUEST"-site (263ROV-6, 281ROV-3, 285ROV-5). Only those animals (126 individuals) were shipboard measured, which were chosen for molecular biological studies. Detailed statistics will follow in the institute's lab.

The size-frequency distribution within the mussel field of "IRINA II" showed clearly one broader peak of mussels from 6cm up to 11 cm length. Within the population at the northern end of the field one more little peak is obviously. It consists of young mussels, which did not exceed a length of 4cm. These distribution patterns indicated, that recruitment processes were successfully in the past. Additionally the mortality seemed to be relative low, because only one slightly peak of dead shells was noticed.

Nevertheless it seemed to be that recently recruitment processes were severely limited over the last year, since the T-logger #4, which was placed during Meteor cruise M60/3, was not overgrown by any Bathymodiolus specimens. For comparison, the growth of young mussels at T-logger #3 of the "QUEST" site indicated that recently recruitment processes are still active.

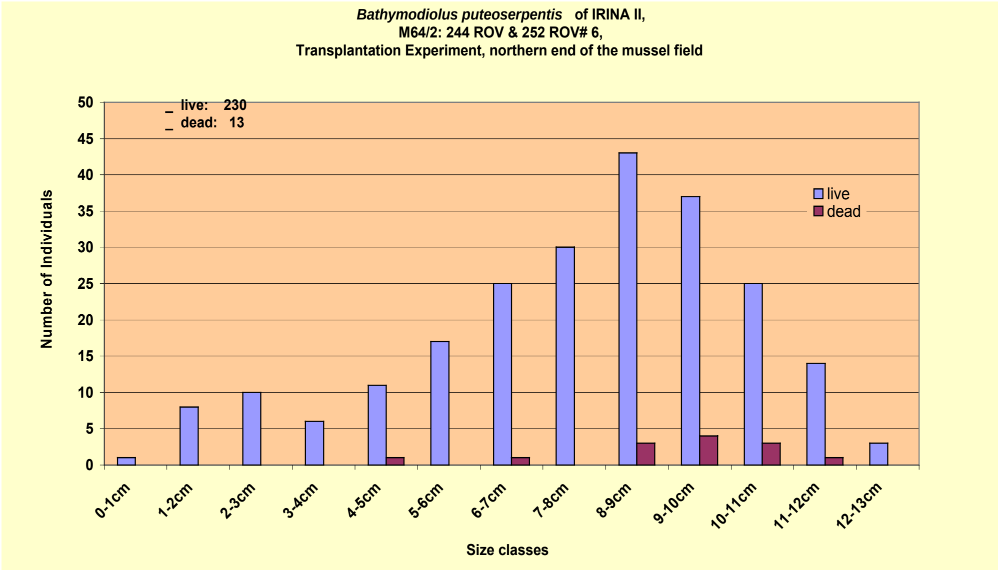

Fig. 2.24 Size-frequency distribution of *Bathymodiolus puteoserpentis* at the northern end of the mussel field in IRINA II during Meteor cruise M64/2.

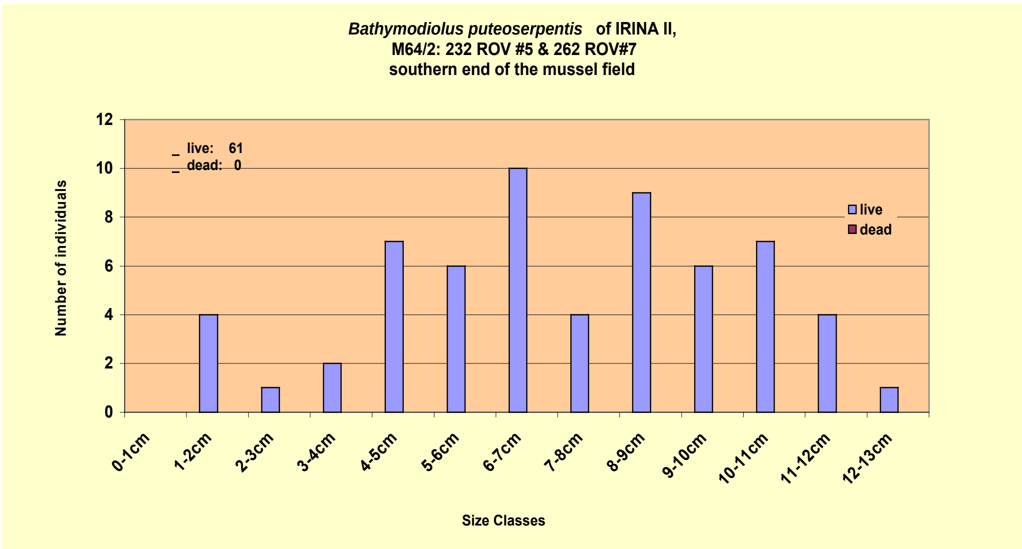

Fig. 2.25 Size-frequency distribution of *Bathymodiolus puteoserpentis* at the southern end of the mussel field in IRINA II during Meteor cruise M64/2.

"ANYA GARDEN"

Kuhn et al. (2004) described the disagreement between the positioning of "ANYA´S GARDEN" given by Gebruk et al. (2000) and their results during the HYDROMAR cruise of M60/3. It can be stated as save that the maker "ANYA" is located 30 m northwest of the "IRINA II" site. Starting at this maker, and going the slope upwards to east, we found during our dive 263ROV (QUEST Dive 57) several structures like *Bathymodiolus* patches with shimmering water, microbial mats and several outcrops, which were in agreement with the Gebruk´s description of "ANYA´s GARDEN". Nevertheless live vesicomyid and thyasirid clams we did not noticed here. Vesicomyid shells we retrieved only at station 258GTV, approx. 20 m N of "IRINA II" (see chapter 2.4.1; Fig. 2.1).

Because during Meteor cruise M60/3 shells of vesicomyid and thyasirid clams were documented nearby this slope, it seemed to be that changes happened, which we could not interpret at this state of knowledge. Instead of this we flew at the slope over large mussel fields consisting of dead *Bathymodiolus* shells, which were inhabited by the snail *Phymorhynchus moskalevi* as well by the squat lobster *Munidopsis crassa*. Here we observed the most *Munidopsis* at LHF-1 especially on outcrops. So we are sure, that the position of "ANYA´s GARDEN" given by Gebruk et al. (2000) is incorrect. "ANYA´s GARDEN" is located at a slope northwest of the "IRINA II" site and hence to the ecofaunistical results it can be regarded as the northwestern branch of "IRINA II".

2.5 Weather conditions

(W. T. Ochsenhirt)

In the afternoon of May 06 2005 FS METEOR left the port of Fortaleza for leg M64/2. A ridge of a subtropical high in the Southwest Atlantic dominated the weather to the beginning of the voyage and METEOR encountered southeasterly trade winds of 4 to 5 Bft. One day later, in the early morning, near 01° South a first larger cloud belt associated with showers was passed. On the next day METEOR crossed the ITCZ (**I**nter **T**ropical **C**onvergence **Z**one) accompanied by frequent and heavy showers and gusty winds up to Bft 6 from variable directions. The normal wind direction outside of the tropical shower area was southeast at first and became east to northeast later. Wind speeds without disturbances ranged from 4 to 5 Bft. The northern edge of the ITCZ extended from 08°N 15°W to 07°N 38°W during this period. METEOR arrived in the area of investigation near 14,8°N 45,0°W on May 10 in the afternoon. This region was still under the influence of the tradewindsystem and steady easterly winds of 4 to 6 Bft predominated with most frequent wind speed of Bft 5. On some days the wind decreased to Bft 3. During the whole time of station work the weather was mostly fair with only few periods of light precipitation. The swell came from easterly directions with height of 1.5 to 2 m, in cases of two swells from different origin up to 3m. In the evening of May 29 METEOR left the working area with easterly course to Dakar. On the transit the centre of the subtropical high was just south of the Azores. Easterly winds of about 5 Bft backed to northeast and north and decreased gradually.

2.6 Station List

(H. Strauss)

Station	Area	Location	Depth	Date	Brief description
217-CTD	S of Logatchev	13° 30.00' N 45° 00.00' W	2666 m	10.05.05	Background station for CTD
218-HS	S-N track into LHF-1	13°30'N 45°00'W to 14°30'N 45°00'N		10.05.05 and 11.05.05	Bathymetry
M219-CTD	QUEST area	14°45,23'N	3017 m	11.05.05	Plume mapping and sampling

Station	Area	Location	Depth	Date	Brief description
		44°58,81'W			
M220-ROV	LHF-1	14°45,28'N 44°58,85'W	3050 m	11.05.05	Terminated early due to technical problems
M221-CTD	S of IRINA II	14°45,11'N 44°58,81'W	3044 m	11.05.05	Plume mapping and sampling
M222-GTV	SW of LHF-1	14°44,99'N 44°58,97'W	3075 m	11.05.05	Sampling hydrothermal sediments
M223-MAPR	LHF-1	14°45,11'N 44°58,81'W		12.05.05	Plume mapping, 5 MAPR, 20 T-sensors, GAPS, Transponder
M224-ROV	QUEST and ANNA LOUISE	14°45,21'N 44°58,81'W and 14°45,21'N 44°58,72'W	3046 m and 3038 m	12.05.05	Deployment of Ocean Bottom Tiltmeter near QUEST area, fluid sampling at ANNA LOUISE
M225-GTV	SW of IRINA II	14°45,19'N 44°58,82'W	3048 m	13.05.05	Sampling at future drilling site
M226-OFOS	Across LHF-1	14°45,42'N 44°58,38'W to 14°44,86'N 44°59,09'W	2954 m to 3108 m	13.05.05	Mapping along NE-SW profile across LHF-1
M227-CTD	NE of Site B	14°45,23'N 44°58,82'W	3020 m	13.05.05	Plume mapping
M228-MAPR	W of IRINA II	14°45,11'N 44°58,81'W	3050 m	13.05.05	12 hrs stationary plume mapping with 5 MAPRs and 20 T-sensors
M229-GTV	W of IRINA I	14°45,07'N 44°58,72'W	3017 m	14.05.05	Sampling at future drilling site
M230-GTV	S of ANNA LOUISE	14°45,00'N 44°58,66'W	2996 m	14.05.05	Sampling at future drilling site
M231-CTD	NW of LHF-1	14°45,28'N 44°58,90'W	3038 m	14.05.05	Plume mapping and sampling
M232-ROV	IRINA II	14°45,11'N 44°58,81'W	3037 m	14.05.05	Mussel experiment with in-situ Profiler measurements and KIPS fluid sampling
M233-CTD	N of LHF-1	14°45,28'N 44°58,76'W	3062 m	15.05.05	Plume mapping
M234-CTD	N of LHF-1	14°45,50'N 44°58,76'W	3127 m	15.05.05	Plume mapping
M235-CTD	N of LHF-1	14°45,56'N 44°58,82'W	3157 m	15.05.05	Plume mapping
M236-CTD	N of LHF-1	14°45,61'N 44°58,89'W	3155 m	15.05.05	Plume mapping
M237-CTD	N of LHF-1	14°45,77'N 44°58,99'W	3200 m	15.05.05	Plume mapping

Station	Area	Location	Depth	Date	Brief description
M238-CTD	N of LHF-1	14°46,02'N 44°59,06'W	3215 m	15.05.05	Plume mapping and sampling
M239-GTV	N of IRINA II	14°45,23'N 44°58,75'W	2988 m	15.05.05	Sampling at future drilling site
M240-HS	E of LHF-1			16.05.05	Bathymetry across two W-E profiles
M241-CTD	N of LHF-1	14°45,82'N 44°58,67'W	3225 m	16.05.05	Plume mapping
M242-CTD	N of LHF-1	14°46,01'N 44°58,80'W	3225 m	16.05.05	Plume mapping and sampling
M243-HS	E of LHF-1			17.05.05	Bathymetry along S-N tracks
M244-ROV	IRINA II	14°45,18'N 44°58,73'W	3032 m	17.05.05	OBT and OBP positioned, biological sampling
M245-CTD	N of LHF-1	14°46,00'N 44°59,40'W	3331 m	18.05.05	Plume mapping
M246-CTD	N of LHF-1	14°46,40'N 44°59,47'W	3539 m	18.05.05	Plume mapping
M247-CTD	N of LHF-1	14°46,60'N 44°59,19'W	3416 m	18.05.05	Plume mapping
M248-CTD	N of LHF-1	14°46,09'N 44°59,00'W	3223 m	18.05.05	Plume mapping and sampling
M249-ROV	ANNA LOUISE and IRINA I	14°45,05'N 44°58,66'W and 14°45,09'N 44°58,71'W	2950 m and 3034 m	18.05.05	Fluid and rock sampling, mussel nets
M250-GTV	S of IRINA II	14°45,16'N 44°58,78'W	3047 m	19.05.05	Sampling at future drilling site
M251-CTD	N of LHF-1	14°46,10'N 44°59,16'W	3297 m	19.05.05	Terminated early due to technical problems
M252-ROV	Site A and IRINA I	14°45,04'N 44°58,63'W and 14°45,09N 44°58,66W	2928 m and 2992 m	19.05.05	Geological and biological sampling, photomosaicing
M253-CTD	N of LHF-1	14°46,09'N 44°59,20 'W	3281 m	20.05.05	Plume mapping and sampling
M254-CTD	N of LHF-1	14°45,90'N 44°59,20'W	3248 m	20.05.05	Plume mapping
M255-CTD	N of LHF-1	14°45,70'N 44°59,30'W	3180 m	20.05.05	Plume mapping
M256-CTD	N of LHF-1	14°45,50'N 44°59,40'W	3157 m	20.05.05	Plume mapping and sampling
M257-ROV	IRINA II and Site	14°45,19'N	3036 m	21.05.05	T-Loggers, fluid and geological sampling

Station	Area	Location	Depth	Date	Brief description
	B	44°58,76'W and 14°45,12'N 44°58,70'W	and 2978 m		
M258-GTV	NW of IRINA II	14°45,21'N 44°58,76'W	3106 m	21.05.05	Geological sampling
M259-GTV	QUEST	14°45,23'N 44°58,83'W	3110 m	21.05.05	Biological sampling (GTV empty)
M260-CTD	N of LHF-1	14°45,94'N 44°59,06'W	3205 m	21.05.05	Plume mapping and sampling
M261-ROV	Site A and IRINA I	14°45,06'N 44°58,64'W and 14°45,09'N 44°58,70'W	2928 m and 2986 m	21.05.05	Fluid and sulphide sampling at Site A, fluid and biological sampling at IRINA I
M262-HS	E of LHF-1			22.05.05	Bathymetry along W-E tracks
M263-ROV	IRINA II QUEST	14°45,20'N 44°58,76'W	3045 m	22.05.05	Biological sampling, OBT re-positioning
M264-CTD	W of LHF-1	14°45,19'N 45°01,02'W	3824 m	23.05.05	Plume mapping and sampling
M265-CTD	SW of LHF-1	14°44,00'N 45°00,00'W	3716 m	23.05.05	Plume mapping
M266-ROV	IRINA II and Site B	14°45,18'N 44°58,74'W and 14°45,10'N 44°58,67'W	3034 m and 3003 m	23.05.05	Profiler and biological sampling, Fluid sampling
M267-CTD	S of LHF-1	14°43,96'N 44°58,97'W	3311 m	24.05.05	Plume mapping and sampling
M268-CTD	S of LHF-1	14°44,02'N 44°57.98'W	2952 m	24.05.05	Plume mapping and sampling
M269-CTD	S of LHF-1	14°44,00'N 44°57,00'W	2861 m	24.05.05	Plume mapping and sampling
M270-CTD	S of LHF-1	14°44,50'N 44°57,70'W	2848 m	24.05.05	Plume mapping and sampling
M271-MOOR	SE of IRINA I	14°45,09'N 44°58,69'W	2992 m	24.05.05	Deployment of 25 m of T-Logger Mooring
M272-ROV	IRINA II	14°45,08'N 44°58,67'W and 14°45,20'N 44°58,74'W	2984 m and 3046 m	24.05.05	Positioning T-Logger-Mooring, Fluid and biological sampling at IRINA II
M273-CTD	NW of LHF-1	14°46,04'N	3250 m	25.05.05	Plume mapping and sampling

Station	Area	Location	Depth	Date	Brief description
		44°59,14'W			
M274-CTD	E of IRINA II	14°45,20'N 44°58,70'W	2731 m	25.05.05	Plume mapping and sampling
M275-CTD	SE of LHF-1	14°44,41'N 44°57,21'W	2909 m	25.05.05	Plume mapping and sampling
M276-CTD	SE of LHF-1	14°45,70'N 44°57,30'W	2912 m	25.05.05	Plume mapping and sampling
M277-ROV	IRINA II	14°45,18'N 44°58,72'W	3046 m	25.05.05	Biological and fluid sampling
M278-OFOS	NW of LHF-1	14°45,78'N 44°59,02'W	3200 m	26.05.05	SE-NW track, terminated early due to technical problems
M279-CTD	NW of QUEST area	14°45,26'N 44°58,85'W	3044 m	26.05.05	Plume mapping and sampling
M280-CTD	NW of LHF-1	14°47,01'N 45°00,00'W	3636 m	26.05.05	Plume mapping and sampling
M281-ROV	QUEST	14°45,21'N 44°58,81'W	3053 m	26.05.05	Benthic chamber deployed at IRINA II, fluid, biological and geological sampling at QUEST site
M282-HS	E of LHF-1	14°45,23'N 44°58,83'W		27.05.05	Bathymetry along W-E tracks
M283-ROV	QUEST and IRINA II	14°45,22'N 44°58,81'W and 14°45,20'N 44°58,72'W	3047 m and 3033 m	27.05.05	QUEST musselbed experiment, Fluid sampling at IRINA II T-measurements
M284-OFOS	NW of LHF-1	14°45,23'N 44°58,83'W		28.05.05	Several tracks NW of LHF-1
M285-ROV	QUEST and NW of LHF-1	14°45,22'N 44°58,79'W	3044 m	28.05.05	Final biological sampling at QUEST, exploration and mapping NW of LHF-1

2.7 Acknowledgments

We would like to thank Captain Kull and his crew for their professionality and exceptionally hard work during the cruise, which contributed to the success of the expedtion. Furthermore, we acknowledge the professional patronage of the German Ministry of Foreign Affairs as well as Captain Berkenheger at the Leitstelle Meteor.

We wish to thank the German Science Foundation (DFG) for funding the cruise and subsequent analytical work in the framework of the priority programm SPP 1144 "From mantle to ocean: Energy-, material-, and life cycles at spreading axes".

2.8 References

Douville E., Charlou J. L., Oelkers E. H., Bienvenu P., Jove Colon C. F., Donval J. P., Fouquet Y., Prieur D., and Appriou P. (2002) The Rainbow vent fluids (36° 14'N, MAR): the influence of ultramafic rocks and phase separation on trace metal content in Mid-Atlantic Ridge hydrothermal fluids. Chemical Geology 184, 37-48.

Gebruk, A.V., Moskalev, L.I., Chevaldonné, P., Sudarikov, S.M. and Chernyaev, E.S. (1997) Hydrothermal vent fauna of the Logatchev area (14°45'N, MAR): preliminary results from first 'Mir' and 'Nautile' dives in 1995. InterRidge News, 6, 10-14.

Gebruk, A.V., Chevaldonné, P., Shank, T. Lutz, R.A. and Vrijenhoek (2000) Deep-sea hydrothermal vent communities of the Logatchev area (14°45'N, Mid-Atlantic Ridge): diverse biotopes and high biomass. J. Mar. Biol., 80, 383-393.

Grasshoff, K., Kremling, K., Ehrhardt, M., 1999. Methods of Seawater Analysis. 3rd edition, 600 p., Wiley-VCH.

Kelley, D.S., Baross, J.A., and Delaney, J.R. (2002) Volcanoes, fluids, and life at mid-ocean ridge spreading centers. Annual Review of Earth and Planetary Sciences 30: 385-491.

Krasnov, S., Cherkashev, G., Stepanova, T., Batuyev, B., Krotov, A., Malin, B., Maslov, M., Markov, V., Poroshina, I., Samovarov, M.A., Lazereva, L., and Ermolayev, I. (1995): Detailed geological studies of hydrothermal fields in the North Atlantic: Geol. Soc. Spec. Publ. 87: 43-64.

Kuhn, T. and cruise participants (2004). Mineralogical, geochemical and biological investigations of hydrothermal systems on the Mid-Atlantic Ridge between 14°45'N and 15°05'N (HYDROMAR I). Meteor Berichte 03-04, Mid-Atlantic Expedition 2004, Cruise No. 60, Leg 3, Leitstelle Meteor, Institut für Meereskunde der Universität Hamburg.

Localli, C., Torsi, G., 2001. Voltammetric trace metal determinations by cathodic and anodic stripping voltammetry in environmental matrices in the presence of mutual interference. Journal of Electroanalytical Chemistry 509, 80-89.

Obata, H., van den Berg, C.M.G., 2001. Determination of picomolar levels of iron in seawater using catalytic stripping voltammetry. Analytical Chemistry 73, 2522- 2528.

Seifert, R., Delling, N., Richnow, H.H., Kempe, S., Hefter, J., and Michaelis, W.(1999). Ethylene and methane in the upper water column of the subtropical Atlantic. Biogeochemistry 44, 73-91.

van Damm, K.L., 2004. Evolution of the hydrothermal system at the East Pacific Rise 9°50'N: geochemical evidence for changes in the upper oceanic crust. In: Mid-Ocean Ridges: Hydrothermal Interactions between the Lithosphere and Oceans.

Wenzhöfer F, Holby O, Glud RN, Nielsen HK, Gundersen JK (2000) In situ microsensor studies of a shallow water hydrothermal vent at Milos, Greece. Marine Chemistry 69, 43-54.

Wenzhöfer F, Glud RN (2002) Benthic carbon mineralization in the Atlantic: A synthesis based on in situ data from the last decade. Deep-Sea Research I 49(7), 1255-1279.